CONTRACTOR REPORT ARLCD-CR-78032

BLAST EFFECTS OF SIMULTANEOUS MULTIPLE-CHARGE DETONATIONS

J. C. HOKANSON
E. D. ESPARZA
A. B. WENZEL
SOUTHWEST RESEARCH INSTITUTE
SAN ANTONIO, TEXAS

P. D. PRICE, PROJECT LEADER
ARRADCOM
DOVER, NEW JERSEY

OCTOBER 1978

US ARMY ARMAMENT RESEARCH AND DEVELOPMENT COMMAND
LARGE CALIBER
WEAPON SYSTEMS LABORATORY
DOVER, NEW JERSEY

The views, opinions, and/or findings contained in this report are those of the author(s) and should not be construed as an official Department of the Army position, policy or decision, unless so designated by other documentation.

Destroy this report when no longer needed. Do not return to the originator.

The citation in this report of the names of commercial firms or commercially available products or services does not constitute official endorsement or approval of such commercial firms, products, or services by the United States Government.

Unclassified

SECURITY CLASSIFICATION OF THIS PAGE (When Data Entered)

REPORT DOCUMENTATION PAGE

READ INSTRUCTIONS BEFORE COMPLETING FORM

1. REPORT NUMBER: Contractor Report ARLCD-CR-78032
2. GOVT ACCESSION NO.
3. RECIPIENT'S CATALOG NUMBER

4. TITLE (and Subtitle): BLAST EFFECTS OF SIMULTANEOUS MULTIPLE-CHARGE DETONATIONS
5. TYPE OF REPORT & PERIOD COVERED: Technical Report
6. PERFORMING ORG. REPORT NUMBER

7. AUTHOR(s): J.C. Hokanson, E.D. Esparza, A.B. Wenzel, SWRI / P.D. Price, ~~ARRADCOM Project Leader~~
8. CONTRACT OR GRANT NUMBER(s): DAAA21-76-C-0254

9. PERFORMING ORGANIZATION NAME AND ADDRESS
Southwest Research Institute
P.O. Drawer 28510
San Antonio, Texas 78284

10. PROGRAM ELEMENT, PROJECT, TASK AREA & WORK UNIT NUMBERS

11. CONTROLLING OFFICE NAME AND ADDRESS
US Army ARRADCOM
ATTN: DRDAR-TSS
Dover, NJ 07801

12. REPORT DATE: ~~OCTOBER 1978~~
13. NUMBER OF PAGES: 115

14. MONITORING AGENCY NAME & ADDRESS (if different from Controlling Office)
US Army ARRADCOM
ATTN: DRDAR-LCM-SF
Dover, NJ 07801

15. SECURITY CLASS. (of this report): Unclassified
15a. DECLASSIFICATION/DOWNGRADING SCHEDULE

16. DISTRIBUTION STATEMENT (of this Report)
Approved for public release; distribution unlimited.

18. > BIF, ARLCD
19. AD-E400 [illegible], CR-78032

17. DISTRIBUTION STATEMENT (of the abstract entered in Block 20, if different from Report)
13. 118 p.

18. SUPPLEMENTARY NOTES

DDC RECEIVED JAN 22 1979 B

19. KEY WORDS (Continue on reverse side if necessary and identify by block number)
Blast Measurements
Simultaneous Detonation
Explosives
Pressure
Impulse
Duration
Time of Arrival

20. ABSTRACT (Continue on reverse side if necessary and identify by block number)
This report describes an experimental program conducted by Southwest Research Institute in support of the Army Plant Modernization Program. Air blast parameters including peak pressure and specific impulse were measured for multiple charges, detonated simultaneously, in three different geometrical configurations: grouped, horizontal and vertical arrays. A series of single charge tests was also conducted to establish a baseline from which the

DD FORM 1 JAN 73 1473 EDITION OF 1 NOV 65 IS OBSOLETE

Unclassified

SECURITY CLASSIFICATION OF THIS PAGE (When Data Entered)

323 510

20. ABSTRACT (Cont'd)

effects of multiple charges could be determined. A model analysis was developed and used to design and interpret the model experiments.

In the experiments, pentolite spheres modeling potential explosive sources were detonated near a reflecting surface. Blast measurements were made directly below the charges and at various slant distances using piezoelectric transducers. The impulse was obtained by numerically integrating the pressure traces. Plots of peak pressure, impulse, duration and arrival time are presented and the differences between single and multiple charges are highlighted.

TABLE OF CONTENTS

LIST OF FIGURES

LIST OF FIGURES (Cont'd)

LIST OF TABLES

INTRODUCTION

This report describes an experimental program conducted by Southwest Research Institute (SwRI) for the U.S. Army Armament R & D Command, Dover, New Jersey under Contract Number DAAA21-76-C-0254. As part of the Army Plant Modernization Program, air blast parameters have been measured in the past for single explosive sources, and propellents and pyrotechnics in their in-process and final product forms.

In a plant process there are often multiple explosive sources within a single room, on a conveyor or near a barricade. Currently, structures which may be loaded by simultaneous or near simultaneous multiple detonations are designed according to Section 4-17 of Reference 1. According to this document, the impulse loading on the structure is approximated by the numerical sum of the impulse which would be generated by each individual explosion whenever the combined duration is less than 1/3 of the response time of the structure. For combined durations longer than 1/3 the structure response time, the actual pressure-time history should be replaced by a fictitious peaked triangular pulse similar to that for a single explosion. The objective of this program is to investigate blast phenomena near a reflective surface due to multiple simultaneous detonations at small scaled distances. This information will be used to supplement the information contained in Reference 1. Eventually, it is hoped that this information will lead to a more realistic design of buildings used for the manufacture of explosives and propellents.

In this program, the blast parameters of several charge geometries were measured at different charge spacings and standoff distances. At large distances, the shock fronts from several charges detonated simultaneously should coalesce and be more or less indistinguishable from that of a single charge with an equivalent amount of explosive. To ensure that measurements were made before the individual shock fronts had begun to coalesce, the transducers were placed at small scaled distances ($Z \leq 1.2$ m/kg$^{1/3}$ or 3.0 ft/lb$^{1/3}$). Since this was an exploratory program, the tests were organized in the following manner.

- The number of charges was held constant at three.
- All three charges were detonated simultaneously.
- The in-process explosive sources were simulated with Composition B spheres.
- Three charge geometries were investigated: Grouped, Horizontal and Vertical Arrays.
- The spacing between charges in the horizontal and vertical array tests was uniform.

The blast parameters measured included peak pressure, specific impulse, positive duration and time of arrival. The pressure-time traces were recorded with piezoelectric transducers and the impulse was obtained by integrating the pressure histories.

A total of 44 tests was conducted in four test geometries. Nine transducers were placed at regular intervals in a straight line. The test charges were suspended above a reflective surface at scaled distances ranging from 0.335 $m/kg^{1/3}$ (0.84 $ft/lb^{1/3}$) to 1.18 $m/kg^{1/3}$ (3.0 $ft/lb^{1/3}$). Each charge was initiated with an exploding bridgewire detonator. A series of single charge tests was used to establish a baseline from which the relative blast output of multiple versus single charges could be determined. This series of tests was also used to check out the instrumentation system, for calibration and to validate the model analysis. A series of tests in which three charges were grouped together was conducted. These tests were designed to determine whether charges packed together behave the same as a single charge of equivalent weight. The horizontal array tests may be thought of as simulating a conveyor system or explosive sources distributed horizontally. Charge spacing and standoff distance were varied in these tests. Of particular interest in the horizontal array tests was the possibility of regions of enhanced pressure and impulse between the charges. The final tests were conducted to determine the blast output of charges suspended above the ground in a vertical array.

In this report a technical discussion is given in which the model law is developed. The model law was used to design the experiments and interpret the data. The section entitled Experimental Program outlines the test program, the instrumentation used to measure the blast parameters and the data reduction methods. The resulting data are presented principally in the form of graphs. Comparison of the blast output of single and multiple charges is made, and tables of all the test data are included as an Appendix to this report.

TECHNICAL DISCUSSION

General

The blast output from the detonation of a single explosive source in the free field has been well defined for many years. A complete description of the blast output is found in Reference 2. To better describe the characteristics of the simultaneous detonation of several charges, a short description of the blast output from a single charge is appropriate.

When an explosive source is detonated, the rapid release of energy causes a sudden increase in pressure in the immediate vicinity of the source. The region of high pressure or shock front is characterized by a near instantaneous increase from ambient conditions (i.e., pressure, particle velocity, density and temperature) to peak shock front conditions. The shock front expands radially from the center of the source at a decreasing rate. The time variations of blast parameters of pressure, density, particle velocity and temperature at any point away from the charge center have similar characteristics. Pressure is shown in Figure 1. The shock front arives at the point in question at some time, t_a, and the pressure rises almost instantaneously to the peak value, P_s. The pressure then decays exponentially to the ambient pressure in a time, t_d. The period from the initial arrival of the shock until the pressure has decayed to the ambient conditions is known as the positive phase duration. Thereafter the pressure drops below the ambient condition for a time longer than the positive phase before returning to the initial value. This period is known as the negative phase duration. Although all of the blast parameters are somewhat similar, the actual positive and negative phase durations for pressure are not necessarily the same for the other shock front parameters.

Consider now the case of three charges detonating simultaneously. The three charges will each produce separate shock fronts which will arrive at some point in space, sequentially. As the observation point moves farther from the charges, the later arriving shock waves will begin to overtake the initial shock. This is because the initial shock front compresses and heats the undisturbed air as it passes through, and in addition, imparts a velocity to the air particles in the direction of shock propagation. Therefore, the subsequent shocks travel through a warmer, denser environment than the initial shock which is also moving in the direction of travel of the first shock. Since the shock velocity of a gas is an increasing function of temperature, the secondary shocks will travel faster than the initial shock. At some point in space, the three individual shocks will coalesce and be similar at the same distance to a shock generated from a single explosive charge with a mass equal to the total of the three charge masses. Thus the characteristic shape of the pressure at some point in space may vary from a single shock front, such as in Figure 1, to three distinct shock front arrivals. Factors governing the type of pressure trace obtained at a given location are the size of the individual charges, the distance between charges and the location of the point in question.

Blast Parameter Scaling

Experimental studies of blast wave phenomena are often difficult and expensive, particularly when conducted on a large scale. Methods of computation of blast wave characteristics are often so involved that one cannot economically repeat these computations while varying, in a systematic manner, all of the physical parameters which may affect the blast wave. Almost from the outset of scientific and engineering studies of air blast, various investigators have attempted to generate model or scaling laws which would widen the applicability of their experiments or analyses.

The most common form of scaling, familiar to anyone who has had even a rudimentary introduction to blast studies, is Hopkinson or "cube-root" scaling. This law was first formulated by B. Hopkinson (Reference 3) and independently by C. Cranz (Reference 4), and states that self-similar blast waves are produced at identical scaled distances from two explosive charges of similar geometry and identical explosive material, but of different size, which are detonated in the same atmosphere. The implications of Hopkinson-Cranz scaling can perhaps be best described by the example illustrated in Figure 2. An observer located a distance R from the center of an explosive source of characteristic dimension d will be subjected to a blast wave with amplitude (peak overpressure) P, duration t_d, and a characteristic time history. The positive impulse I of the blast wave, defined by

$$I = \int_{t_a}^{t_a + t_d} p(t)dt \qquad (1)$$

where t_a is arrival time of the shock front and p(t) is the wave form of the time-varying overpressure, is often used to characterize the blast wave. The Hopkinson-Cranz scaling law then states that an observer stationed a distance λR from the center of a similar explosive source of characteristic dimension λd detonated in the same atmosphere will feel a blast wave of similar wave form, identical amplitude P, duration λt_d, and impulse λI. All characteristic times such as arrival time t_a are scaled by the same factor as the length scale factor λ. In such scaling, both pressures and velocities are unchanged at homologous times.

Hopkinson-Cranz scaling has been shown by many investigators to apply over a very wide range of distances and explosive source energies. An example of early published work is that of Stoner and Bleakney (Reference 5) which showed that such scaling would apply for a limited range of distances and source energies. The list of other investigations corroborating this law is too lengthy to include here, but a report by Kingery, et al., (Reference 6) showing very good agreement between blast data obtained during a field test with a 100-ton TNT detonation and predicted values scaled from experiments with 1- to 8-lb charges, will serve to indicate the usefulness of this ubiquitous law. It has, in fact, become so universally used that blast data are almost always presented in terms of the Hopkinson-scaled parameters:

$$Z = R/W^{1/3} \quad \text{(scaled distance)}$$

$$T = T/W^{1/3} \quad \text{(scaled time)} \qquad (2)$$

$$\zeta = I/W^{1/3} \quad \text{(scaled impulse)}$$

This law implies that all quantities with dimension of pressure and velocity are unchanged in the scaling. Thus, side-on pressure, dynamic pressure, and reflected pressure all remain identical at homologous times, and both shock velocity and time histories of particle velocity are unchanged.

Model Analysis

In a program such as this one, it is often beneficial to conduct a model analysis prior to the beginning of testing. The purpose of the model analysis is to design a series of scaled experiments which will simulate in a realistic fashion the pressure-time histories of large-scale or prototype detonations of multiple charges. The problem addressed by the model analysis developed below is that of three charges detonating simultaneously. The charges are suspended above an infinitely long, infinitely wide and infinitely stiff reflecting surface. The object of the model analysis is to develop the scaling relationships for the pressure and impulse which are applied at various points along this surface.

The first step in developing a model analysis is to list all the parameters which are required to characterize the phenomena. Table 1 is a list of the 24 parameters which are required to characterize the explosive charge, the atmospheric conditions, the shock front, charge locations and the reflecting plane. To characterize the explosive charge, the energy release of the explosive, E, charge radius r, density ρ_e, detonation velocity a_e, and the explosive products specific heat ratio γ_e are required. The effective limit for explosive detonation g is listed because, as is well known, there exists a minimum charge linear dimension below which it is impossible to initiate or propagate a detonation. This parameter will define a lower limit for the scale at which the tests will be conducted.

The medium in which the detonation occurs is characterized in the analysis by the ambient air pressure P_a, sonic velocity in air a_a, ambient air density ρ_a, ambient air temperature θ_a, the specific heat ratio of air, γ_a and the specific entropy, S. The shock itself is characterized by the velocity U_1, gas density ρ_s, particle velocity u_s and a shock front temperature θ_s.

The remaining parameters are used to characterize the geometry of encounter and the responses to be measured. In this program it is desired to measure the pressure P and impulse I as a function of time t, as well as the arrival time of the shock wave t_a and the shock wave duration t_d. The position of the point where responses can be determined by three coordinates: the standoff distance R, the shock front encounter angle Ψ, and the spacing between charges, s_1.

The second step in developing a model law is the derivation of scaled quantities, called pi-terms, from the list of important parameters. The procedure of deriving the pi-terms is described in Chapters 2 and 3 of Reference 7. For brevity, only the resulting pi-terms are presented here. Twenty pi-terms can be derived from the 24 parameters listed in Table 1. One possible set of pi-terms, or nondimensional quantities, is listed in Table 2.

The first four pi-terms are statements of geometric similarity. That is, all lengths in the prototype must be scaled by the constant λ in the model for the two systems to be equivalent. The shock wave encounter angle Φ is identical in equivalent systems. Pi-terms five to seven state that similiar explosives must be used in the model and prototype systems, and pi terms six to eleven require that similiar atmospheres exist in the model and prototype systems.

Pi-terms 13 to 19 are the response pi-terms in this analysis. These terms impose no restrictions on the model, but rather define how to scale the model measurements of pressure, impulse, arrival time and duration in order to make prototype scale predictions of the same parameters.

All twenty pi-terms listed in Table 2 can be satisfied providing replica modeling is used. In a replica model, the same materials are used in the model and prototype systems, and all geometric quantities are scaled by the scale factor λ. By examination of the remaining pi-terms, the scale factors for quantities other than length can be established. The use of the same explosives and atmosphere in the two systems implies that all densities, temperatures and specific heats will be identical in the model and prototype systems. Since the same atmosphere is used, pi-terms 7 to 9 further imply that velocities and pi-term 16 implies that pressure will be invariant between systems. That the scale factor for energy is λ^3 can be established by observing π_{16} and noting that the scale factors for pressure and length are 1.0 and λ respectively. Similarly, π_{19} shows the scale factor for impulse is λ, and π_{20} shows the scale factor for time is λ.

Table 3 summarizes the replica scaling law for miltiple detonations. The replica model law is essentially an extention of the Hopkinson-Cranz scaling of blast parameters. Several pi-terms have been added to account for the extra parameters needed to characterize the test geometry and to account for the fact that the initial blast front compresses, heats the initially undistrubed air and imparts a net velocity in the direction of shock front propagation.

The model analysis developed above was used to design the model experiment so that the prototype situation, three charges detonating simultaneously near a reflecting plane, could be modeled accurately, and so that the parameters required to created a blast-resistant structure would be available. The designer primarily needs to know the pressure and impulse acting on a structure and he will sometimes use duration measurements when they are available. Arrival time measurements are useful when multiple shock fronts are present.

If one were to write an equation for the pressure, impulse, time of arrival or duration at some point on the target, he would be defining a 12 parameter space. That is, each of the responses is a function of the first 12 pi-terms in Table 2. However,many of the parameters in each of the pi-terms are essentially constant and may be eliminated from the analysis without significant loss of accuracy. For example γ_e, ρ_e, a_e, P_a, a_a, ρ_a, γ_a and θ_a are all invariant. If the size of the charge is above the minimum size required to sustain detonation, the effective limit for explosive detonation g may be ignored. Under these circumstances, the following functional relationships for pressure, impulse, arrival time and duration can be written:

$$P = f_1\left(\frac{r}{R}, \frac{s_i}{R}, \Phi, \frac{R}{E^{1/3}}, \frac{t}{R}\right) \tag{3}$$

$$\frac{I}{E^{1/3}} = f_2\left(\frac{r}{R}, \frac{s_i}{R}, \Phi, \frac{R}{E^{1/3}}, \frac{t}{R}\right) \tag{4}$$

$$\frac{t_a}{E^{1/3}} = f_3\left(\frac{r}{R}, \frac{s_i}{R}, \Phi, \frac{R}{E^{1/3}}\right) \tag{5}$$

$$\frac{t_d}{E^{1/3}} = f_4\left(\frac{r}{R}, \frac{s_i}{R}, \Phi, \frac{R}{E^{1/3}}\right) \tag{6}$$

In this program only one explosive type will be used; therefore, the parameter E can be replaced by the charge weight W, resulting in a more familiar form for Equations 3 to 6. In addition,if we recognize that only the peak value of pressure and the impulse will be used by designers, the following relations are obtained:

$$P = f_1\left(\frac{r}{R}, \frac{s_i}{R}, \Phi, \frac{R}{W^{1/3}}\right) \tag{7}$$

$$\frac{I}{W^{1/3}} = f_2\left(\frac{r}{R}, \frac{s_i}{R}, \Phi, \frac{R}{W^{1/3}}\right) \tag{8}$$

$$\frac{t_a}{W^{1/3}} = f_3\left(\frac{r}{R}, \frac{s_i}{R}, \Phi, \frac{R}{W^{1/3}}\right) \tag{9}$$

$$\frac{t_d}{W^{1/3}} = f_4\left(\frac{r}{R}, \frac{s_i}{R}, \Phi, \frac{R}{W^{1/3}}\right) \tag{10}$$

The data accumulated during this program can be used to predict full scale measurements of P, I, t_a and t_d provided the prototype experiments use the same explosive and the measurements are made over the same range of values of the six parameters in the above functions. The equation relating the four responses to the independent variables is not derived as part of this program; instead the data are presented in a graphical form. Only the peak values of the pressure and the impulse are presented and all four responses are plotted as a function of Φ and $R/W^{1/3}$. Separate plots for the different charge geometries are presented.

EXPERIMENTAL PROGRAM

General

The objective of this test program was to investigate the blast effects on a barricade due to the simultaneous detonation of three charges at small scaled distances. To accomplish this objective, a technique for measuring the blast pressures and impulses at scaled distances of 0.32 to 1.2 $m/kg^{1/3}$ (0.80 - 3.0 $ft/lb^{1/3}$) was devised. The program consisted of exploding either one or three spherical Composition B charges at various distances above the ground surface. The Composition B charges were cast by The Explosive Processing group of the Naval Surface Weapons Center, White Oak Laboratory, Maryland, and had relatively uniform mass and diameter. Pressure-time histories were recorded with piezoelectric transducers mounted in metal canisters buried in the ground. Impulse measurements were obtained by integrating the pressure-time histories.

The program consisted of four series of tests as summarized in Table 4. In Test Series 1, a single charge weighing either 0.65 kg (1.43 lb) or 2.29 kg (5.05 lb) was detonated from 0.29 to 1.56 m (0.95 - 5.13 ft) above the reflecting plane. This series of tests was conducted to validate the experimental technique and transducer calibration by generating data which could be compared directly with data in the literature. In addition, this series of tests served as a baseline from which the effects of three charges detonating simultaneously could be evaluated. Test Series 1A was conducted to examine the validity of the model law by detonating a different scaled size charge at an equivalent scaled distance. A total of 15 Series 1 tests was conducted at four different scaled distances: 0.335, 0.5, 0.672, 1.2 $m/kg^{1/3}$ (0.84, 1.25, 1.70, 3.0 $ft/lb^{1/3}$). A schematic diagram of the charge placement and gage positioning is given in Figure 3a.

Test Series 2 was conducted to determine how the blast output of three charges which are grouped together differs from the blast output of a single charge. The test configuration for this series is shown schematically in Figure 3b. Notice that the standoff distance R is measured in this case as the distance from the ground surface up to the center of mass of the three charges. A total of nine tests at the three scaled distances, Z = 0.478, 0.716 and 0.960 m/kg1/3 (1.2, 1.81, 2.42 $ft/lb^{1/3}$), was conducted in Test Series 2. For the grouped array tests, the total weight of the three charges was used in computing the scaled distance Z. This convention facilitates comparison with the single charge test results.

Test Series 3 was conducted to investigate the variations of blast output of three charges which are distributed in a horizontal array for various charge spacings and standoff distances. The test configuration for this test series is shown schematically in Figure 3c. A total of 16 tests was conducted in this test series. Three scaled distances were investigated, Z = 0.719, 0.960 and 1.19 $m/kg^{1/3}$ (1.81, 2.42, 3.01 $ft/lb^{1/3}$), as well as three charge spacings, s = 0.366, 0.71 and 1.07 m (1.2, 2.33 and 3.5 ft). Of particular interest in this test series was the possibility of regions of enhanced pressure or impulse at gage locations between charges over what would be expected if only one charge was present.

The final test series was designed to investigate the blast output of three charges which are placed in a vertical array. This situation is shown schematically in Figure 3d. A total of four tests was conducted at a scaled distance, $Z = 0.51$ m/kg$^{1/3}$, (1.29 ft/lb$^{1/3}$), and a charge spacing of 0.145 m (0.475 ft). As was the case for the grouped charge arrays, the standoff distance, R, is measured from the ground surface to the center of mass of the three charges, and W is the total charge weight. This convention is used to facilitate comparison with the single charge test results.

Transducer Placement

In order to perform the measurements, a reflective surface, capable of withstanding the loads due to the exploding charges and of holding the transducers in place, had to be designed. After some consideration, it was decided to use the ground as the reflecting plane rather than a more conventional test stand, because in some tests the three charges would have a separation distance of as much as 2.08 m (6.8 ft). In order to satisfy the assumption in the model analysis that the reflecting plane was effectively infinite in extent in all horizontal directions and infinitely stiff, a conventional steel test stand would have to be wider, longer and thicker than was practical, therefore, the ground, which has infinite dimensions and stiffness, was chosen as the most advantageous reflecting plane.

The gages were installed in separate fixtures, as shown in Figure 4. Each canister had provisions for removing the surface plate so that the transducer and cable could be serviced without taking the canister out of the ground. The bottom cavity of the canister in Figure 4 was designed to hold several coils of microdot cable, to allow enough slack to remove the cover plate and transducer. The cable exited the canister through a NPT coupler and up to the ground surface. The portion of the cable outside the canister was encased in 1.59 cm (0.625 in) garden hose. Water tightness of the entire assembly was assured by using gaskets between the surface and base plates, and by sealing both ends of the garden hose with silicon rubber.

Three different transducer types were used in this program, and all three types could be used with the canisters. The PCB 102A03 transducer threaded directly onto the surface plate as shown in Figure 4. The remaining two transducer types threaded into cylindrical plugs 3.19 cm (1.25 in) in diameter and 3.10 cm (1.22 in) tall. Steel plugs were used with the PCB 109A02 gages while silicon rubber plugs were used with Susquehanna Instruments ST-2. The plugs protruded slightly above the canister body so that no movement of the plug was possible once the surface plate was installed. The transducer protruded 0.635 cm (0.25 in) above the canister body so that the sensitive diaphragm was flush with the surface plate. Gaps between the transducer and surface plate were filled with modeling clay to provide a uniformly flat top surface.

The canisters were buried in the ground so that the surface plate and the transducer diaphragm were flush with the ground surface. The transducer cable enclosed by the garden hose exited the ground a minimum of 1.22 m (4.0 ft) from the gage line. The nine canisters were buried at 0.361 m

(1.18 ft) intervals. Once the transducers were placed, they remained in the ground in their original positions until the test program was completed.

Test Procedure

All 44 tests were performed at an outdoor explosives site on the SwRI grounds. A typical test was conducted by first installing the pressure transducers in the nine canisters. The type of transducer installed at any measurement location was determined by the pressure expected to be generated by the test. While the instrumentation was being readied, the ground surface surrounding the canisters was leveled. On many occasions it was easier to remove the top 0.8 to 1.6 cm (0.31 - 0.62 in) of soil and replace it with new soil, as previous tests had compacted the soil to the point where it was unworkable. After the ground surface and instrumentation was prepared, the charge was suspended from a bar 2.44 m (8 ft) high at the correct standoff distance above the ground. The charges were held in place above the gage line by light string running to two points on the ground as shown in Figure 5. After all charges had been secured, a final electrical continuity check of all firing and instrumentation lines was made; the detonators were placed in the center of the spherical charges and positioned so that no fragments would be likely to strike the transducer. The detonators used in this program were Reynolds Industries RP-81 electronic bridgewire detonators. These EBW's are used extensively where simultaneity of detonation of multiple charges is desired. When connected in series, up to 8 charges can be detonated with a simultaneity not worse than 0.125 μs. After the detonators were placed and the area cleared, the exploding bridgewire firing system was triggered. The data were recorded on magnetic tape and five channels were backed up by Biomation recorder. Oscillograph records were made from the data on magnetic tape and polaroid prints made of the Biomation recordings. Typical damage to the ground surface produced by a test is shown in Figure 6.

Instrumentation System

Several different transducers were used in this project to obtain the pressure-time data. Each transducer was selected depending on the peak pressure expected at a given measurement location. The majority of the data were recorded using piezoelectric transducers, although a few measurements were made with a piezoresistive type.

The piezoelectric transducers utilize a ceramic or crystal to generate an electrical charge which is proportional to the stress imparted by the blast wave. Two models, 102A03 and 109A02, made by PCB Piezotronics and one model, ST-2, made by Susquehanna Instruments were used in this project. The PCB transducers use a quartz sensing element with a resonant frequency of 500 kHz. The model 102A03 has a pressure range of 6.9 to 138,000 kPa (1-20,000 psi), while the model 109A02 has a range of 13.8 to 827,000 kPa (2-120,000 psi). These two models are made to withstand up to 20,000 g's of shock acceleration. They contain a built-in amplifier which provides a low impedence, voltage-mode output for improved signal-to-noise ratio, long-line driving capability and good low frequency response as compared to the high impedence, charge-mode output of other piezoelectric transducers.

The Susquehanna ST-2 transducer uses a lead-metaniobate sensing element having a natural frequency of 250 kHz and a pressure range of 0.69 to 3,450 kPa (0.1 to 500 psi). The one piezoresistive transducer used was a Kulite Model HFG-375-1,000 having a natural frequency of 500 kHz and a pressure range of 0-6,000 kPa (0-1,000 psi). This unit was balanced, calibrated and powered with a B&F Model 1-700 signal conditioner. The output was amplified with a B&F Model 702A-10D differential amplifier having a frequency response of 0-100 kHz before being recorded on magnetic tape.

The piezoelectric transducers were connected as shown in Figure 7. Their outputs were also recorded on an Ampex FR-1900 Wideband II magnetic tape recorder which has frequency response of 0-500 kHz at a record speed of 3.05 m/s (120 ips). The data were played back with a reduction speed ratio of 64 into a Bell & Howell Model 1-124 oscillograph recorder with a 5 kHz CEC response galvanometer. The resultant frequency response of the playback system was then 0-320 kHz. For quick-look analysis, the output of some of the transducers was redundantly recorded on Biomation Models 802 and 1015 transient digital recorders with a frequency response of at least 0-50 kHz.

The pressure transducers were dynamically calibrated using a hydraulic calibrator consisting of a triangular chamber filled with oil. Two symmetric ports are provided for flush mounting a reference and a test transducer. The pressure pulse is generated by dropping a weight down a guide tube onto a piston which extends through the top of the chamber. This device produces a half-sine, positive pressure pulse with peak amplitudes from 0.7 MPa (100 psi) to more than 100 MPa (14,500 psi) and rise times of 1 to 2 milliseconds. Different weights and drop heights are used to vary the peak amplitudes. Figure 8 shows samples of typical calibration pressure pulses. The reference piezoresistive transducer used was first calibrated using a dead-weight hydraulic tester to check its sensitivity. It in turn, was used to determine the pressure input to the test transducer.

Data Reduction

The oscillograph traces and polaroid photographs obtained from each test were used to obtain peak pressures, positive impulses, arrival times and positive phase durations. The data were reduced by manually digitizing the records using a Hewlett-Packard Model 9830 microprocessor and a Hewlett-Packard Model 9864A digitizing plotter. The BASIC program which was used to digitize the pressure-time traces also performed the following services:

1. integrate the pressure-time trace
2. retain peak positive impulse
3. retain arrival time of each blast front
4. retain peak pressure associated with each blast front arrival
5. retain total positive duration

The pressure impulse and time traces were plotted for each test in the format shown in Figure 9. In addition, the pressure-time trace was stored on magnetic tape along with Items 2-5 listed previously. After all the data had been reduced for a given test, a separate program was used to print a summary of Items 2-5 in a convenient form for checking errors and plotting the data. The data are printed by this program in both scaled and raw form.

EXPERIMENTAL RESULTS

General

The results of the experimental program are presented in this section in graphic form. The scaling law derived in the model analysis and presented in equations 7-10 states that pressure, impulse, positive duration and time of arrival are a function of the scaled distance Z, the scaled charge separation s_1/r and the shock front encounter angle Φ^*. In the general solution, a five parameter space must be considered to properly scale the data. The results presented in this section, however, define a four parameter space. This is because the scaled charge size, r/R, was held relatively constant during the test program ($0.0425 \leq r/R \leq 0.154$). This fact does not negate the model law, but only places a restriction that the use of this data be limited to situations where r/R is in the range of 0.0425 to 0.154. Care should be exercised whenever the data presented in this report is used for predictions outside this range in r/R.

In this section, graphs of pressure, scaled specific impulse, scaled positive duration and scaled time of arrival are presented as a function of the scaled position. At each value of x/R, the average response parameters, along with the maximum and minimum recorded values, have been plotted while taking advantage of the symmetry about P5 in the transducer array. Measurements at P1 and P9, for example, are plotted together. Where appropriate, two curves are presented on each graph. The first is a solid line drawn through the average points as near as possible while maintaining a smooth transition from point to point and the correct slope (zero) at $x/R = 0$. The second line is transferred from the appropriate single charge figure and is presented such that the relative blast output of a single charge versus multiple charges can be visualized in a convenient manner. In order to easily visualize the differences between different scaled distances or charge spacings, all of the plots for a given blast parameter are presented on one page for each of the four test geometries. Each figure is labeled to indicate the test series, the scaled standoff distance and the scaled charge separation distance. All of the pressure, impulse, duration and arrival time data presented in this section appear in tabular form in Appendix A. For the convenience of the reader, the data are presented on the figures and in the Appendix in both metric and English units.

Pressure Data

The peak pressure data accumulated during this program are shown in Figures 10 to 14. Figure 10 summarizes the peak pressures resulting from the detonation of a single charge at four scaled distances from a reflecting surface. Two scaled charge sizes were investigated in the single charge tests to validate the model analysis (0.68 kg (1.5 lb) and 2.29 kg (5.05lb)). Since the charge size was scaled as dictated by π_1 of the model law, one would expect pressure to be a function of only the position at which it was

---

*For convenience in presenting the data, the angle Φ will be represented on the figures and in the discussions which follow by its horizontal (x) and vertical (R) components.

measured. This is demonstrated by the A and B series tests ($Z = 0.50$ m/kg$^{1/3}$ (1.25 ft/lb$^{1/3}$)) and the R and S series tests, ($Z = 1.19$ m/kg$^{1/3}$ (2.99 ft/lb$^{1/3}$)) where a single line can be drawn through all of the test data. Note that there is a consistent trend in the four pressure curves shown in Figure 10. As the measuring point moves away from directly under the charge ($x/R = 0$), the peak pressure decays very slowly until x/R approaches 0.2. This narrow region of gradual pressure change is followed by a region in which the pressure decays substantially until x/R is about 1.5. For values of x/R greater than 1.5, the decay of pressure with increasing x/R is again quite gradual. These three regions may be conveniently thought of as (a) essentially reflected pressure, (b) transition from reflected to side-on pressure and (c) a region which approximates side-on pressure.*

The pressure generated by three 0.23 kg (0.51 lb) charges grouped together as in Figure 3b, is shown in Figure 11. Three different scaled distances were investigated for this charge configuration. The solid curve in Figure 11 represents an "eyeball" fit to the data generated by the grouped array. The dashed line represents the single charge data for equal scaled distances. Note that the comparisons given in Figure 11 are between three 0.23 kg (0.51 lb) charges and a single 0.65 kg (1.43 lb) charge. This comparison is not intended to demonstrate agreement between single charges and grouped charges but rather to indicate differences in magnitude and tendency. The reader is reminded that standoff distance (Z) of the group array is measured to the center of mass of the three charges. The curves shown in Figure 11 exhibit a trend consistent with the variations in pressure with x/R for the single charges; however, the pressures are reduced. This reduction may be due to a lower energy density of the three charges. As expected, the gap between the pressure curves for the single charge and the grouped array decreases as x/R becomes large, subsequently coalescing at large x/R values.

Figure 12 presents the variation in pressure for three charges in a horizontal array at three different scaled distances. The charges in these tests were separated by 0.71 m (2.33 ft). Above each graph in Figure 12, the physical charge locations, relative to the location of the pressure transducers are represented by circles. This convention is used to aid the reader in visualizing the location of the charges. The comparisons shown on Figure 12 are between three 0.23 kg (0.51 lb) charges and a single 0.65 kg (1.43 lb) charge placed at equivalent scaled standoff distances from a reflective plane. The standoff distance for the horizontal array is computed as the vertical distance to the center of mass of the three charges, divided by the total mass of the explosive detonated (i.e., 0.69 kg (1.52 lb)). Again, the solid line represents the trend of the horizontal array data, and the single charge results are represented by the dashed line. Not that for series I and J, the pressure due to the horizontal array exceeds the single charge pressure curve at scaled positions of 0.5 to over 3.5. Only directly under the center charge ($0 \leq x/R \leq 0.5$) is the pressure from the horizontal array less than that given by the

*As x/R becomes large, the pressure curve approaches the side-on pressure which would be generated by a charge with twice the explosive mass at the same position (7). As the slant distance from the charges to the measurement position becomes larger, the pressure in the third region better approximates the side-on values.

equivalent single charge curve. This is because contributions from the outside charges arrive too late to positively reinforce the pressure measured directly under the center charge. The converse is also true; contributions from the center charge arrive too late to contribute significantly to the pressure under the outside charges. Indeed the pressures measured directly below the charges in Figure 12 are equal within the experimental scatter. The implication of this observation is that it is unfair to compare the single charge results with the pressure from 1/3 the explosive at positions directly under the charges. However, the intention of presenting the dashed line of Figure 12 was not to demonstrate agreement between the single and multiple charge results, but rather to highlight the differences, in both magnitude and general tendency, due to distributing the charge weight in a horizontal array.

To this point, the discussion of the variation in pressure due to changing the scaled standoff distance for the horizontal array concentrated on test series I and J, but not N. This is because no single charge tests at a scaled standoff of 0.83 $m/kg^{1/3}$ (2.09 $ft/lb^{1/3}$) were conducted due to an oversight when the program was planned. To place the series N results into perspective, it was decided to present the single charge curve for $Z = 0.67$ $m/kg^{1/3}$ (1.69 $ft/lb^{1/3}$) in Figure 12. A dotted line is used to emphasize the single charge curve presented for a smaller Z-value. Note that the equivalent curve for $Z = 0.83$ $m/kg^{1/3}$ (2.09 $ft/lb^{1/3}$) would fall somewhat below the dotted line on the series N plot because of the larger standoff distance. Note that the trends described above for the series I and J tests also apply to the series N results.

Figure 13 shows the variation in peak pressure due to charge spacing for horizontal array tests. Three different charge spacings were investigated (5.76, 11.2 and 16.8 charge diameters), while holding the scaled standoff distance constant at $Z = 0.83$ $m/kg^{1/3}$ (2.09 $ft/in^{1/3}$). The charge location is again represented on this figure by a circle and the single charge curve for $Z = 0.67$ $m/kg^{1/3}$ (1.67 $ft/lb^{1/3}$) is presented in absence of data at $Z = 0.83$ $m/kg^{1/3}$ (2.09 $ft/lb^{1/3}$). The correct reference line would fall slightly below the dotted line on each of the figures. Several observations can be drawn from Figure 13. First note that the effect of greater charge spacings is to move the position of maximum pressure towards large values of x/R. For small charge spacings, series P, the pressure curve for the horizontal array approximates that for a single charge. Since no measurements were made between charges, it is unclear whether a region of enhanced pressure similar to that described in the previous section and shown on Figure 11, exists.

For the intermediate charge spacing, series N, a narrow region of enhanced pressure exists halfway between the charges, and a broader region exists for $x/R > 1.0$. These two regions of enhanced pressure are due to the superposition of the blast output of the two charges nearest the measurement position. The highest pressures occur at $x/R = 0.45$, or halfway between charges, because at this point the shock fronts from both charges arrive simultaneously enhancing the pressure. The single charge blast output exceeds that of the horizontal array in series N for $0 \leq x/R \leq 0.3$ and series Q for $0 \leq x/R \leq 1.1$. The reasons for this apparent discrepancy were described previously, and are due to comparing the output of a single charge with that of 1/3 the explosive at equivalent distances. Beyond $x/R = 0.3$ for series N and 1.1 for series Q, superposition of the blast

output of the two nearest charges results in significantly higher pressures than would be observed from a single charge. Although only a narrow region in x/R was explored in these tests, it is apparent that the point where the horizontal array pressure begins to approximate the single charge results is a function of the charge spacing. Closely spaced charges will approximate single charge pressures at smaller scaled positions than widely spaced charges.

The peak pressures resulting from three charges placed in a vertical array are shown in Figure 14. In this case the charge spacing was fairly narrow, 2.28 charge diameters. The comparison shown on Figure 14 is between three 0.23 kg (0.51 lb) charges and one 0.65 kg (1.43 lb) charge. The standoff distance for the vertical array is computed in the vertical distances to the center of mass divided by the cube root of the total mass of explosive detonated. Notice that at scaled distances approaching x/R = 0 and x/R ~ 1.75, the peak pressure for the vertical array tests exceeds that for a single charge. Unfortunately, only one combination of charge spacing and standoff distance was investigated for vertical arrays. It is therefore not clear whether regions of enhanced pressure would exist for different combinations of Z and s. Further vertical array tests should be conducted to see if the trends shown in Figure 14 apply to other charge spacings and standoff distances.

Impulse Data

The impulse data obtained by numerically integrating the pressure-time curves is given in Figures 15 to 19. All of the impulse data is plotted in scaled format as dictated by Equation 8. As noted previously, the impulse from multiple charge tests is scaled by the total charge weight detonated. Scatter in the data, represented by the line drawn from the minimum to the maximum value recorded at a given value of x/R, is generally larger for impulse than for peak pressure. Several factors contribute to the larger scatter, including thermal drift and uncertainties in determining the positive duration. The impulse for single charges at four scaled distances from a reflecting plane is shown in Figure 15. As mentioned in Section III, the scaled charge size was varied in the A-B and R-S test series. According to the model law, the impulse from different charge weights (at a constant Z) can be collapsed to a single curve by scaling the impulse by the cube root of the charge weight. This is demonstrated in the A-B and R-S graphs in Figure 15.

Consistent trends in the impulse curves in Figure 15 can be observed. At small values of x/R, generally less than 0.5, the impulse decreases slightly. This region may be thought of as a region of essentially reflected impulse and corresponds to the region of essentially reflected pressure previously discussed. For values of x/R greater than 0.5, the impulse declines more rapidly.

Figure 16 presents the impulse generated by the grouped array at three different scaled distances. The general trend exhibited by the single charge tests is followed by the grouped array tests. Note that the disparity between the single charge and the grouped array tests is not as great as was true for pressure. This is particularly true at x/R = 0, where the impulse measured for the grouped array essentially equaled the single charge results. As is expected the impulses for the grouped array appear to converge towards the single charge results for larger values of x/R.

Figures 17 and 18 present the variation in impulse for horizontal arrays due to variation in charge standoff and charge spacing. Note that the position of the charges has been included in these figures as was done in the previous section. All of the trends discussed in the previous section for peak pressure are directly applicable to the impulse curves. As seen in Figure 17, a region of enhanced impulse is found between the two nearest charges. This region of enhanced response is more pronounced than for pressure (Figure 12). The enhanced impulse is probably caused partially by the contribution to the impulse from the third charge and by a slight elongation of the positive duration. The effect of varying the charge spacing on impulse is shown in Figure 18. Notice that the general shape of the impulse curves are quite similar to the pressure curves shown in Figure 13, but discrepancies between the horizontal array and the single charge results are generally more pronounced. The one exception to this observation occurs when the charges were spaced the farthest apart, Series Q. Here the impulse is nearly constant at 450 Pa-s/kg$^{1/3}$ (50 psi-ms/lb$^{1/3}$) over the entire range of x/R. Another observation which can be drawn from the horizontal array tests, Figures 17 and 18, is that as x/R becomes large, the curves for the single and horizontal array impulse begin to converge. This is particularly apparent for the curves shown in Figure 17. For wide charge spacings, (Series Q), the point at which the two curves begin to overlap is beyond the range of x/R tested.

The impulse resulting from three charges placed in a vertical array are shown in Figure 19. The variations in impulse with x/R is virtually the same as for pressure (Figure 14), and therefore the comments made in the section for pressure are directly applicable to Figure 19.

Duration Data

The duration data accumulated during this program are given in Figures 20-24. All of the duration data are presented in a scaled format as required by Equation 10. For multiple charge tests, the duration is scaled by the total charge weight detonated rather than by the weight of an individual charge. Scatter in the data is greater for duration than for any other parameter measured during the program. The factors contributing to the scatter are the same which affect the reproducibility of the impulse measurements: thermal drift and uncertainty in determining the time at which the pressure drops below the time axis. Several observations can be drawn from Figures 20-24, which apply to all charge geometries. First, the general trend is for the duration to gradually increase as x/R gets larger. The duration measurements were seldom below 0.15 ms/kg$^{1/3}$ (0.115 ms/lb$^{1/3}$) or greater than 1.0 ms/lb$^{1/3}$ (0.768 ms/lb$^{1/3}$); a change of less than one decade. Apparent exceptions to this observation are found in the duration measurements for the horizontally spaced charges (Figure 22) where the duration declines directly under the outside charge. Note, however, that as x/R increases from zero, the duration increases until the measuring point is halfway between charges. Further increases in x/R moves the measuring point closer to the outside charge, and the duration in turn decreases until the measuring point is directly under the charge. Beyond this value of x/R, the duration increases monotomically. Except for the decrease in the duration directly under the outside charge for the horizontal array, no significant variation in the duration with charge geometry was observed.

Time of Arrival Data

The time of arrival of the initial shock front is shown in Figure 25. All of the arrival time data are presented in a scaled format as dictated by Equation 9. Scatter in the data is the smallest observed during the program. All of the plots in Figure 25 present the initial shock front arrival at each gage. The distance which is used to calculate Z for each point is the distance from the gage to the nearest charge. The charge weight used to scale the time of arrival and in computing the scaled distance is the total charge weight detonated for single charge, grouped and vertical array tests, but the weight of an individual charge for the horizontal array tests. The scaling relationships for arrival time collapse the data to where all four charge geometries could be plotted on one figure without increasing the scatter appreciably.

Comparison of Single Charge Results

Pressure and impulse are most often presented as plots of either normally reflected or side-on parameters as a function of the scaled distance Z. However, for many applications it is desirable to know the pressure acting on a reflecting surface at positions where neither side-on nor normally reflective measurements are appropriate. For this reason, Figures 26 and 27 represent a composite of data from this report and from references 7 and 9. In these figures the peak pressure and the scaled specific impulse are plotted as a function of the scaled position x/R. Each curve in these figures is for a different value of the scaled standoff distance Z, and this value is indicated on the legend in the upper left hand corner of the figures. Note that the charge weight used in computing Z and in scaling the impulse is the equivalent weight of TNT and not the weight of the explosive itself. This was done because different explosives were used to generate the original data. For example, the data from this report are based on measurements with Pentolite. Data from references 8 and 9 are based on limited measurements with Pentolite and primarily Composition C-4 measurements.

CONCLUSIONS AND RECOMMENDATIONS

A total of 44 tests was conducted at scaled distances ranging from 0.335 $m/kg^{1/3}$ (0.84 $ft/lb^{1/3}$) to 1.18 $m/kg^{1/3}$ (3.0 $ft/lb^{1/3}$). Four different charge geometries were studied: single charges and grouped, horizontal and vertical arrays. Based on the results of these tests the following observations can be made:

(1) The validity of the model law has been verified for single charges by numerous researchers (2, 3, 4), which is consistent with the single charge data contained in this report. No attempt to verify the model law for multiple detonations was made during this project.

(2) The pressure and impulse for grouped arrays at small scaled distances are lower than for single charges. The disparity between grouped array and single charge pressure is more pronounced than for impulse.

(3) For horizontal arrays, regions exist where the pressure and impulse exceed what would be expected from a single charge. The location of maximum response is dependent on the charge spacing and the standoff distance, but generally is found halfway between charges. Other regions of enhanced pressure and impulse exist just beyond the outside charge. For very wide charge spacings, the pressure and impulse are nearly constant over the entire range in x/R. For very narrow charge spacings, the regions of enhanced pressure are less pronounced than for intermediate charge spacings.

(4) Only one combination of charge spacings and standoff distances was investigated for vertical arrays. The results indicated that two regions of enhanced pressure and impulse exist: one directly under the vertical array and another for $x/R > 1.5$.

(5) The tests conducted verified the expectation that at large scaled distances, the blast parameters measured for multiple charges could approach those of a single charge. The distance at which the curves begin to coalesce is apparently the greatest for widely spaced horizontal arrays and the smallest for grouped arrays.

(6) No significant variations in the positive duration were observed for the different test geometries.

Based on the above observations, the following recommendations are made:

(1) Although the scaling law has not been verified for multiple detonations, the measurements in this report can be used to obtain a more rational design for munition processing plants. Caution should be exercised, however, when extrapolation of these results is required beyond the scaled distances, positions, or charge sizes tested.

(2) Multiple detonation tests with several different charge size and standoff distance combinations should be planned to verify the complete model analysis.

(3) Only one combination of scaled distance and charge spacing was investigated for vertical arrays. These tests should be repeated to determine whether the trends described in (4) of the conclusions will exist for other values of Z and s/r.

(4) The gage placement for the horizontal array tests resulted in poor resolution of the variation in response as a function of x/R. particularly in the region between charges. Should tests of this nature be repeated in the future, more measurement positions should be provided in this critical region.

(5) Computer programs which could predict the pressure and impulse acting on a barrier due to multiple charge detonations do not exist at the present time. A three dimensional program would be required, and even if available would be very expensive to run. A cheaper and probably as accurate prediction technique can be devised, based on empirical observation and Equations 8-10. However, the data presented in this report are probably insufficient to accomplish this goal. Therefore, further multiple detonation tests should be conducted and an attempt should be made to generate empirical prediction techniques.

REFERENCES

1. "Structures to Resist the Effects of Accidental Explosions", Department of the Army Technical Manual TM5-1300, June 1969, pp. 465.

2. W. E. Baker, Explosions In Air, University of Texas Press, Austin, Texas, 1973.

3. B. Hopkinson, British Ordnance Board Minutes 13565, 1915.

4. C. Cranz, Lehrbuch der Ballistik, Springer-Verlag, Berlin, 1926.

5. R. G. Stoner and W. Bleakney, "The Attenuation of Spherical Shock Waves in Air," Journal of Applied Physics, Vol. 19, No. 7, pp. 670-678, July 1948.

6. C. N. Kingery, et al, "Surface Air Blast Measurements from a 100 Ton TNT Detonation," BRL Memorandum Report No. 1410, Aberdeen Proving Ground, Maryland, June 1952.

7. W. E. Baker, P. S. Westine and F. T. Dodge, Similarity Methods in Engineering Dynamics, Spartan Books, 1973.

8. A. B. Wenzel and E. D. Esparza, "Measurements of Pressure and Impulse at Close Distances from Explosive Charges Buried and in Air", Final Report, Contract No. DAAK 02-71-C-0393, SwRI Project No. 02-3132, August 1972.

9. J. J. Kulesz, E. D. Esparza and A. B. Wenzel, "Blast Measurements at Close Standoff Distances for Various Explosive Geometries," Final Report, Contract No. DAAA21-76-C-0219, SwRI Project No. 02-4563, May 1977.

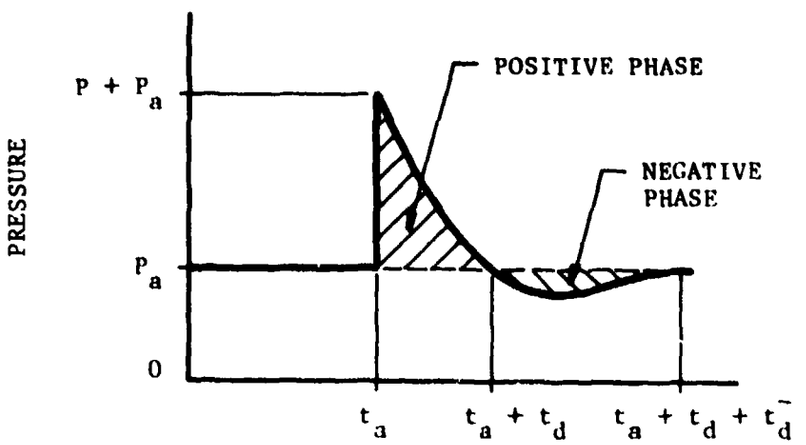

FIGURE 1. IDEAL PRESSURE-TIME HISTORY

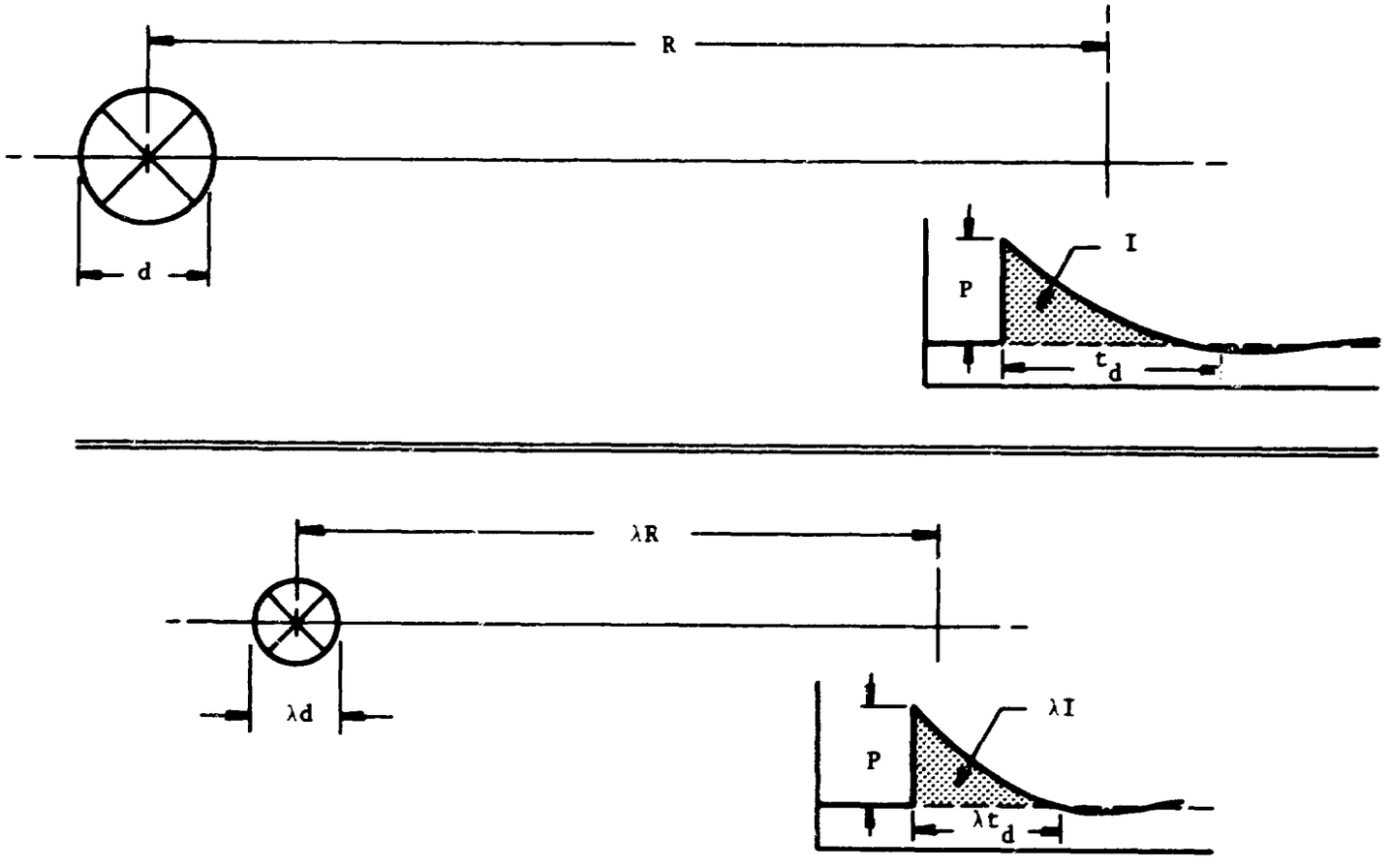

FIGURE 2. HOPKINSON-CRANZ BLAST WAVE SCALING

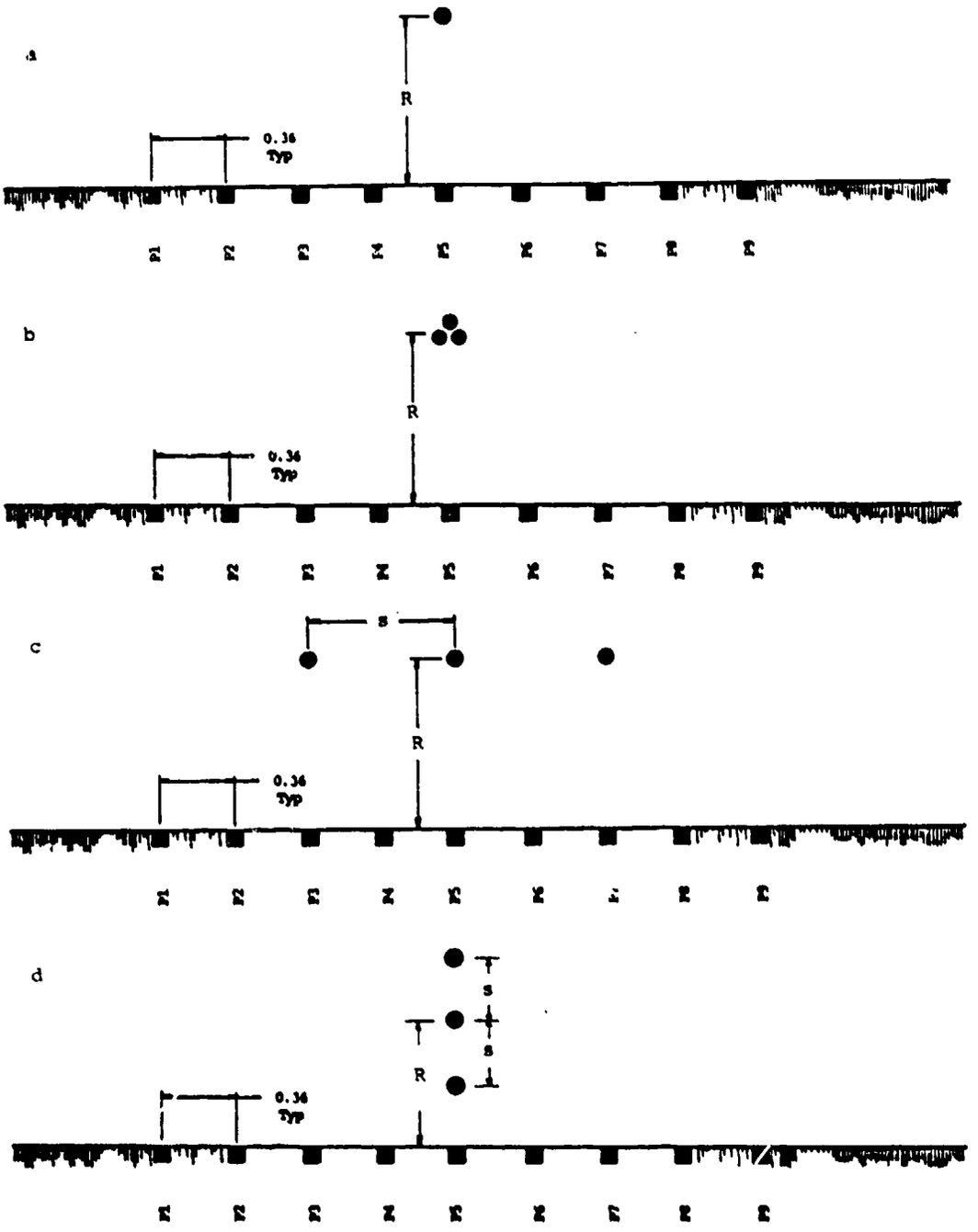

Figure 3. Transducer Arrangement and Charge Placement for the (a) Single Charge, (b) Grouped Array, (c) Horizontal Array and (d) Vertical Array tests.

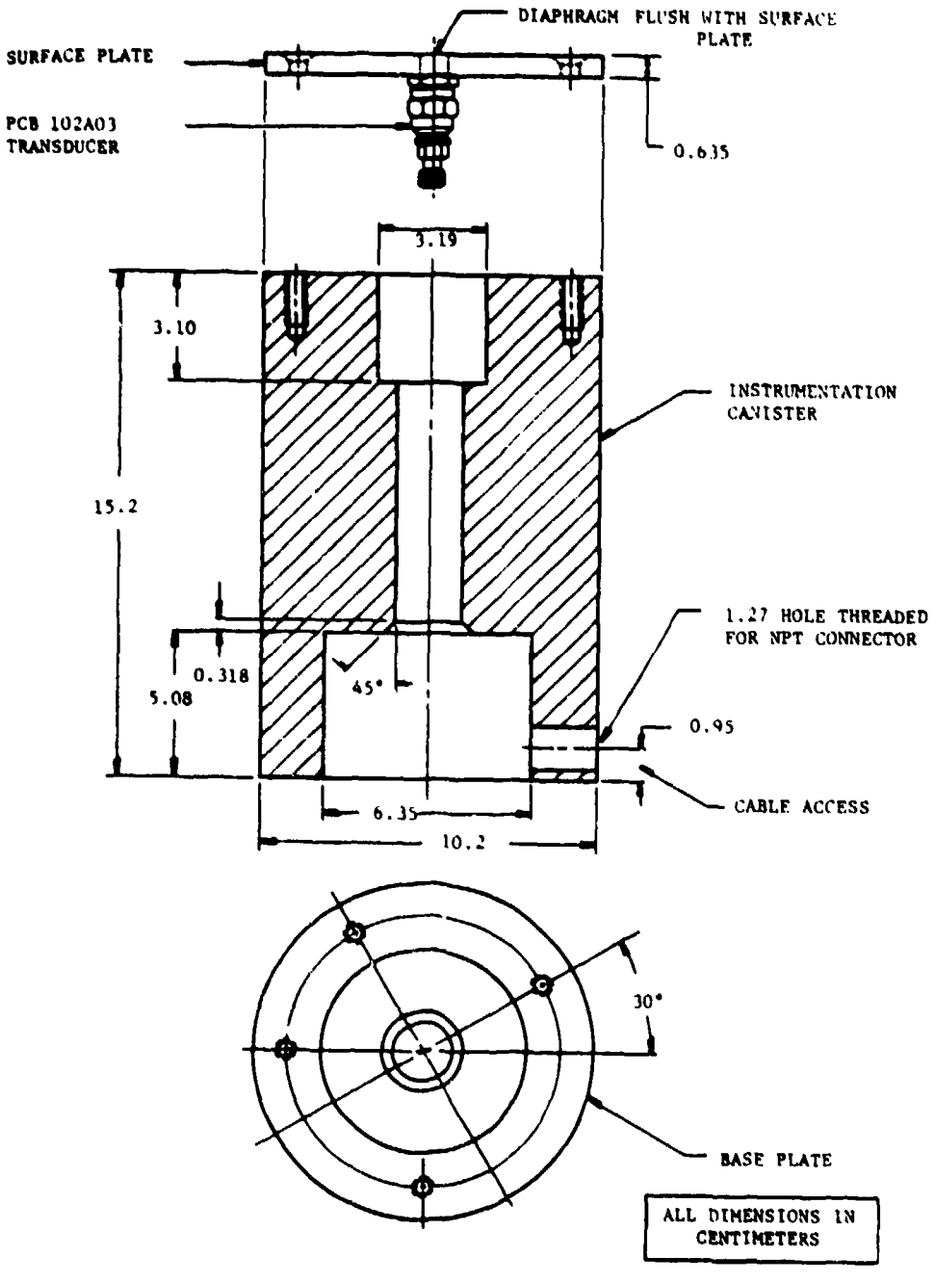

FIGURE 4. EXPLODED DIAGRAM OF THE PRESSURE MEASUREMENT ASSEMBLY

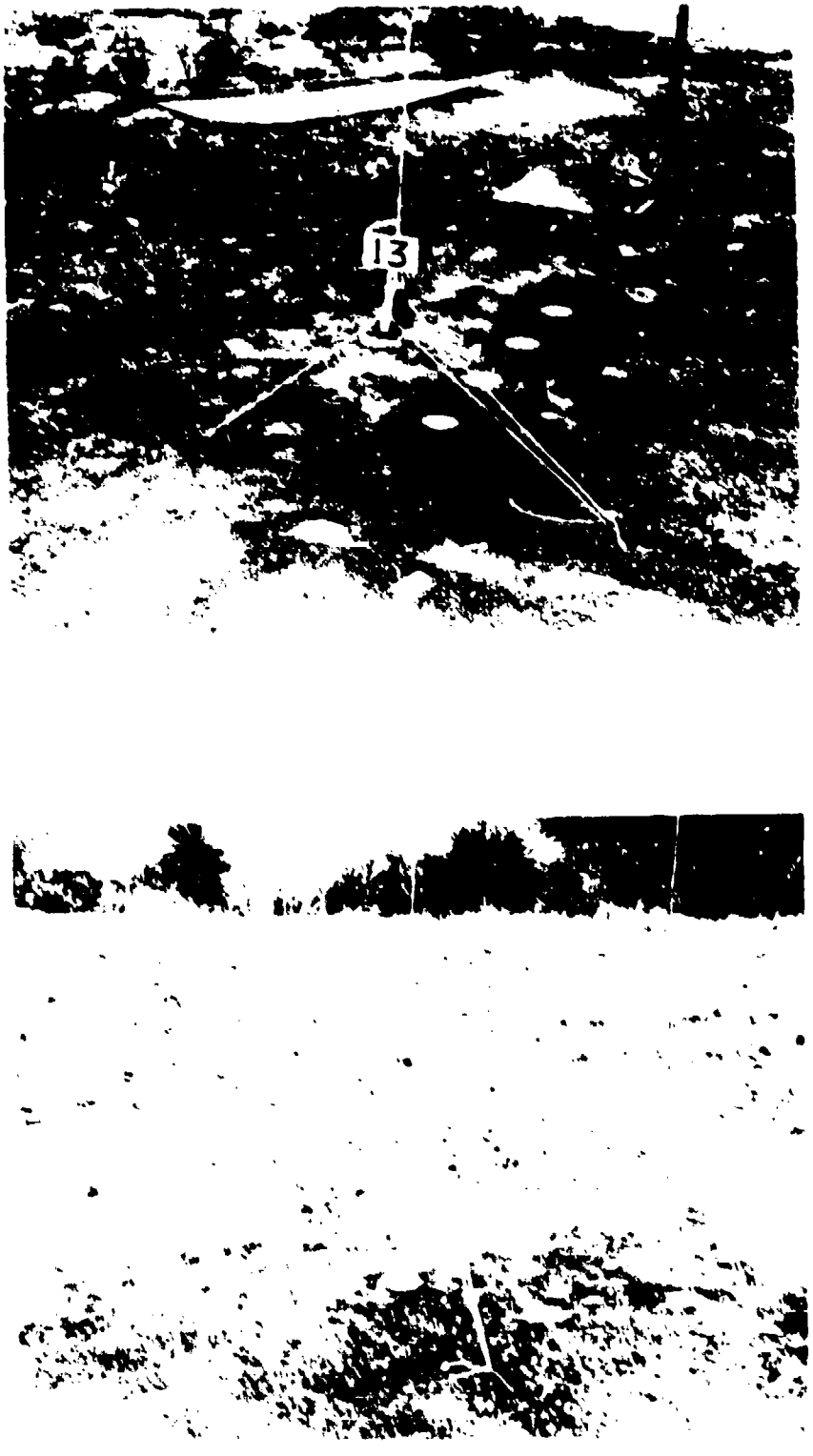

FIGURE 5. TYPICAL TEST ARRANGEMENT FOR THE GROUPED ARRAY AND THE HORIZONTAL ARRAY TESTS

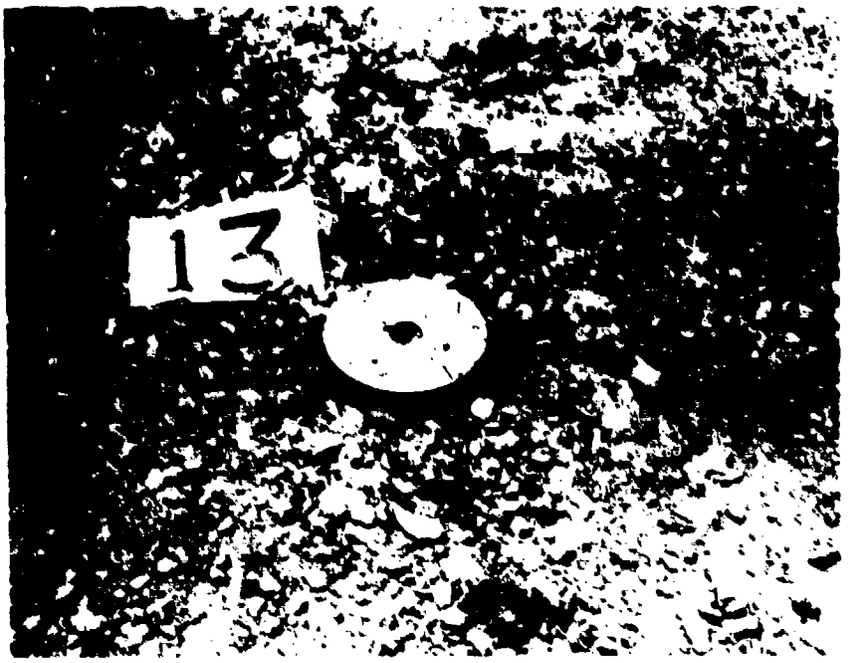

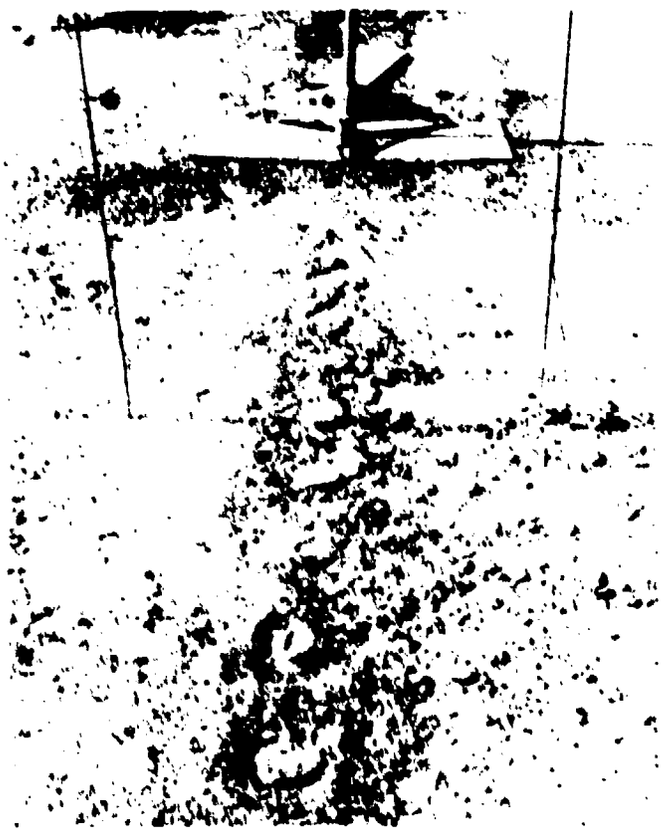

FIGURE 6. DAMAGE TO GROUND SURFACE FROM A TYPICAL GROUPED ARRAY TEST

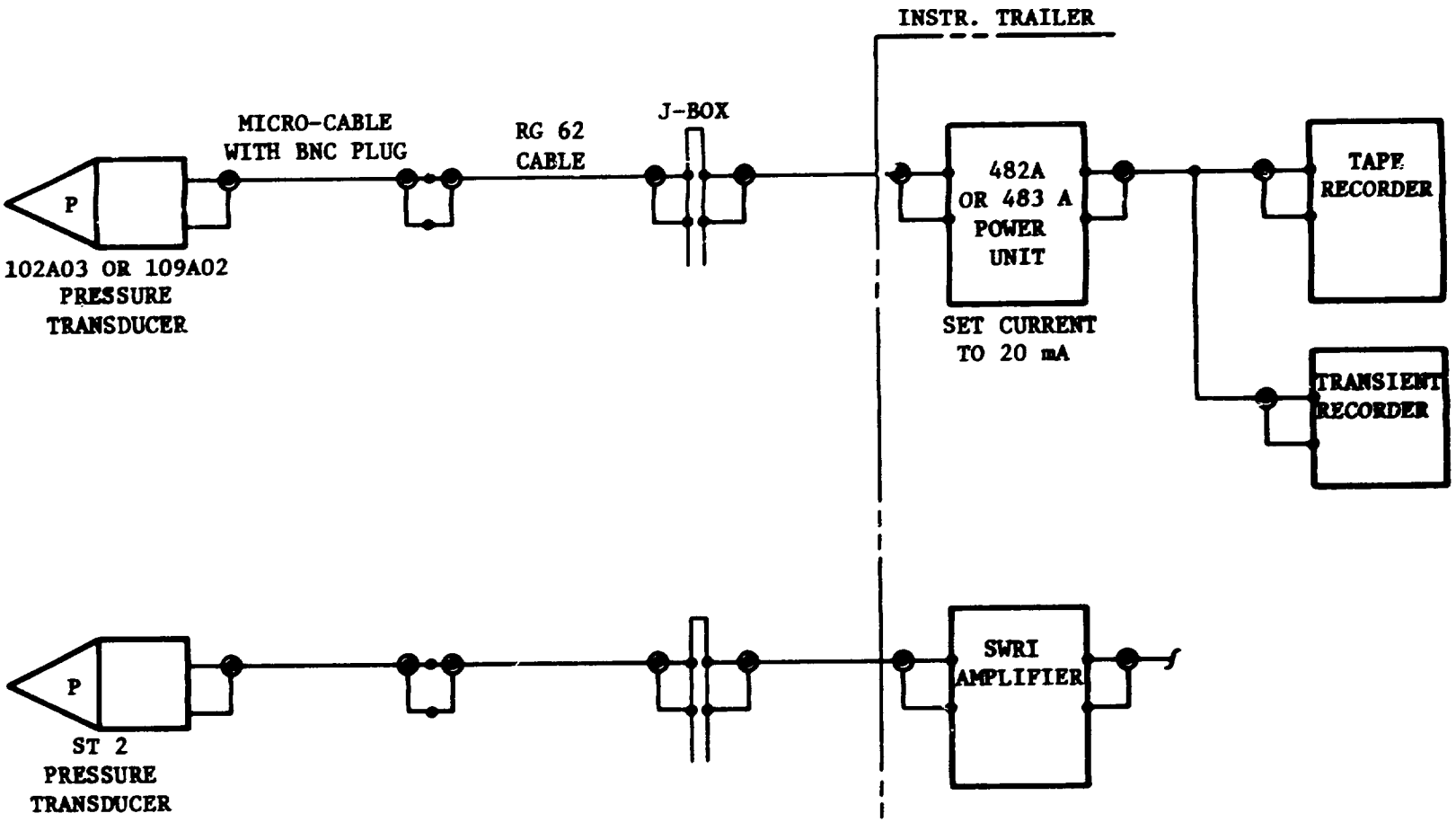

FIGURE 7. DIAGRAM OF PIEZOELECTRIC TRANSDUCER MEASUREMENT SYSTEM

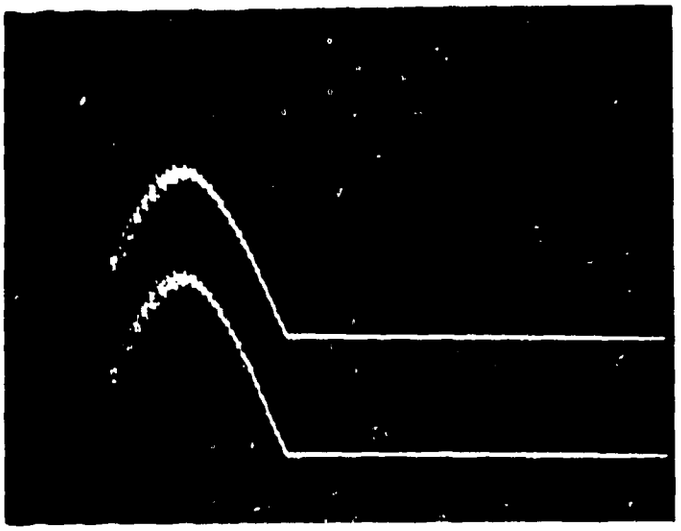

Upper Trace: Ref. Transducer
Lower Trace: Test Transducer
Peak Pressure: 38.3 MPa (5560 psi)
Sweep: 1.0 ms/division

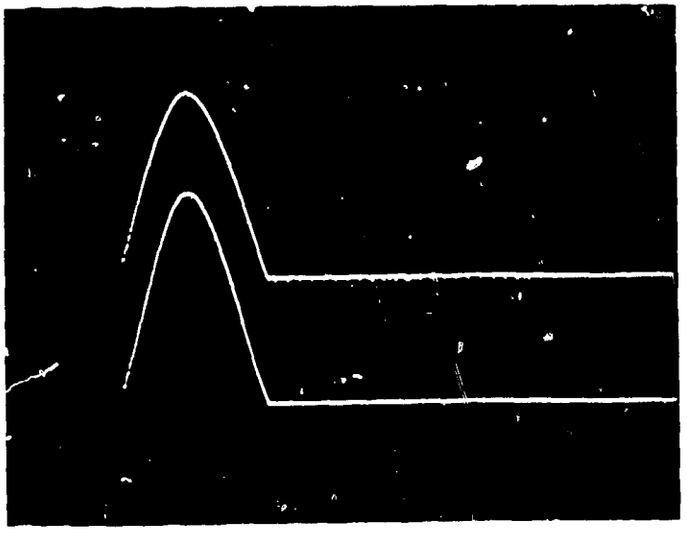

Upper Trace: Ref. Transducer
Lower Trace: Test Transducer
Peak Pressure: 46.0 MPa (6670 psi)
Sweep: 1.0 ms/division

FIGURE 8. CALIBRATION TRACES FOR PRESSURE TRANSDUCERS

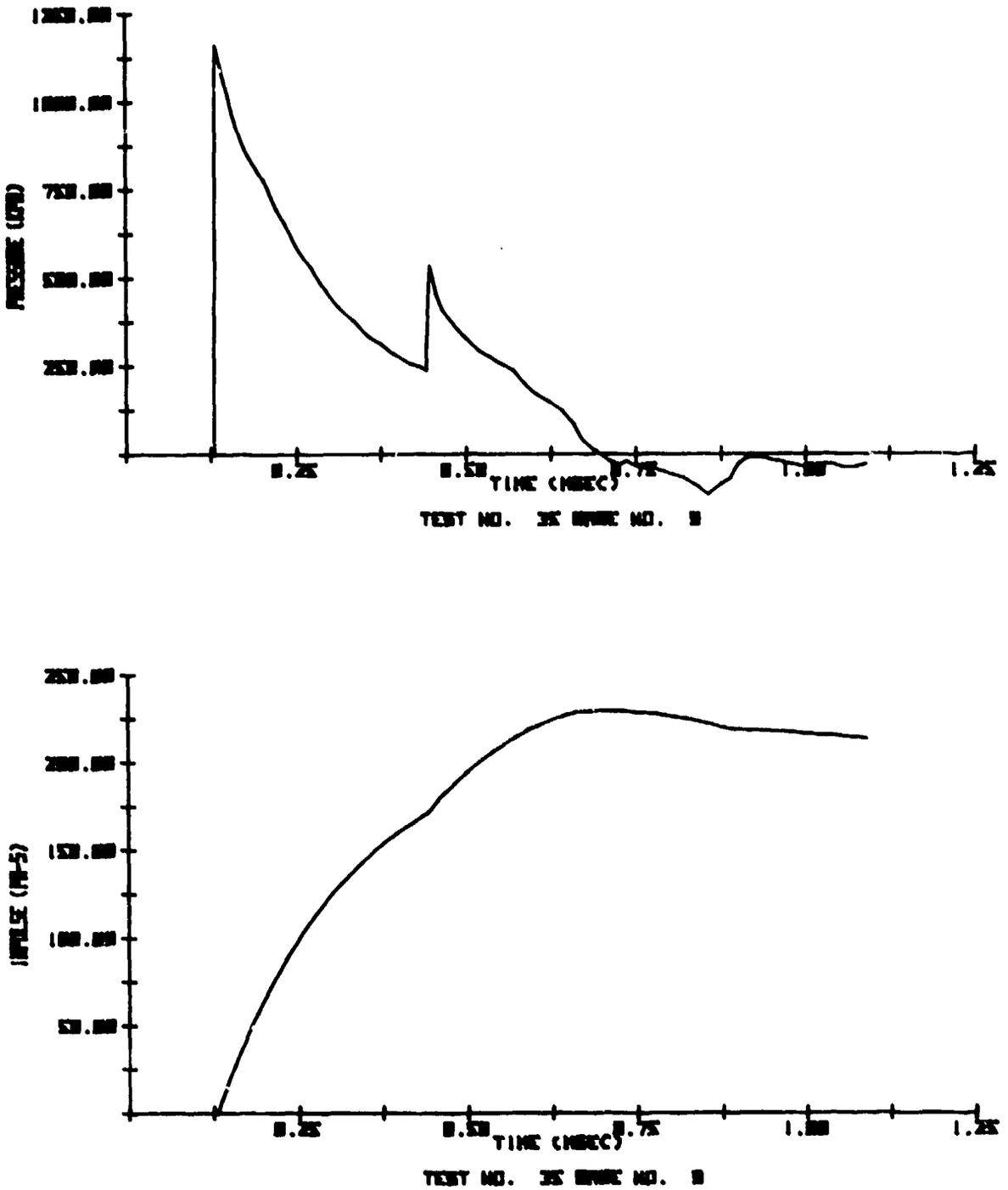

FIGURE 9. SAMPLE OF REDUCED DATA FOR GAGE 9, TEST 35 (HORIZONTAL ARRAY)

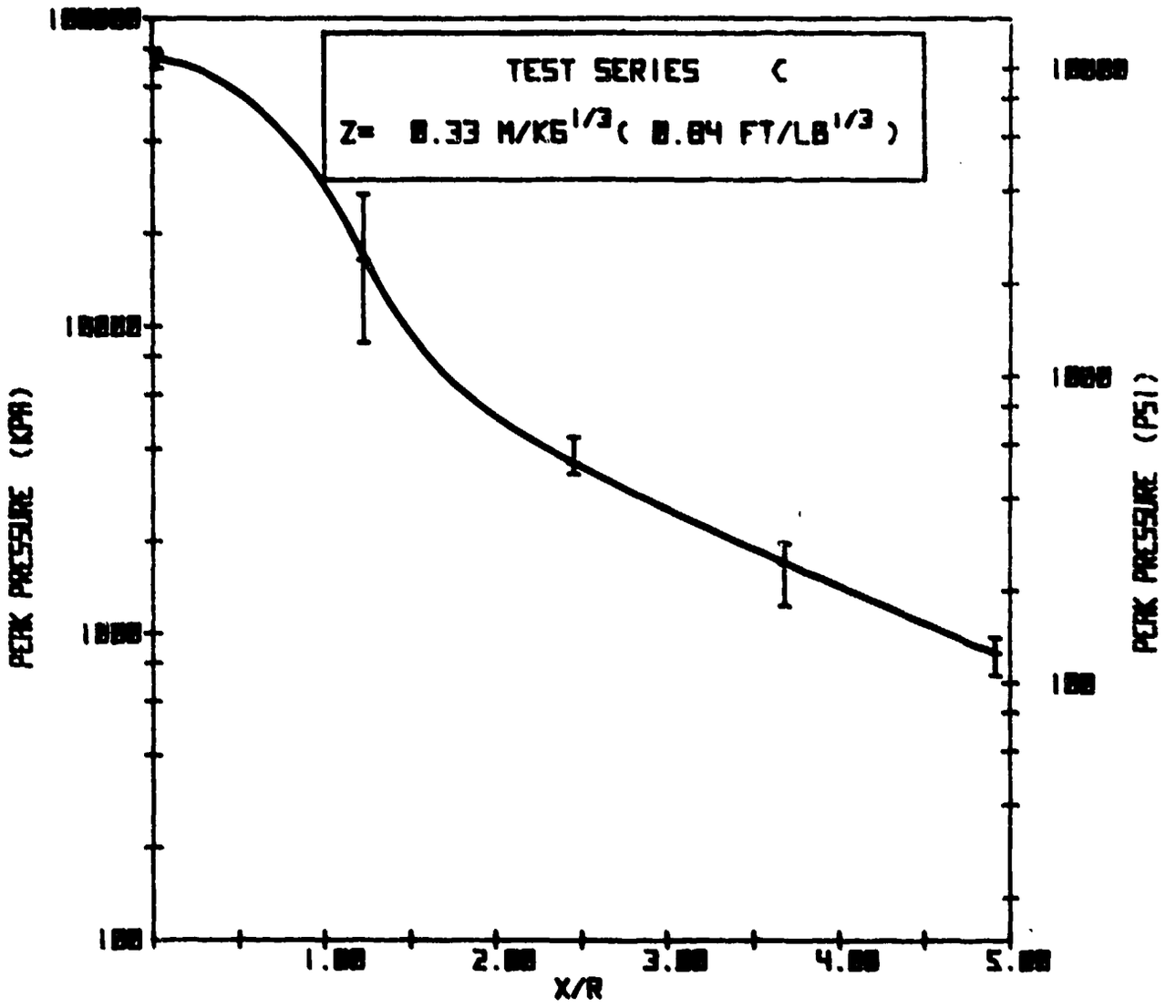

FIGURE 10. PEAK PRESSURE FOR SINGLE CHARGE TESTS

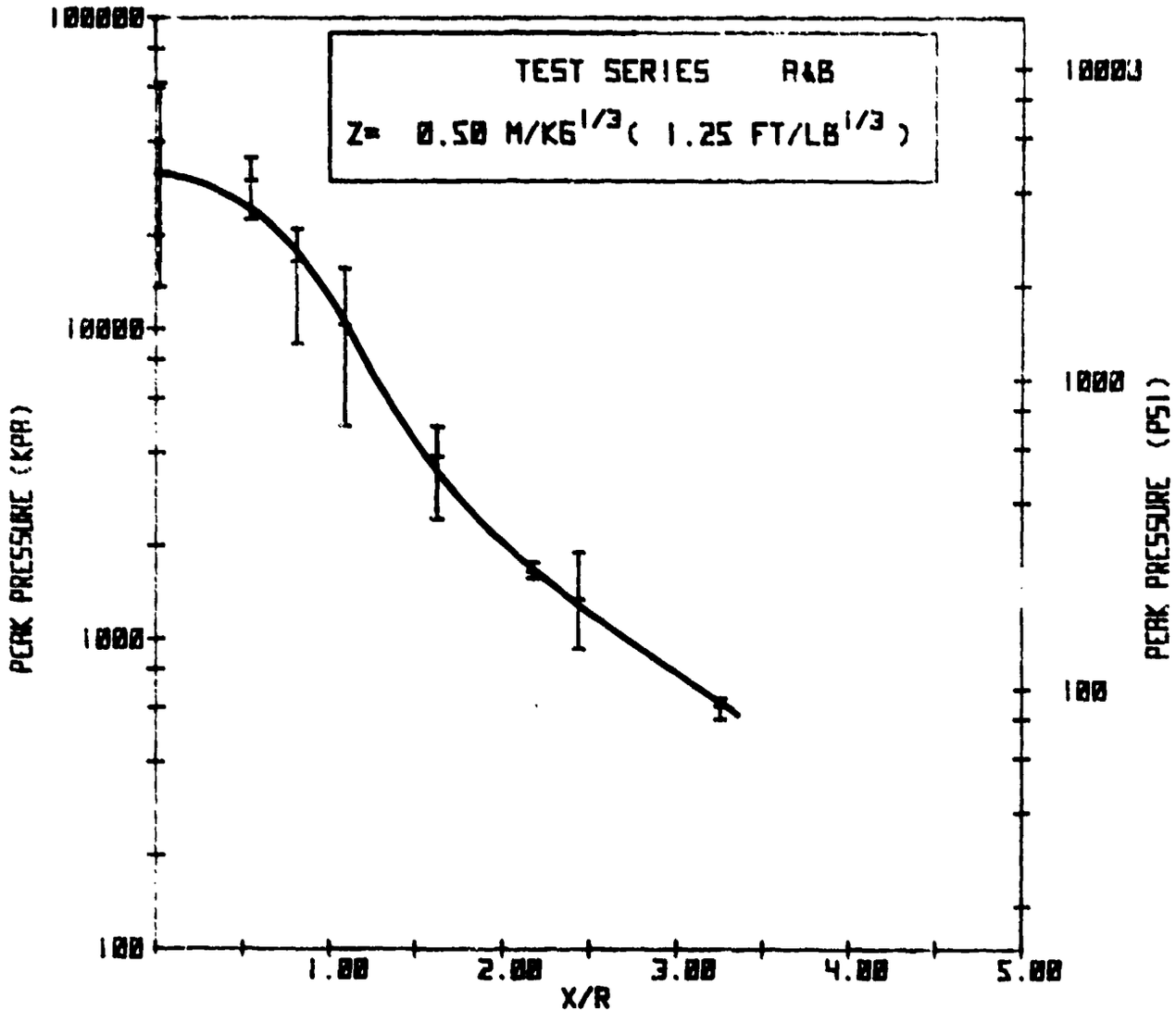

FIGURE 10. PEAK PRESSURE FOR SINGLE CHARGE TESTS (CONT'D)

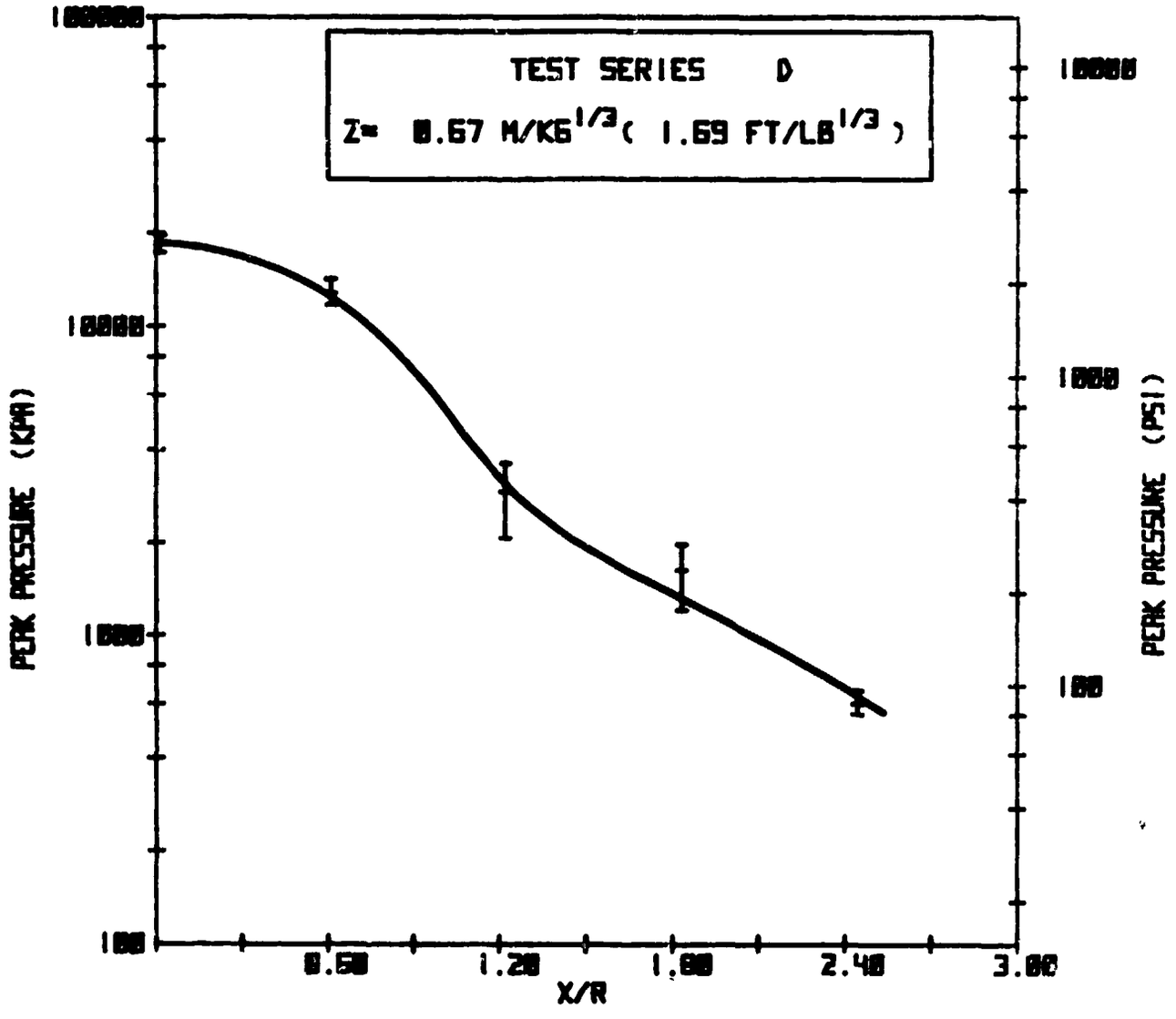

FIGURE 10. PEAK PRESSURE FOR SINGLE CHARGE TESTS (CONT'D)

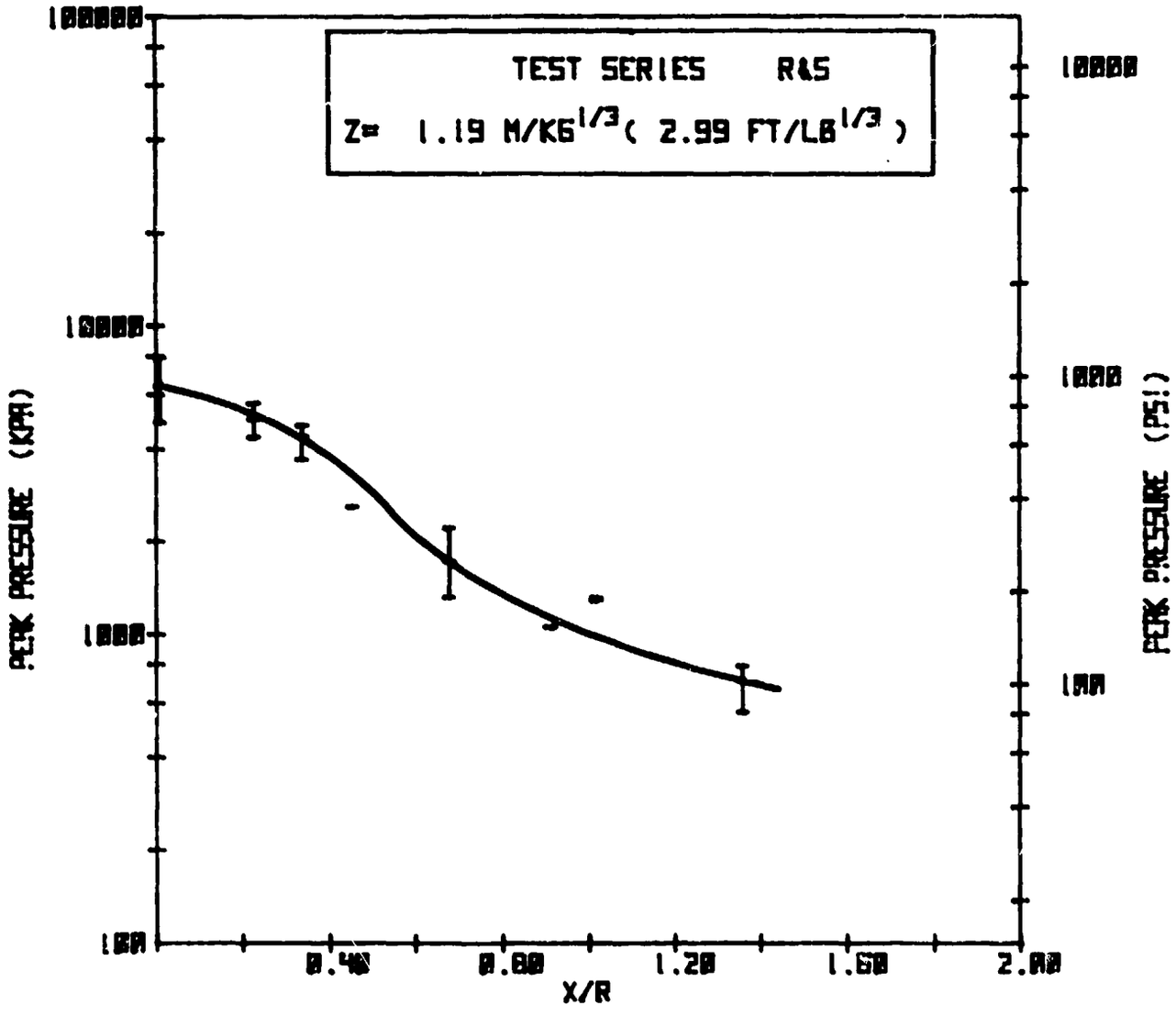

FIGURE 10. PEAK PRESSURE FOR SINGLE CHARGE TESTS (CONT'D)

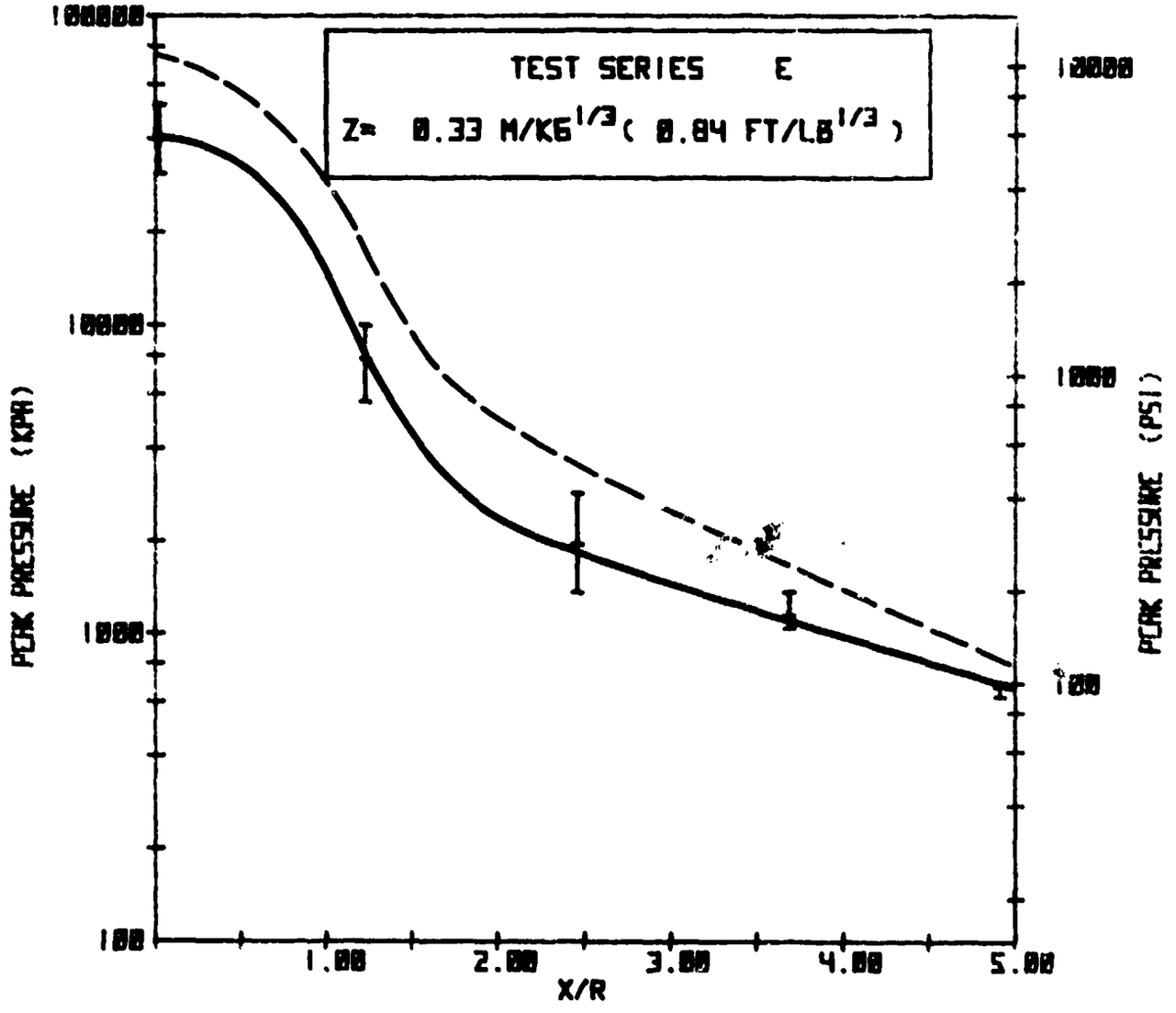

FIGURE 11. PEAK PRESSURE FOR GROUPED ARRAY TESTS

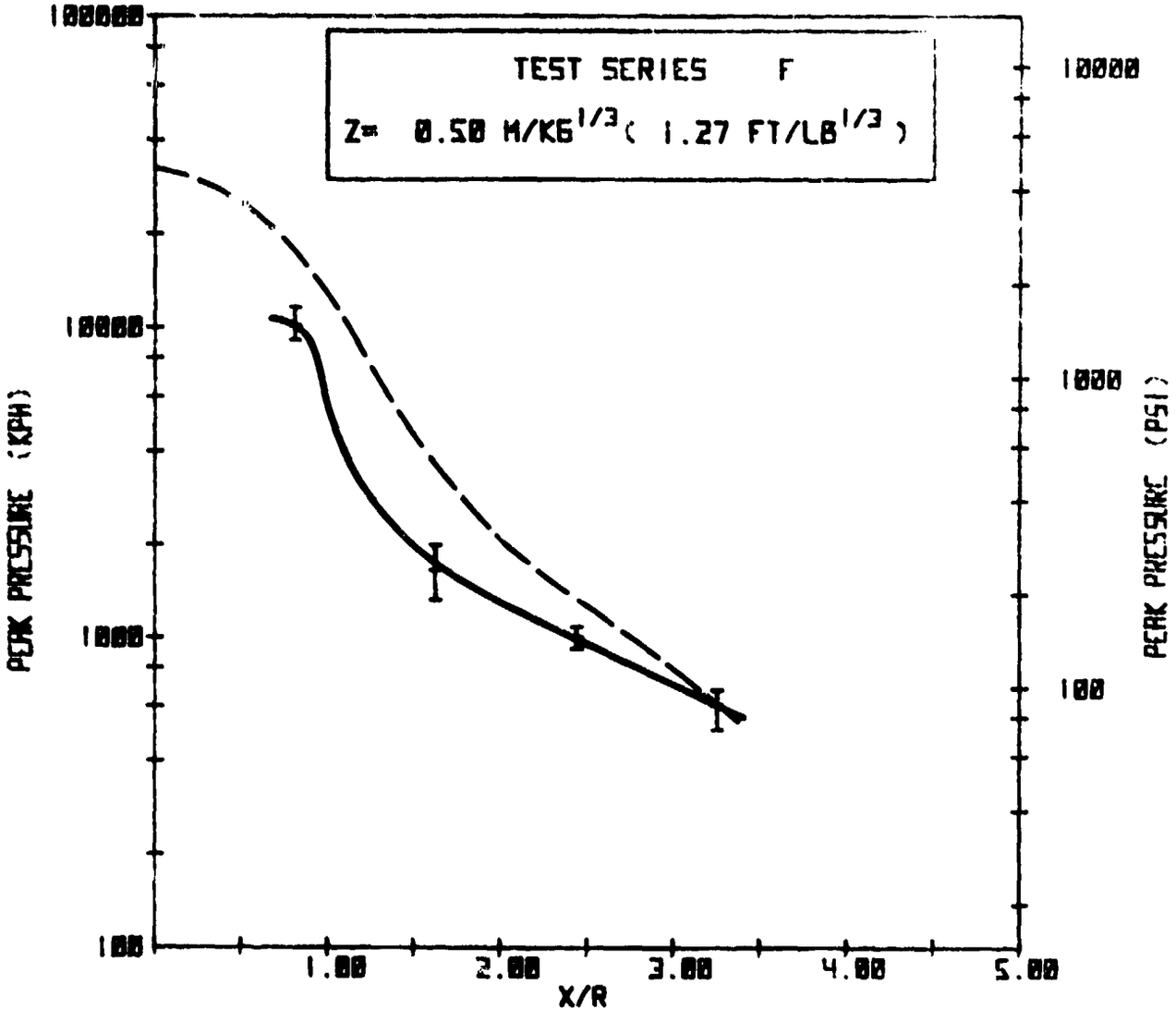

FIGURE 11. PEAK PRESSURE FOR GROUPED ARRAY TESTS (CONT'D)

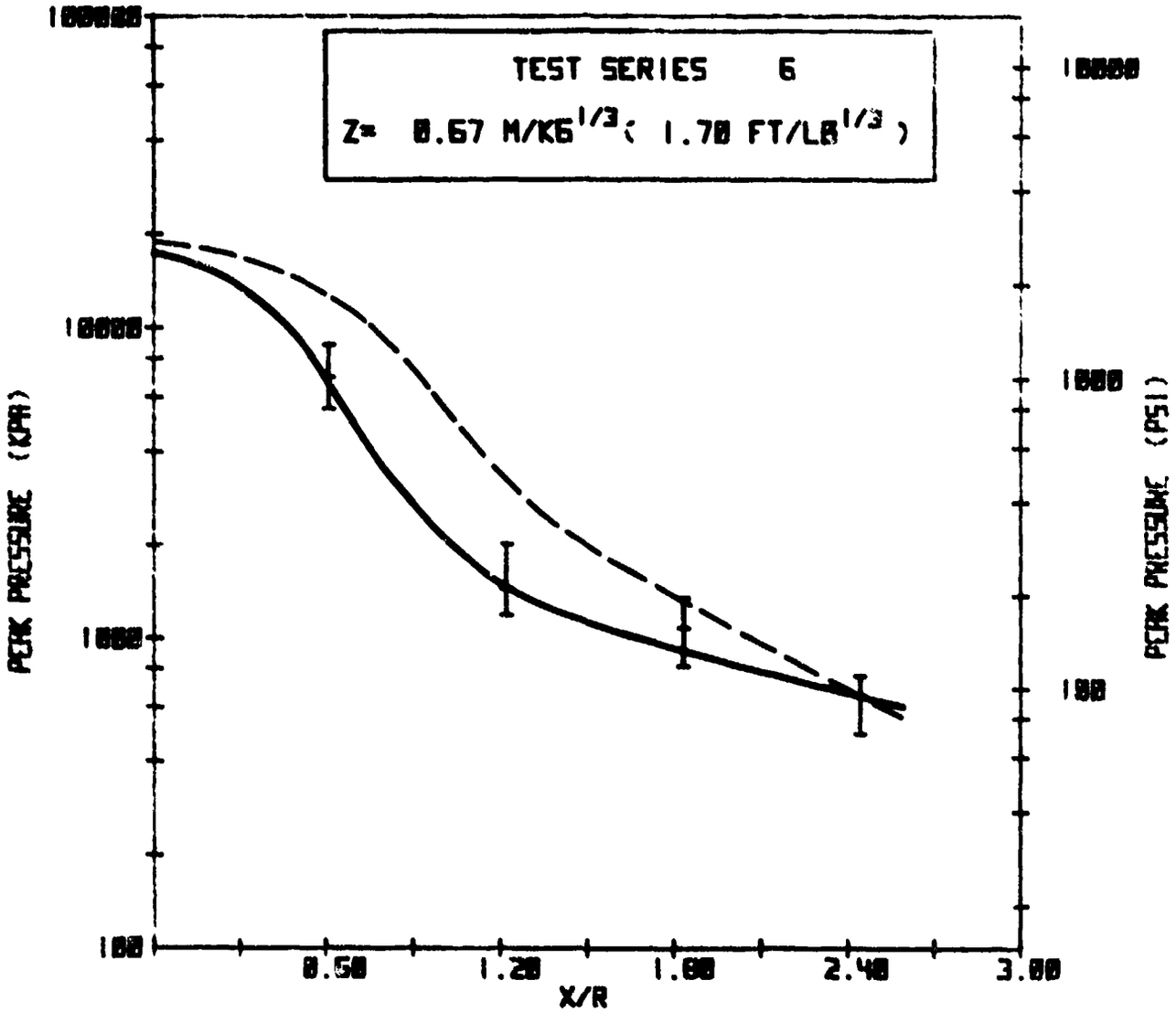

FIGURE 11. PEAK PRESSURE FOR GROUPED ARRAY TESTS (CONT'D)

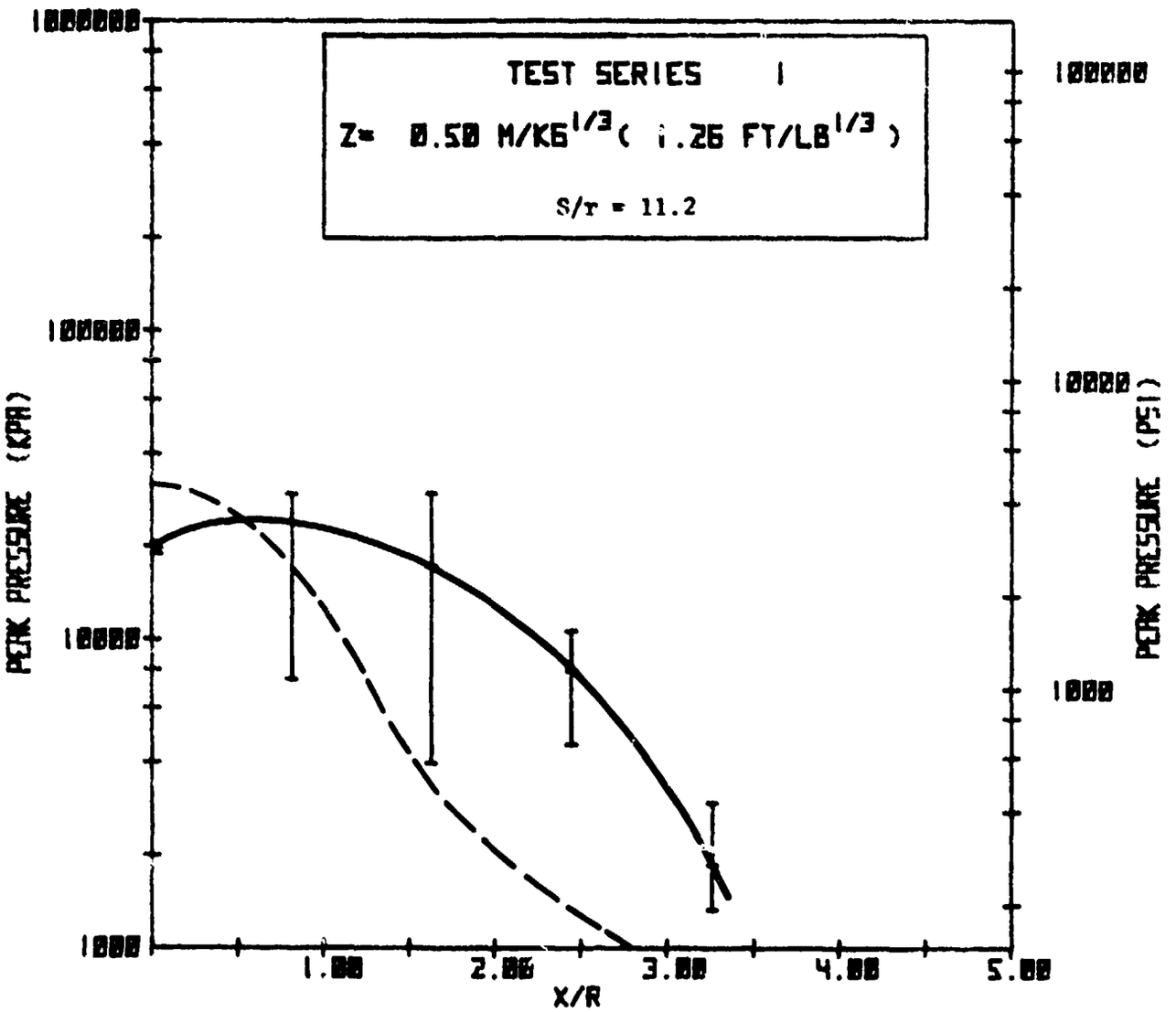

FIGURE 12. PEAK PRESSURE VARIATIONS DUE TO CHARGE STANDOFF FOR HORIZONTAL ARRAY TESTS

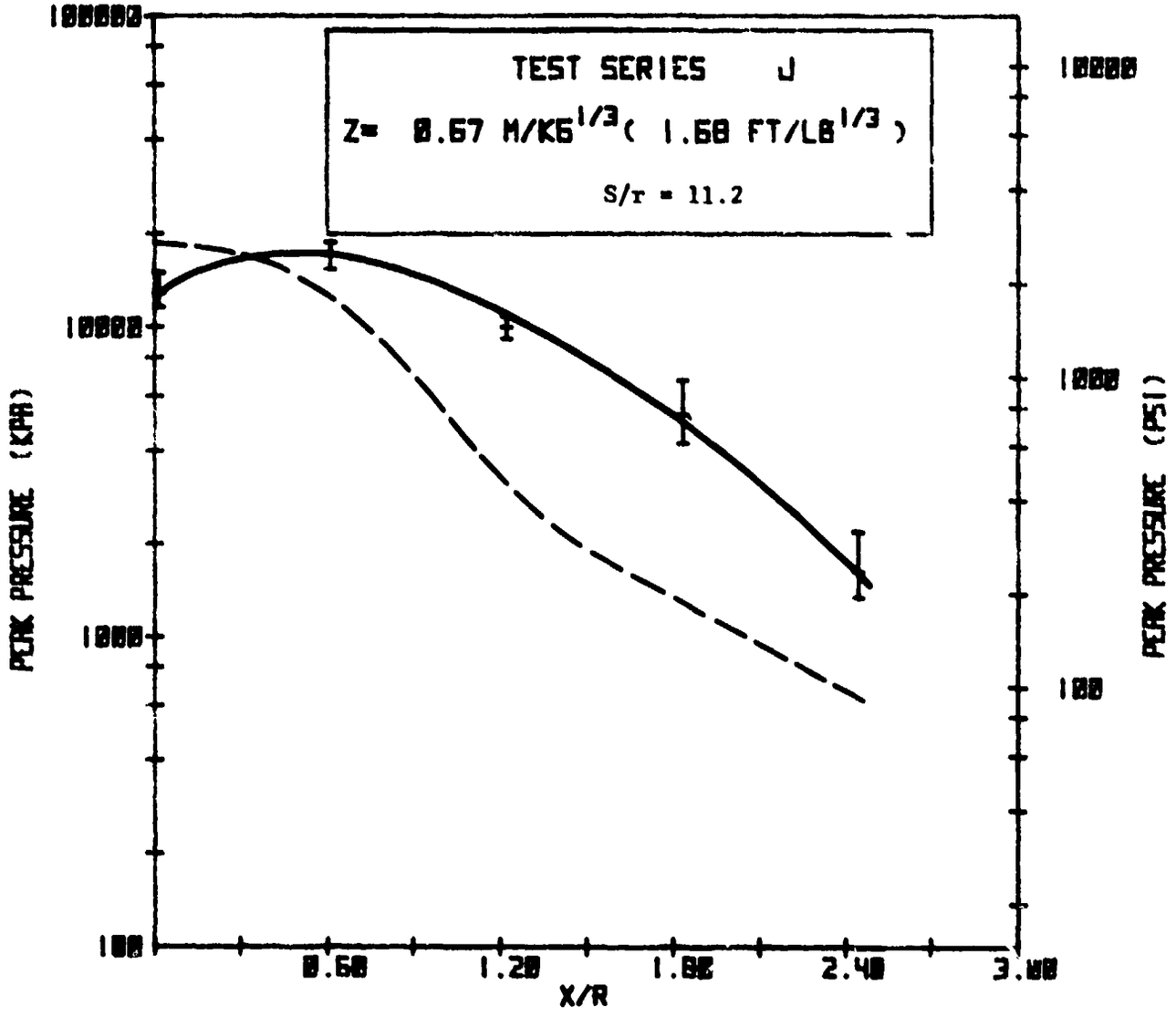

FIGURE 12. PEAK PRESSURE VARIATIONS DUE TO CHARGE STANDOFF FOR HORIZONTAL ARRAY TESTS (CONT'D)

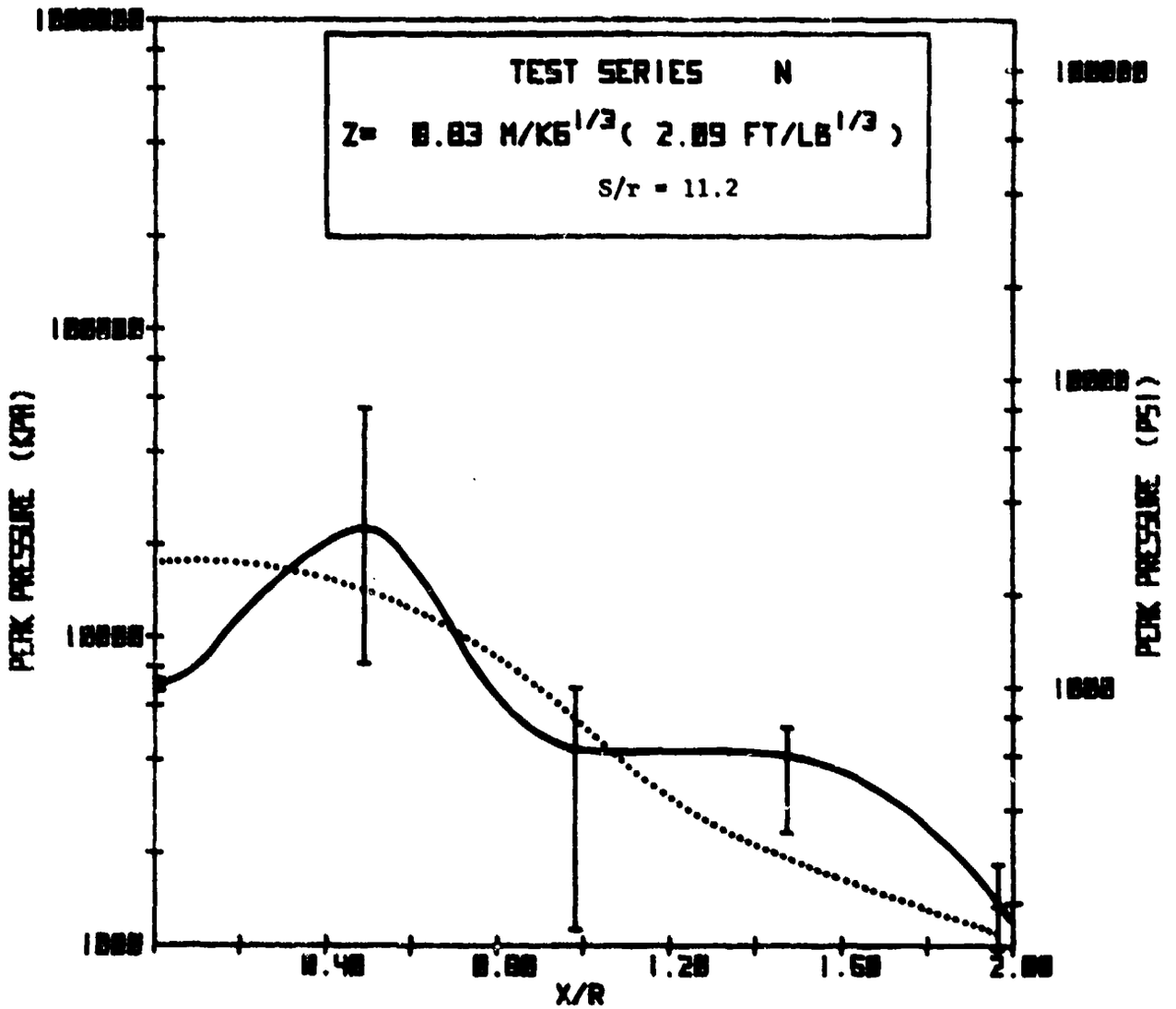

FIGURE 12. PEAK PRESSURE VARIATIONS DUE TO CHARGE STANDOFF FOR HORIZONTAL ARRAY TESTS (CONT'D)

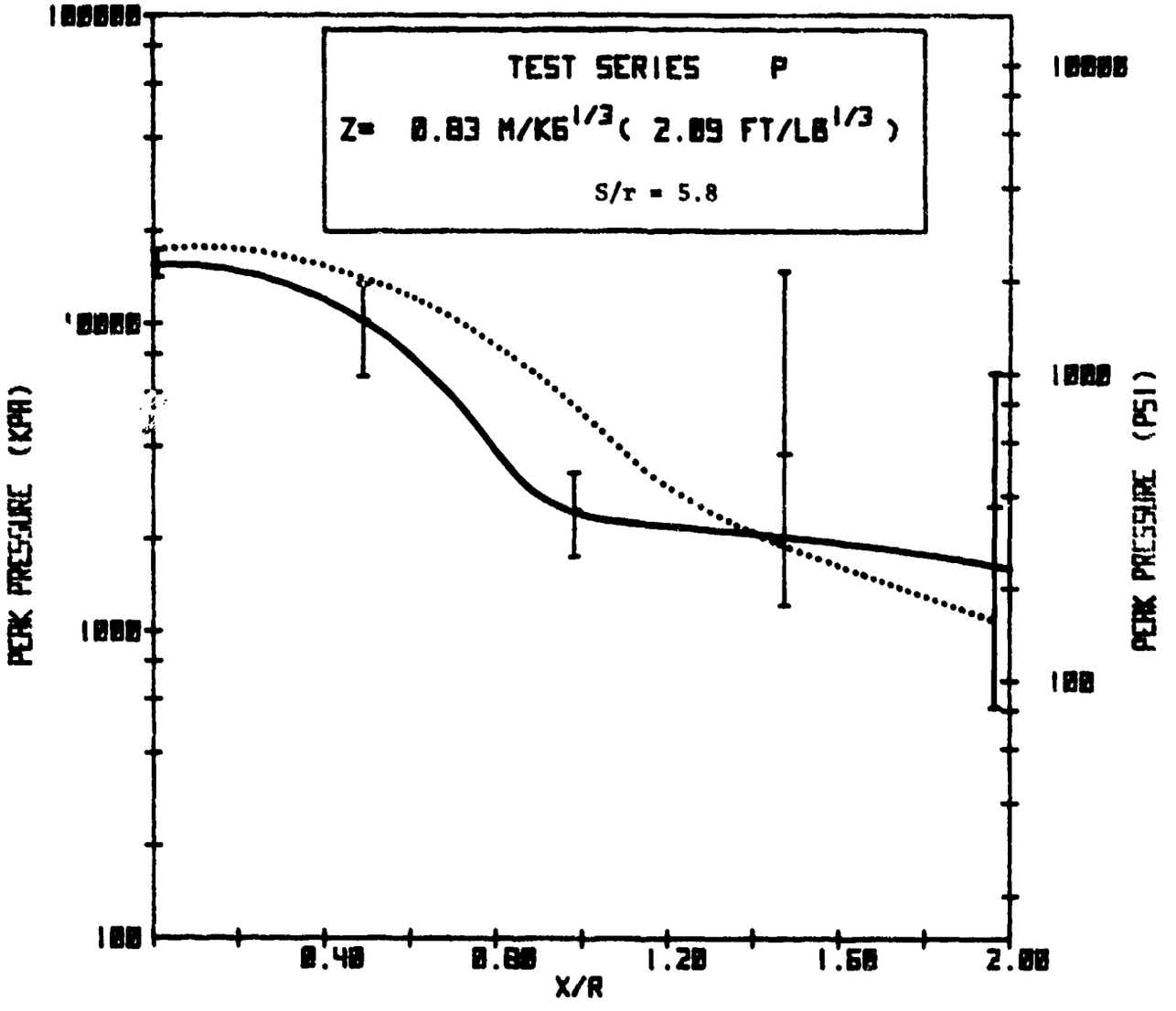

FIGURE 13. PEAK PRESSURE VARIATIONS DUE TO CHARGE SPACING FOR HORIZONTAL ARRAY TESTS

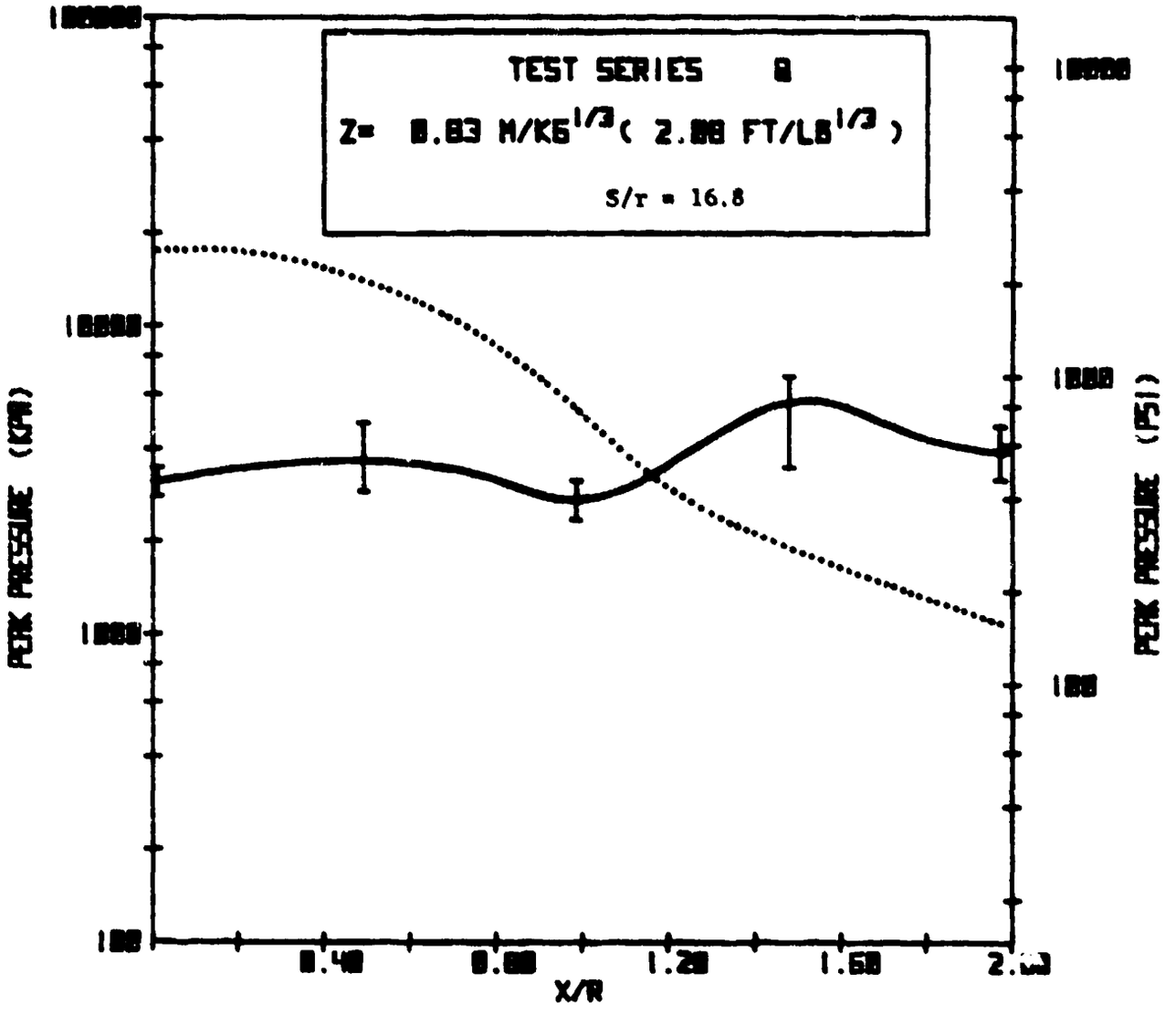

FIGURE 13. PEAK PRESSURE VARIATIONS DUE TO CHARGE SPACING FOR HORIZONTAL ARRAY TESTS (CONT'D)

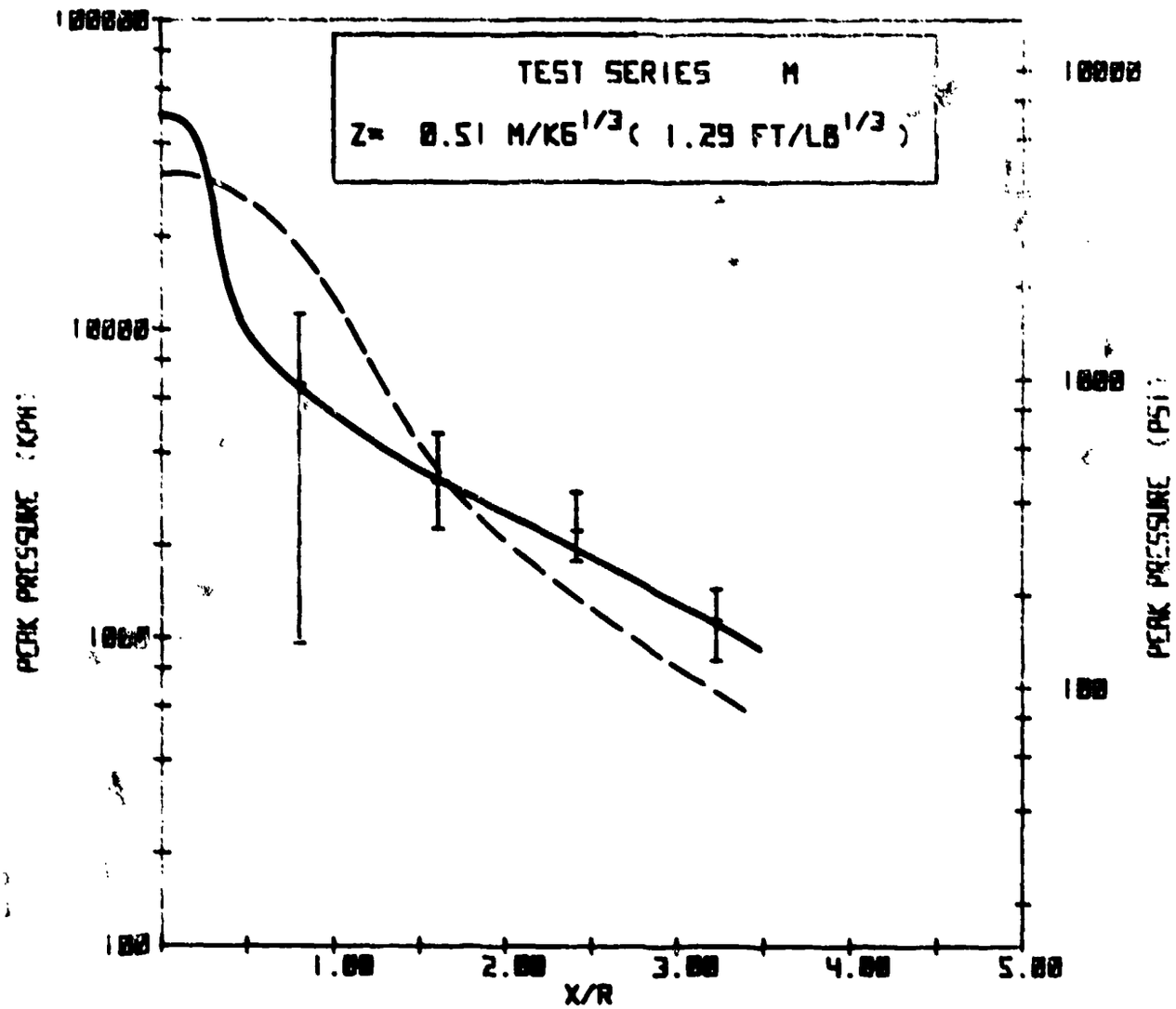

FIGURE 14. PEAK PRESSURE FOR VERTICAL ARRAY TESTS

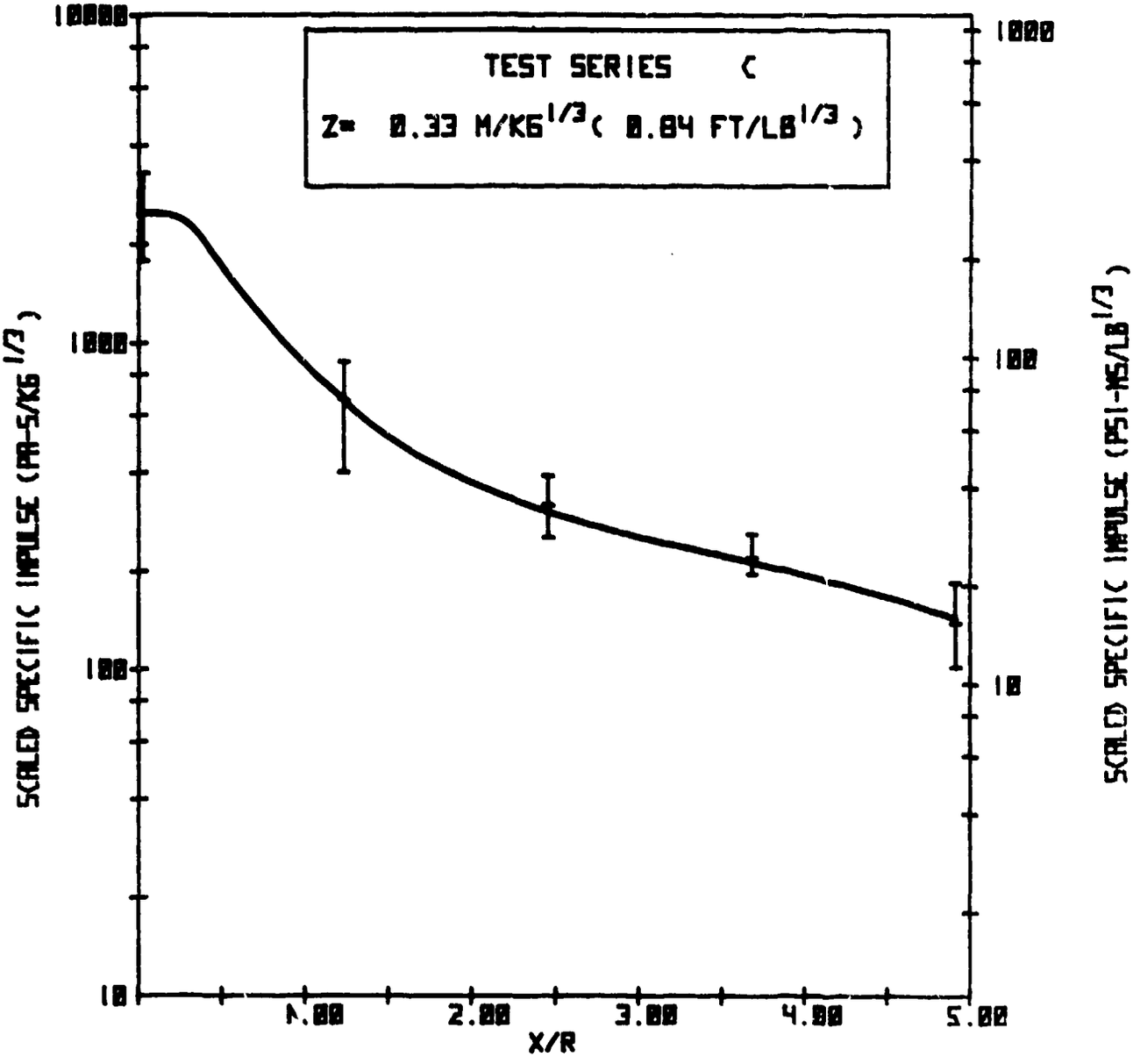

FIGURE 15. SPECIFIC IMPULSE FOR SINGLE CHARGE TESTS

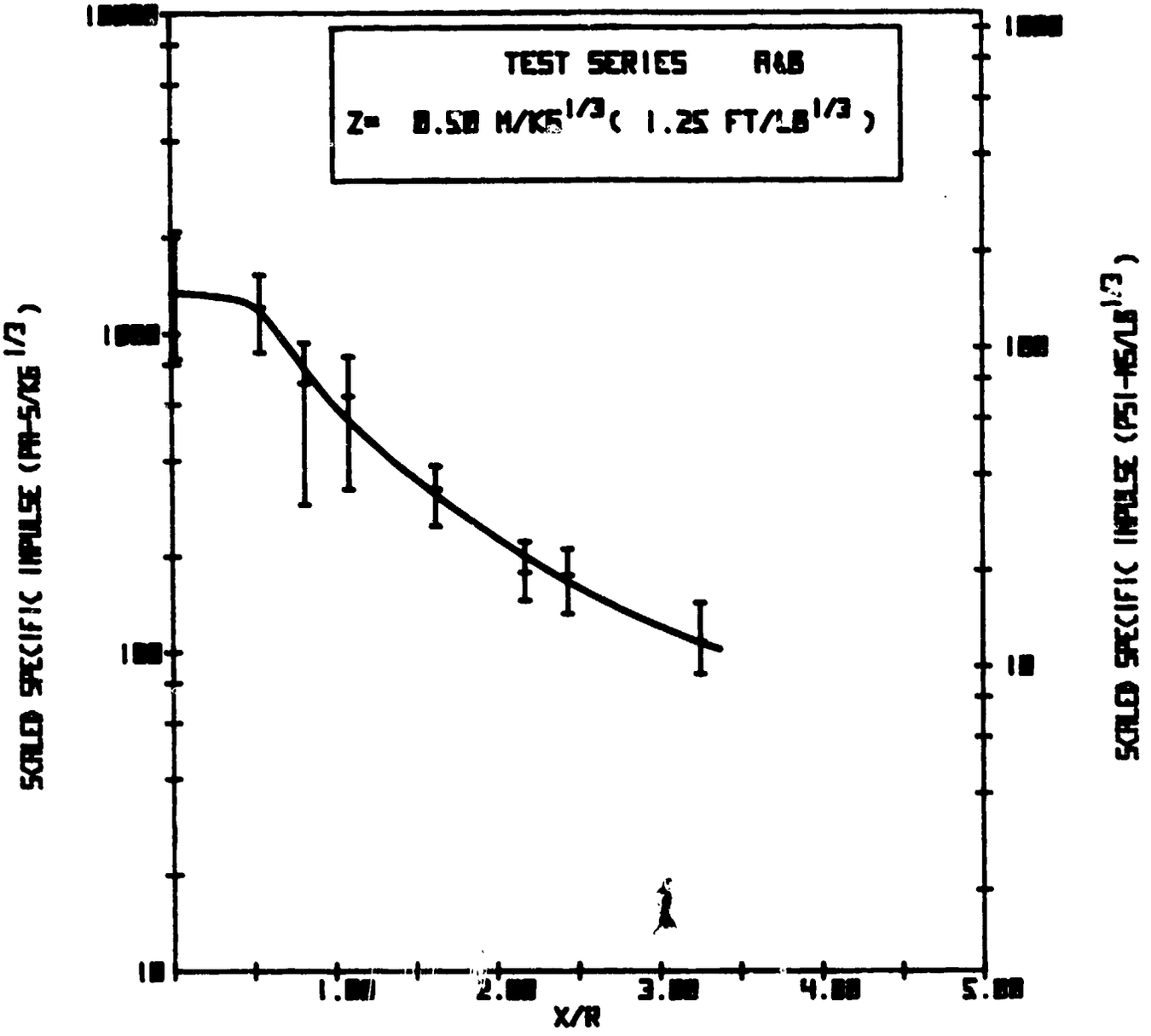

FIGURE 15. SPECIFIC IMPULSE FOR SINGLE CHARGE TESTS (CONT'D)

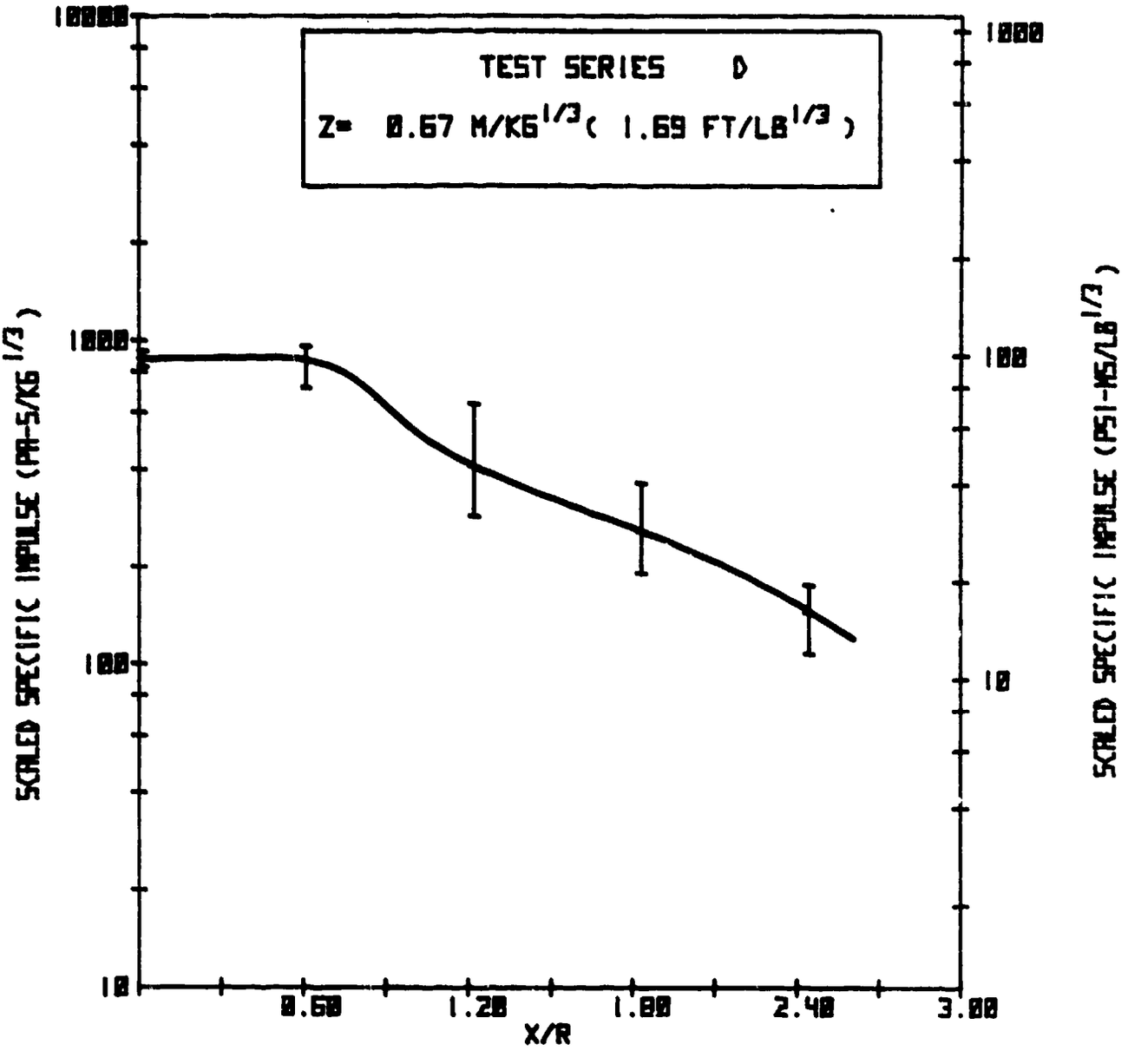

FIGURE 15. SPECIFIC IMPULSE FOR SINGLE CHARGE TESTS (CONT'D)

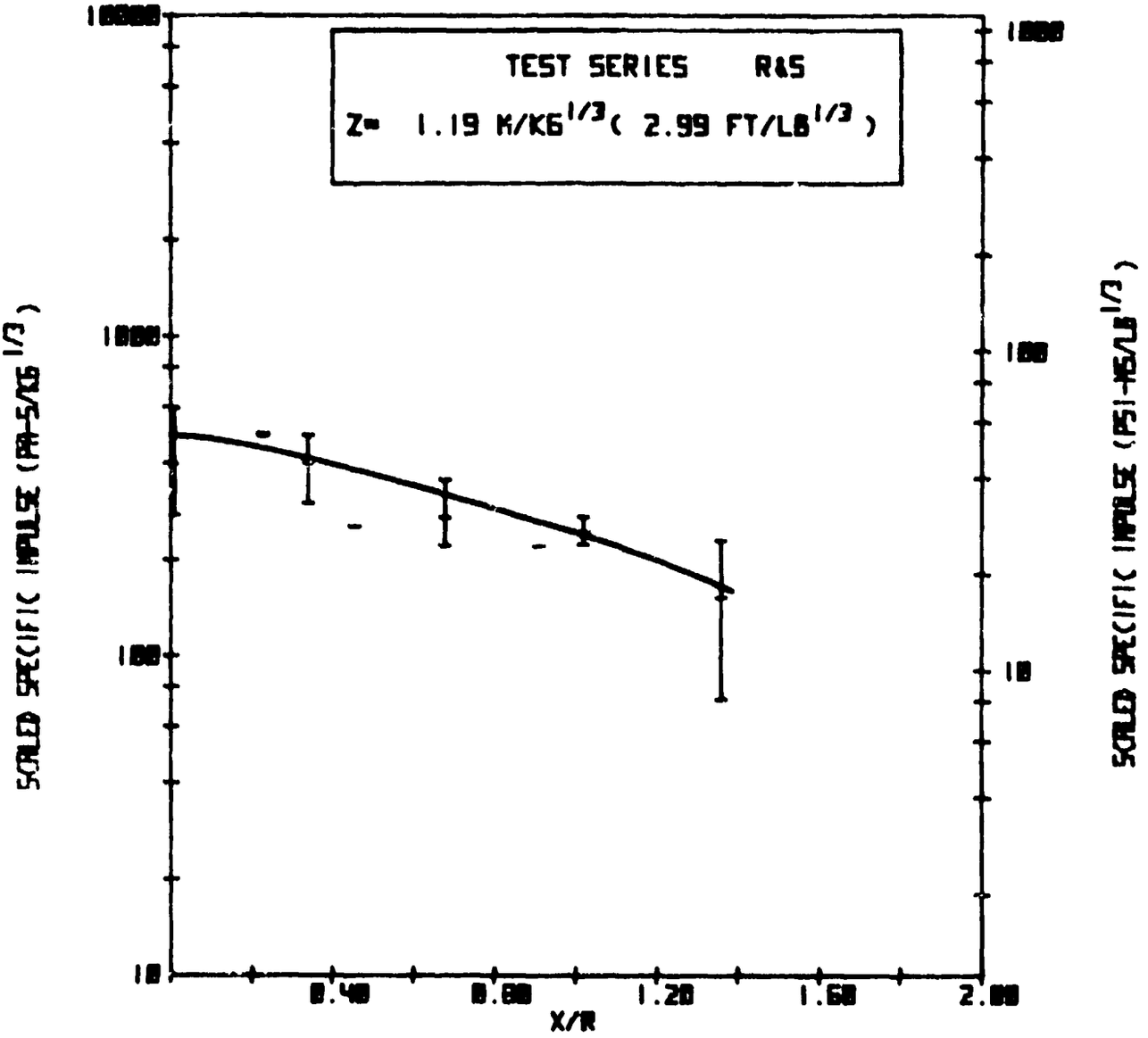

FIGURE 15. SPECIFIC IMPULSE FOR SINGLE CHARGE TESTS (CONT'D)

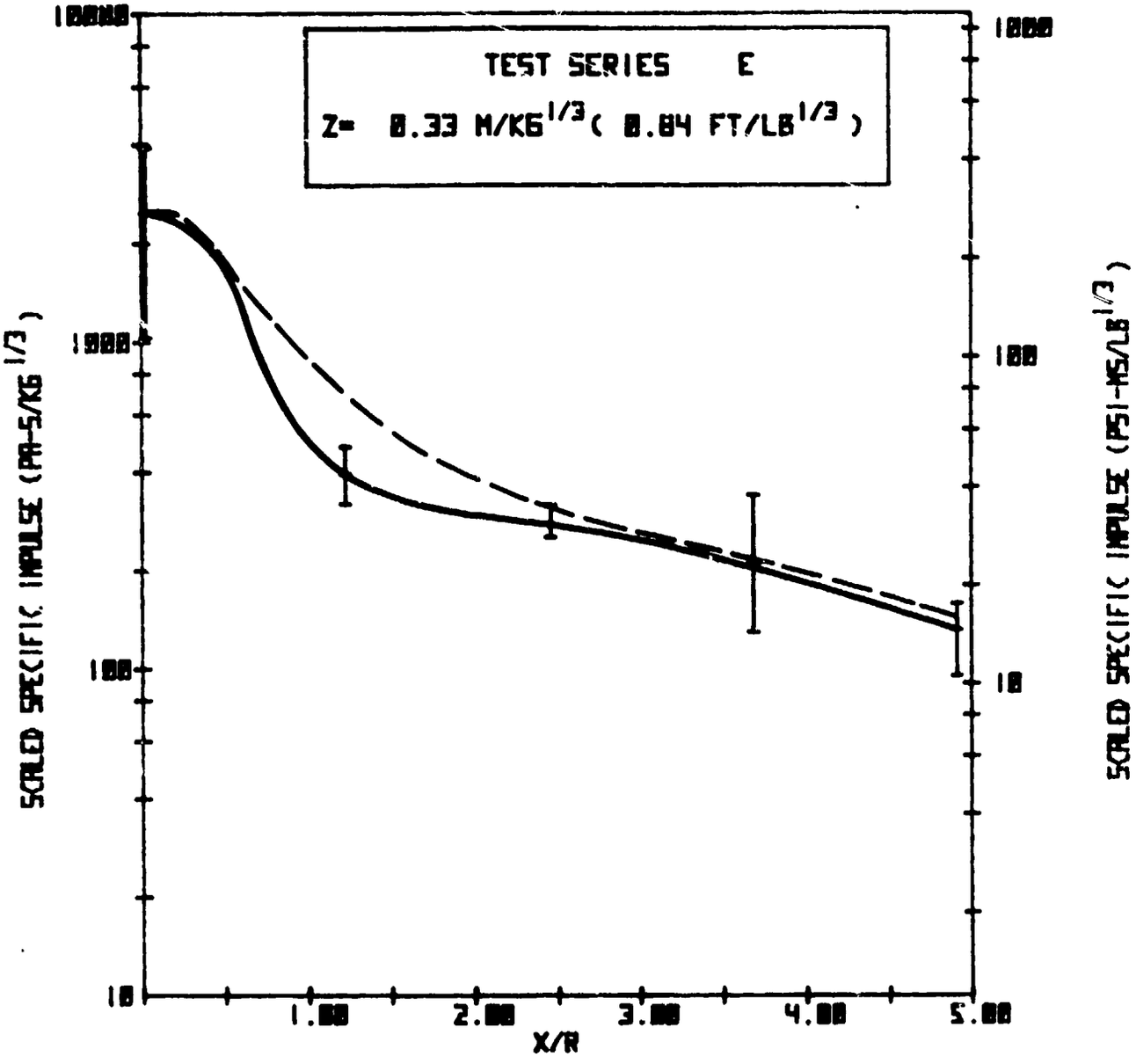

FIGURE 16. SPECIFIC IMPULSE FOR GROUPED ARRAY TESTS

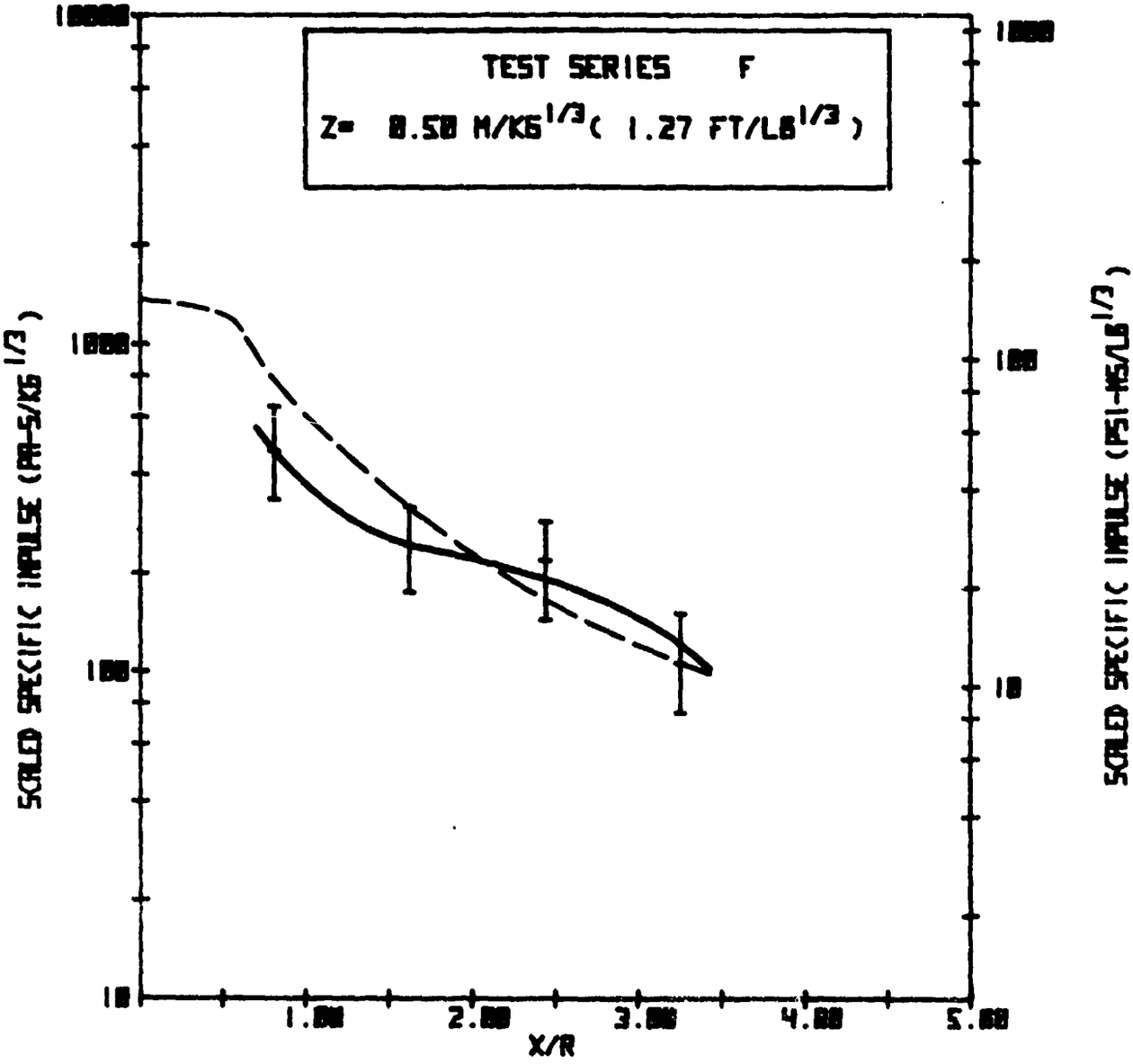

FIGURE 16. SPECIFIC IMPULSE FOR GROUPED ARRAY TESTS (CONT'D)

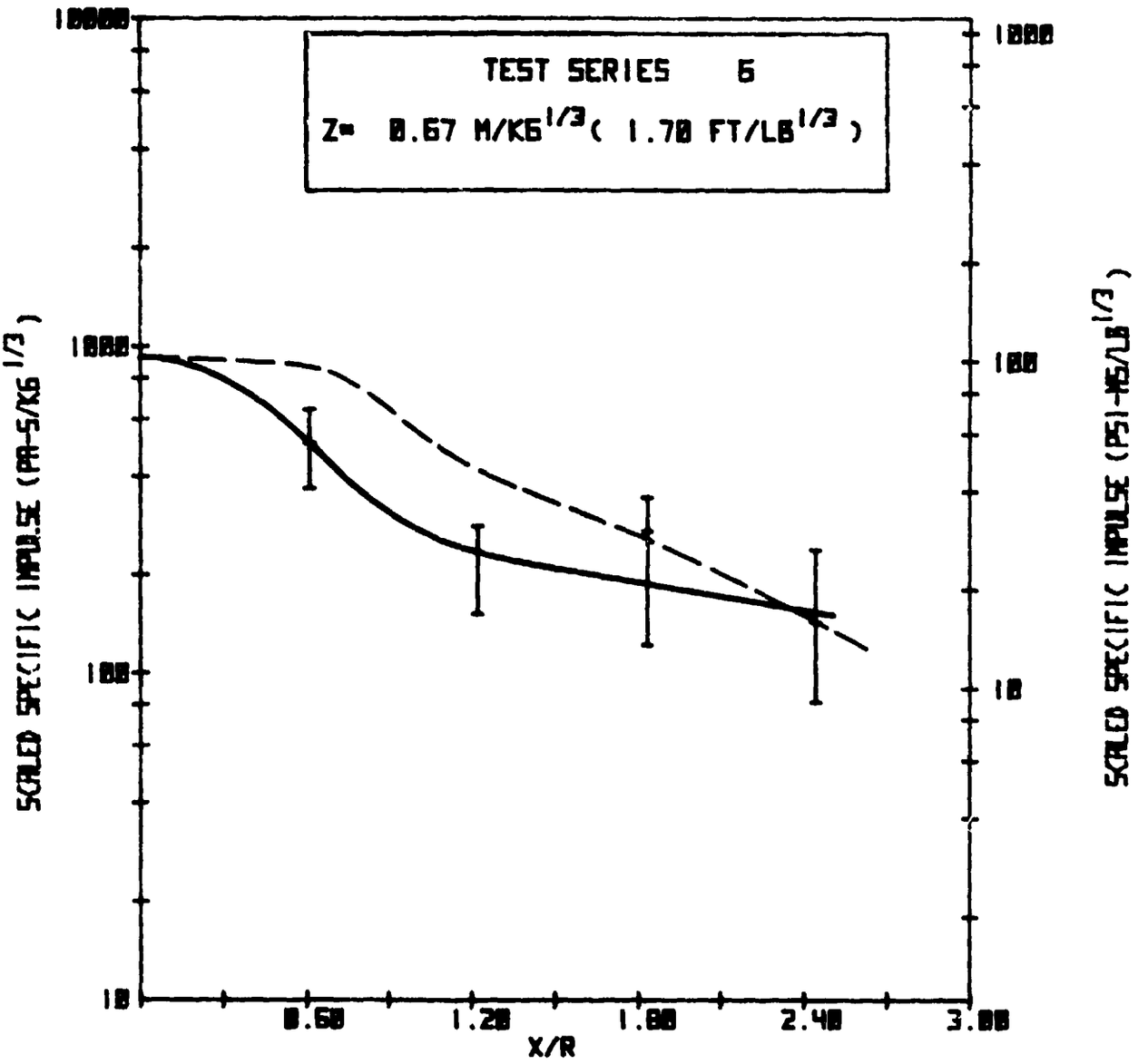

FIGURE 16. SPECIFIC IMPULSE FOR GROUPED ARRAY TESTS (CONT'D)

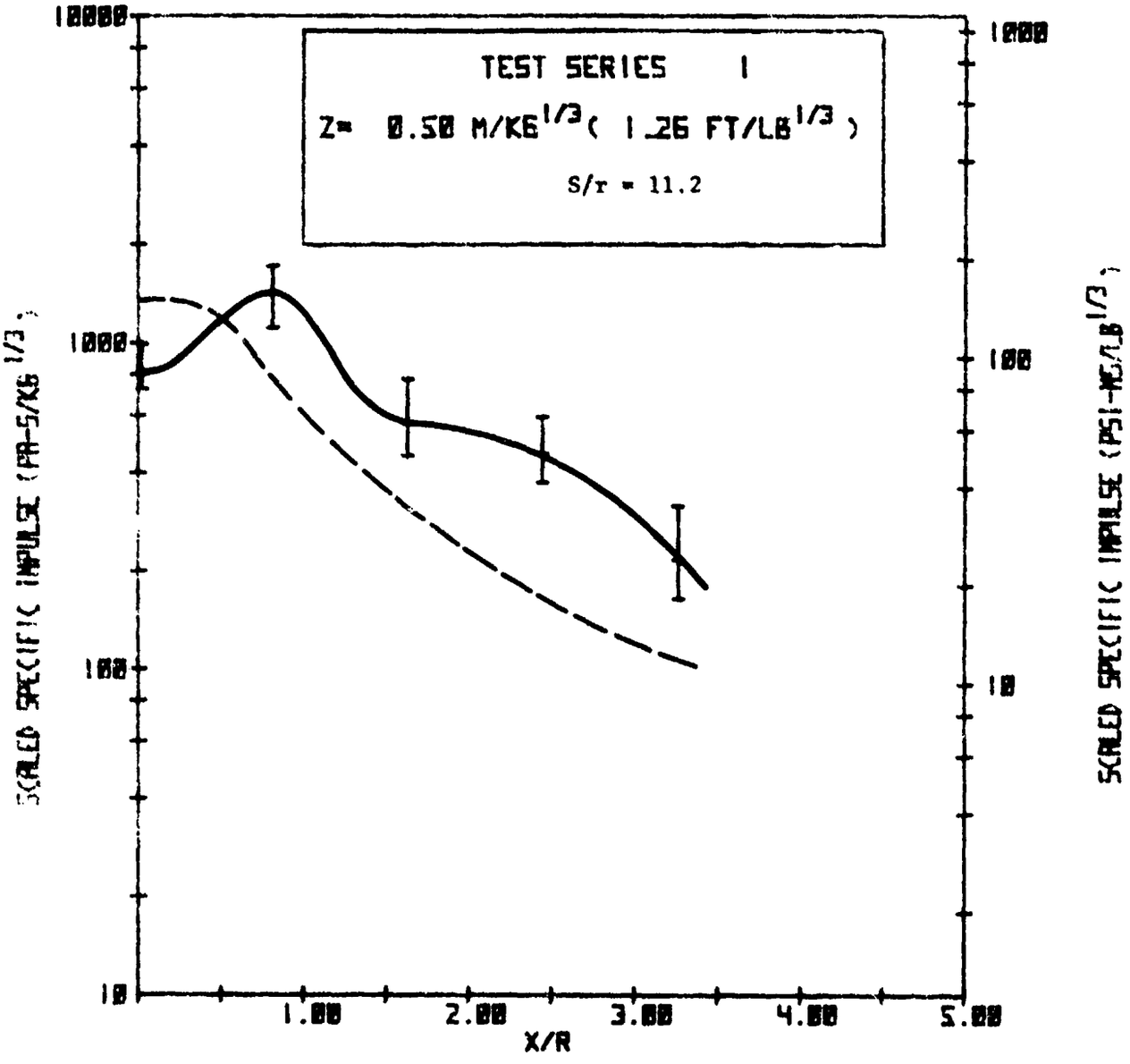

FIGURE 17. SPECIFIC IMPULSE VARIATIONS DUE TO CHARGE STANDOFF FOR HORIZONTAL ARRAY TESTS

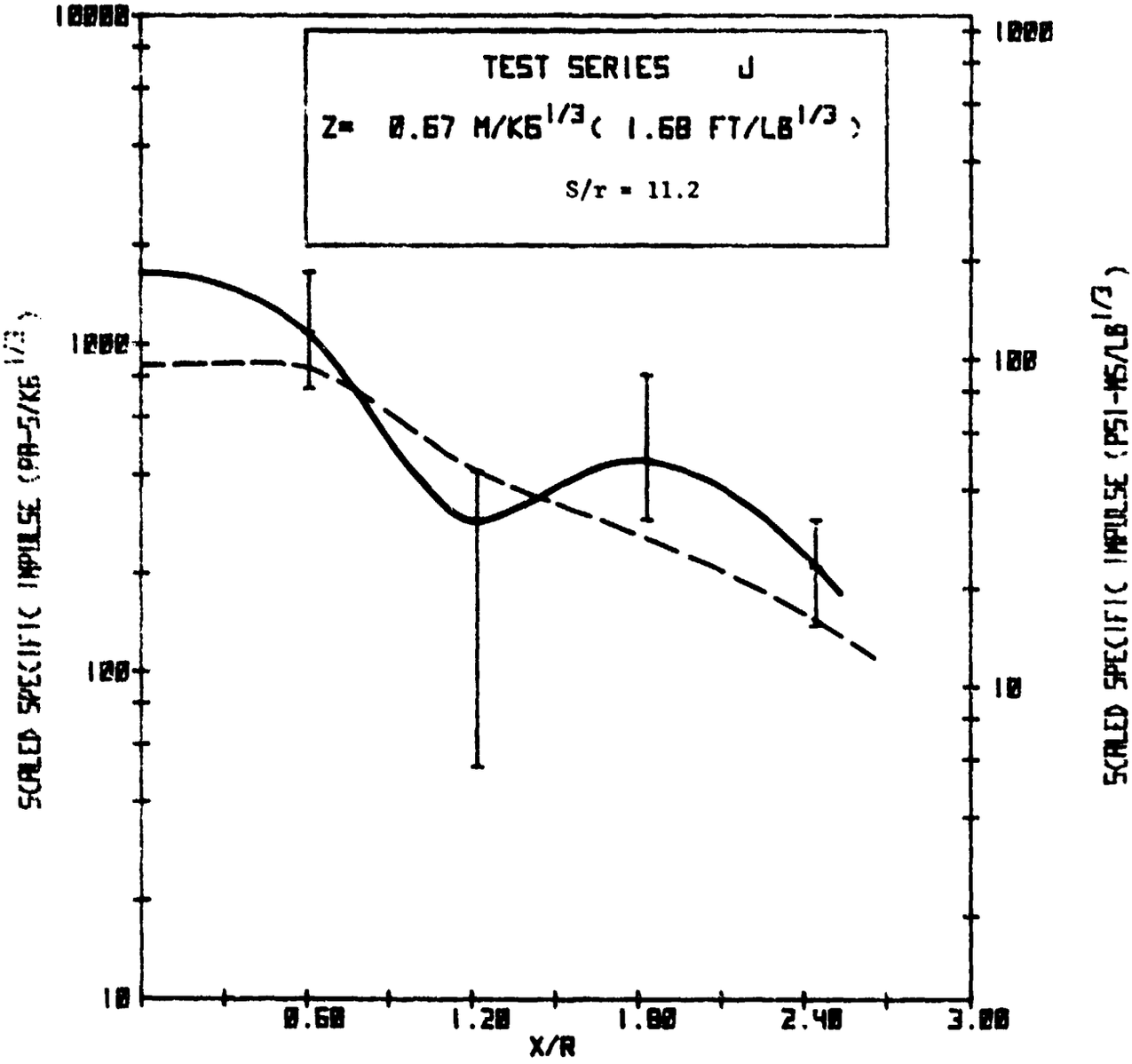

FIGURE 17. SPECIFIC IMPULSE VARIATIONS DUE TO CHARGE STANDOFF FOR HORIZONTAL ARRAY TESTS (CONT'D)

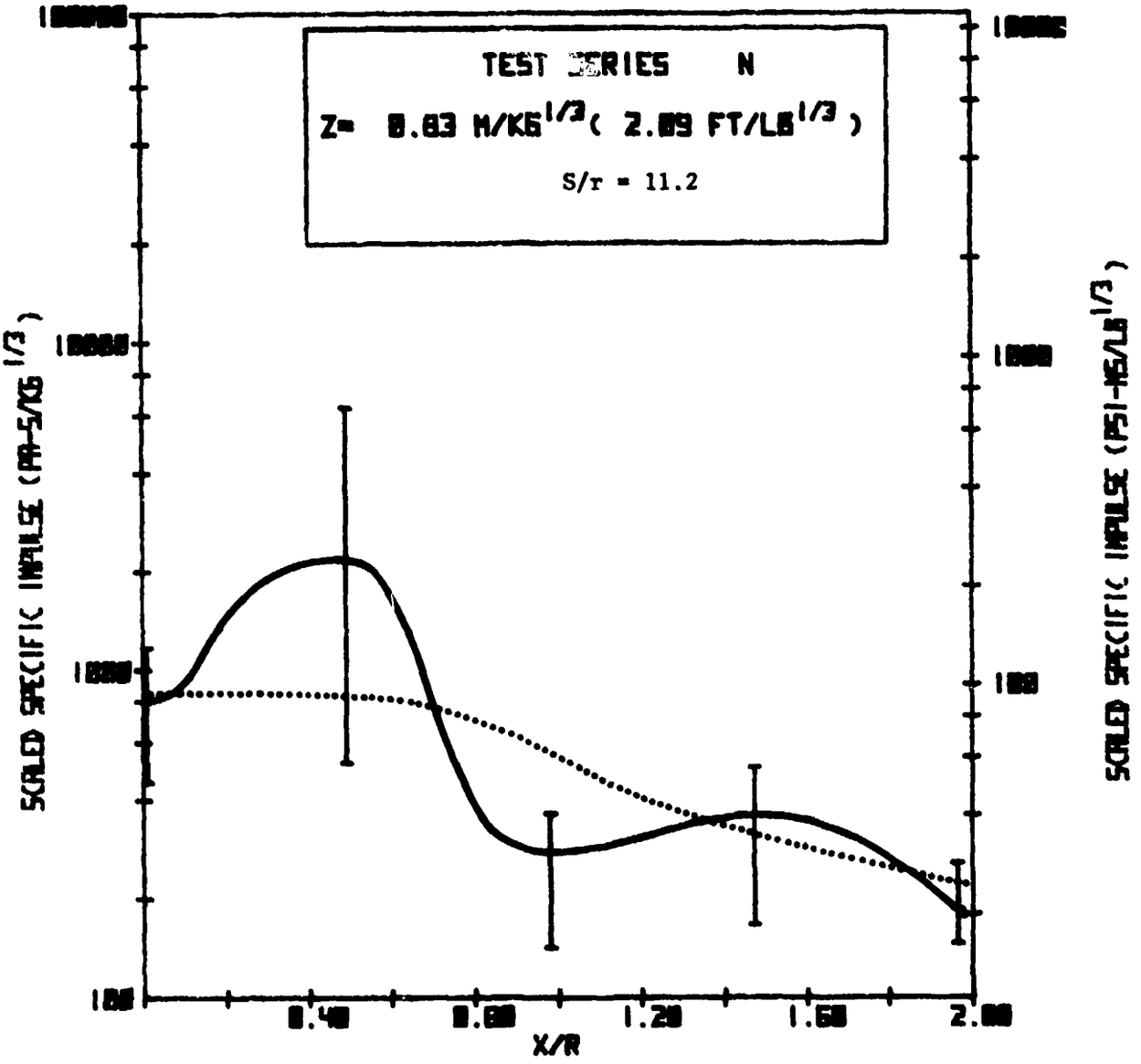

FIGURE 17. SPECIFIC IMPULSE VARIATIONS DUE TO CHARGE STANDOFF FOR HORIZONTAL ARRAY TESTS(CONT'D)

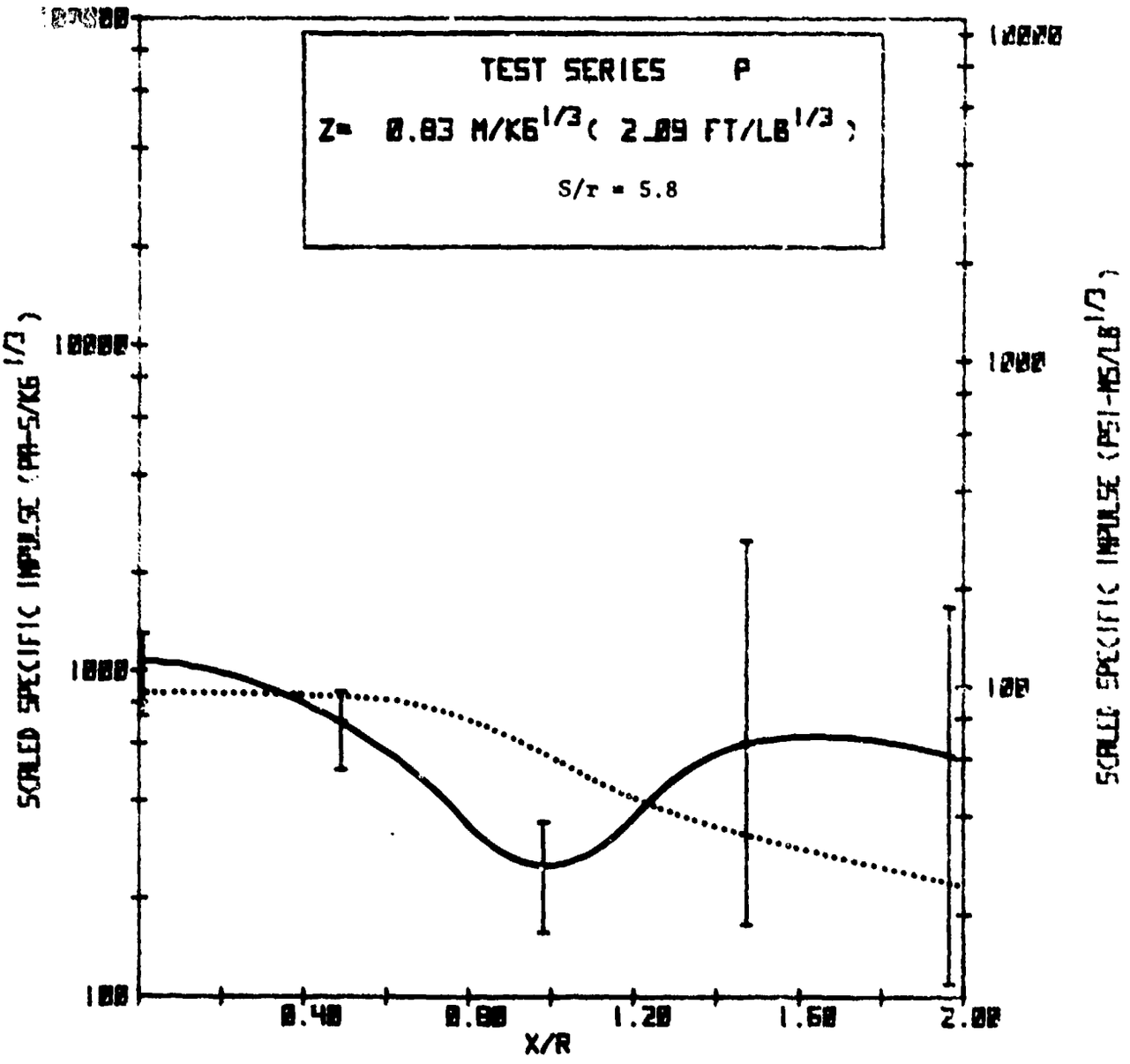

FIGURE 18. SPECIFIC IMPULSE VARIATIONS DUE TO CHARGE SPACING FOR HORIZONTAL ARRAY TESTS (CONT'D)

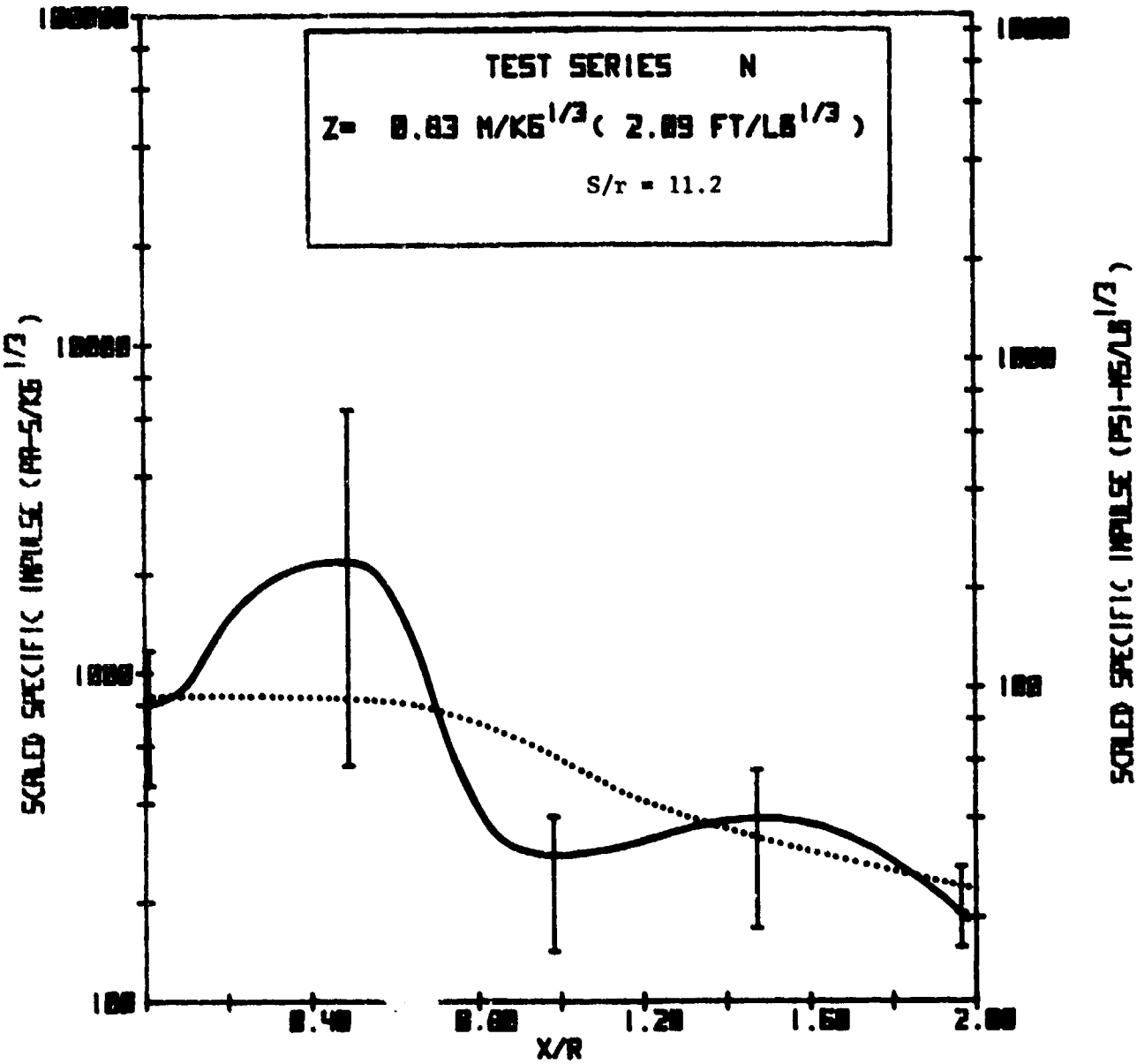

FIGURE 18. SPECIFIC IMPULSE VARIATIONS DUE TO CHARGE SPACING FOR HORIZONTAL ARRAY TESTS (CONT'D)

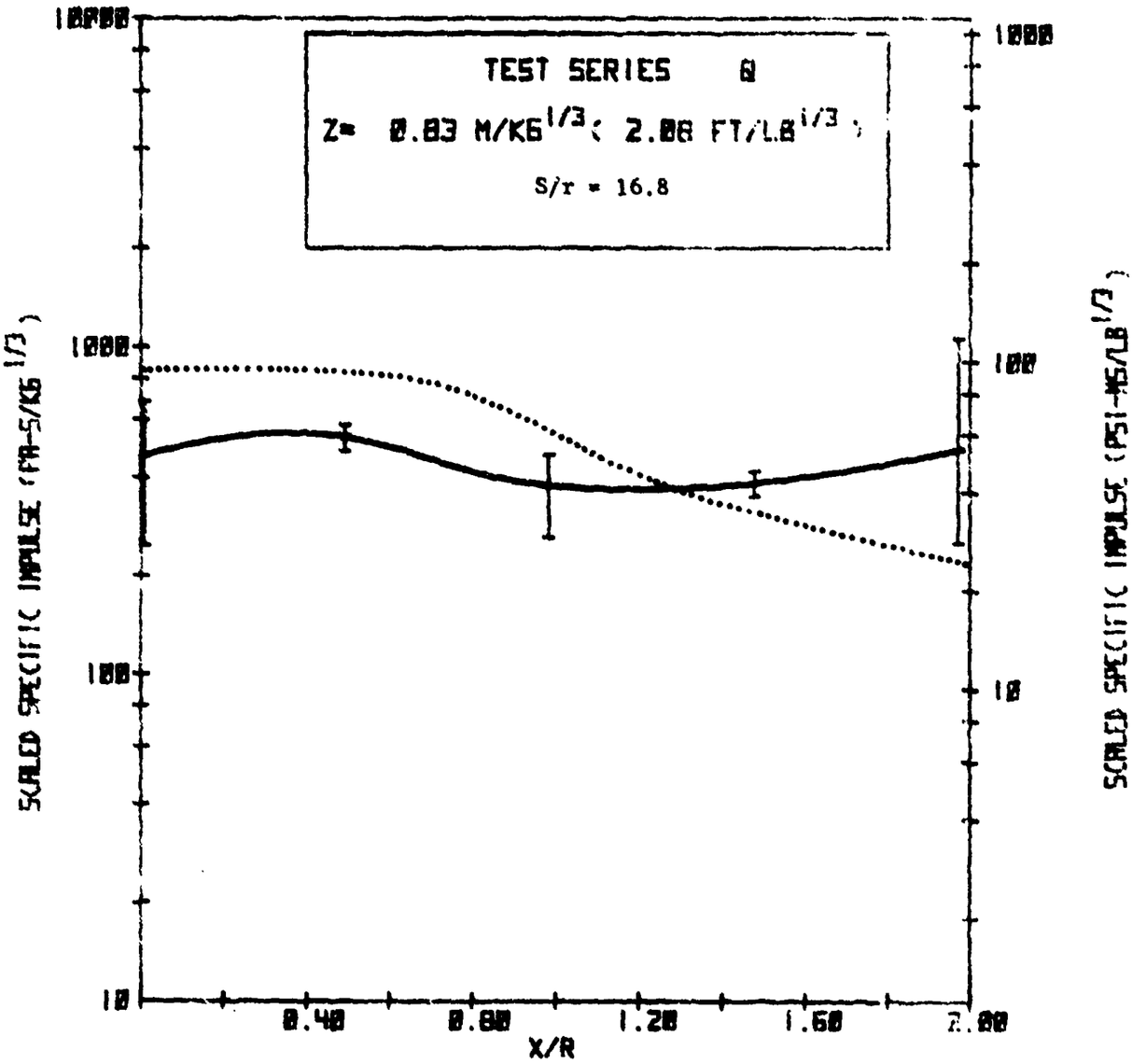

FIGURE 18. SPECIFIC IMPULSE VARIATIONS DUE TO CHARGE SPACING FOR HORIZONTAL ARRAY TESTS (CONT'D)

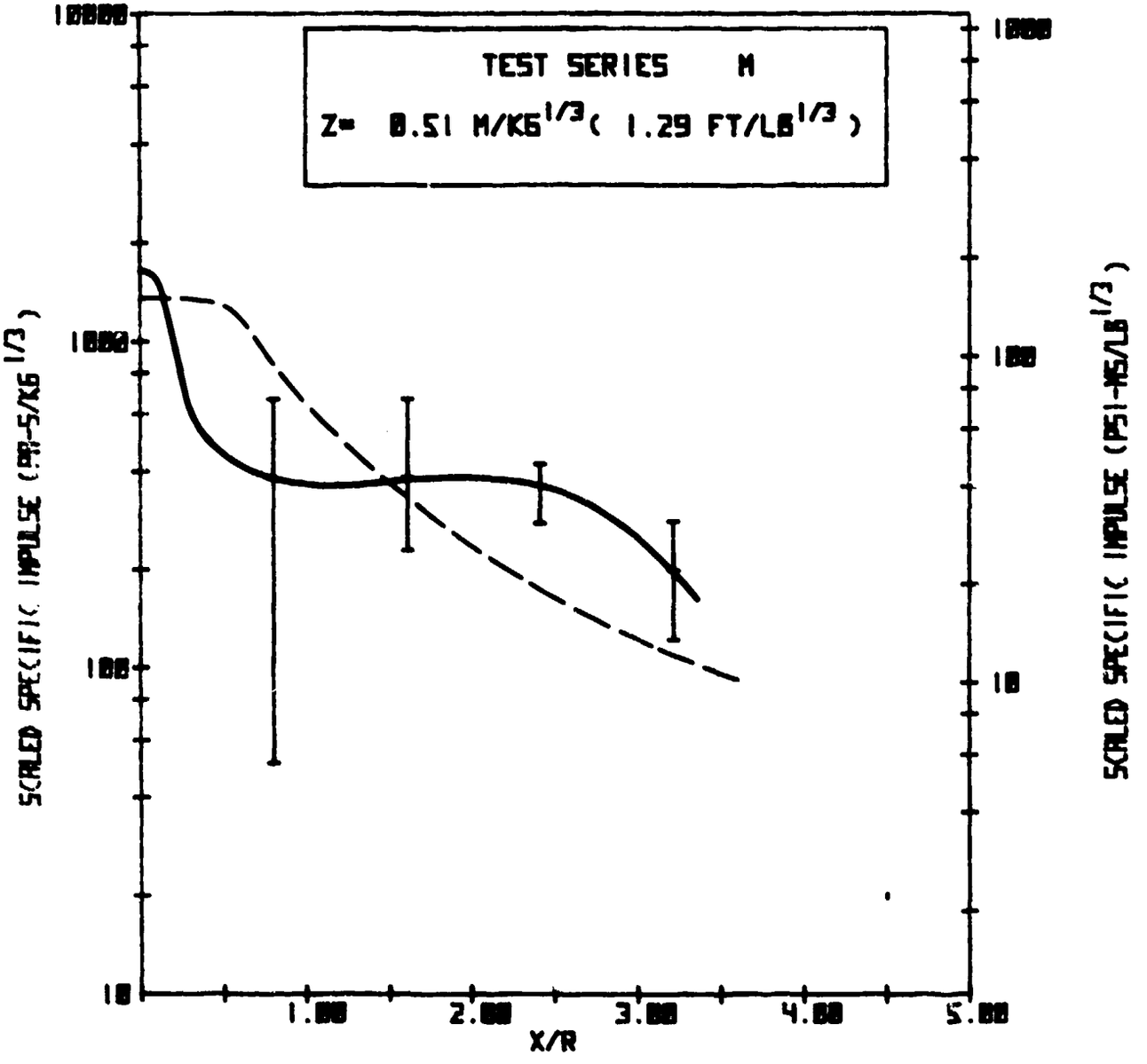

FIGURE 19. SPECIFIC IMPULSE FOR VERTICAL ARRAY TESTS

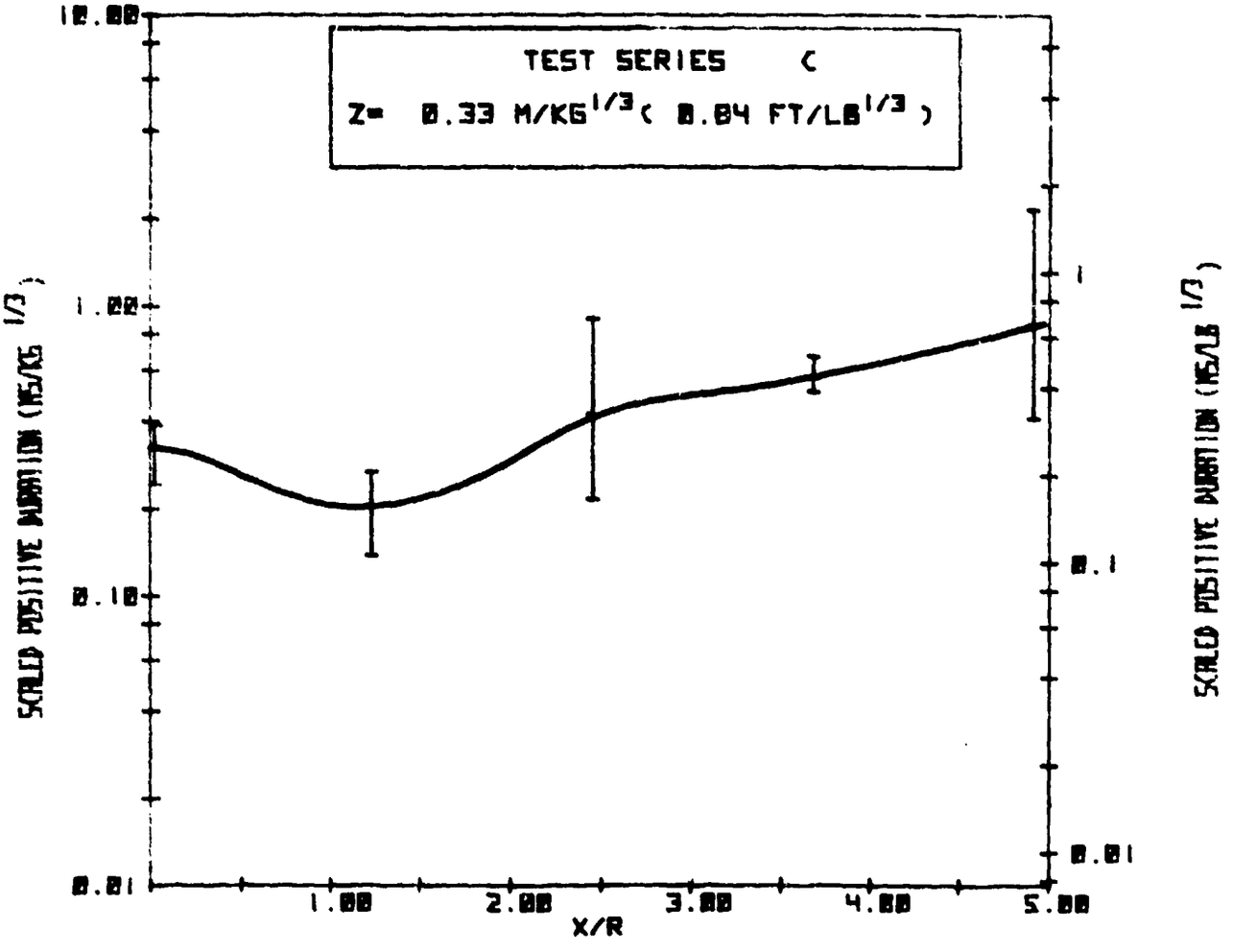

FIGURE 20. POSITIVE DURATION FOR SINGLE CHARGE TESTS

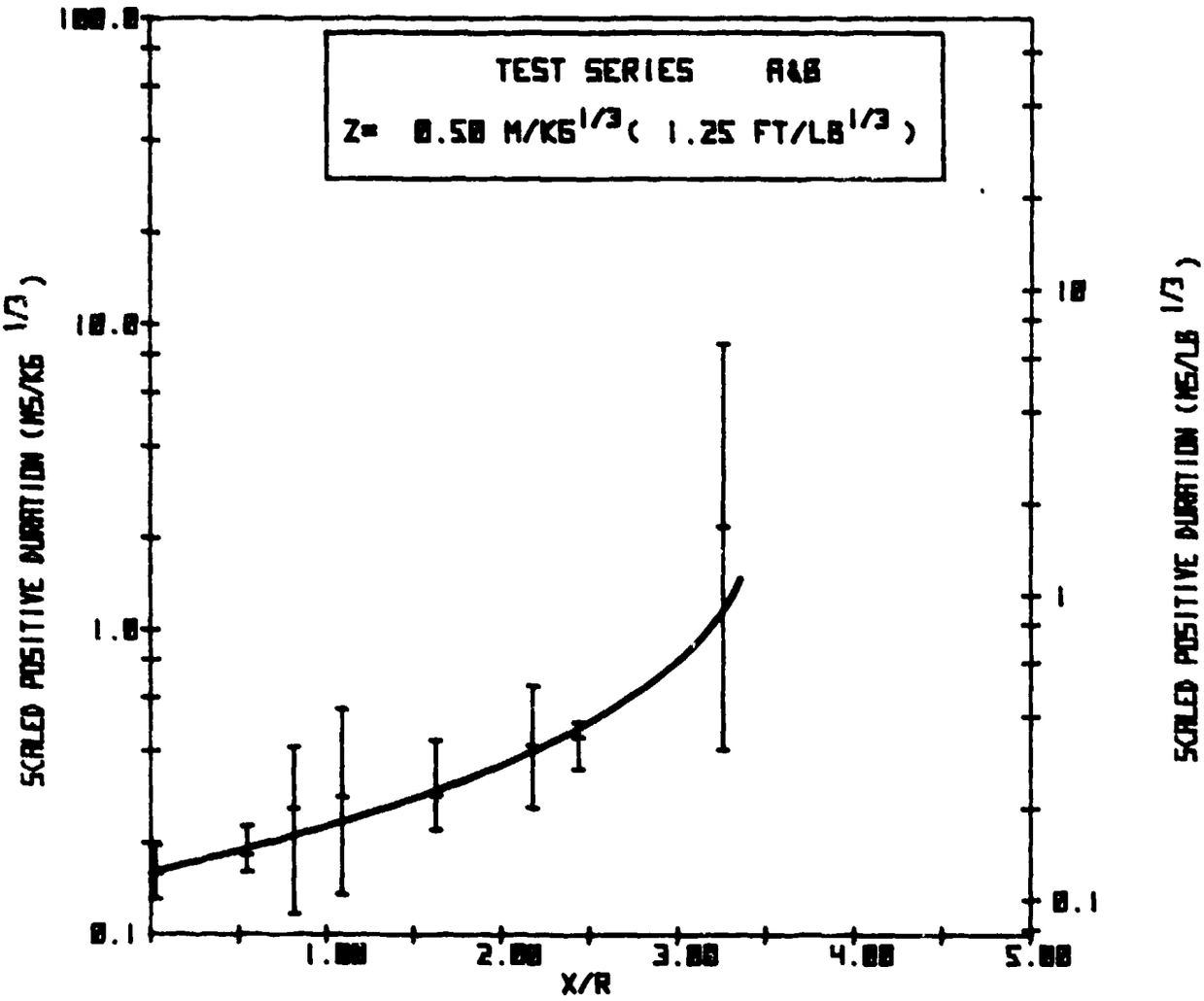

FIGURE 20. POSITIVE DURATION FOR SINGLE CHARGE TESTS (CONT'D)

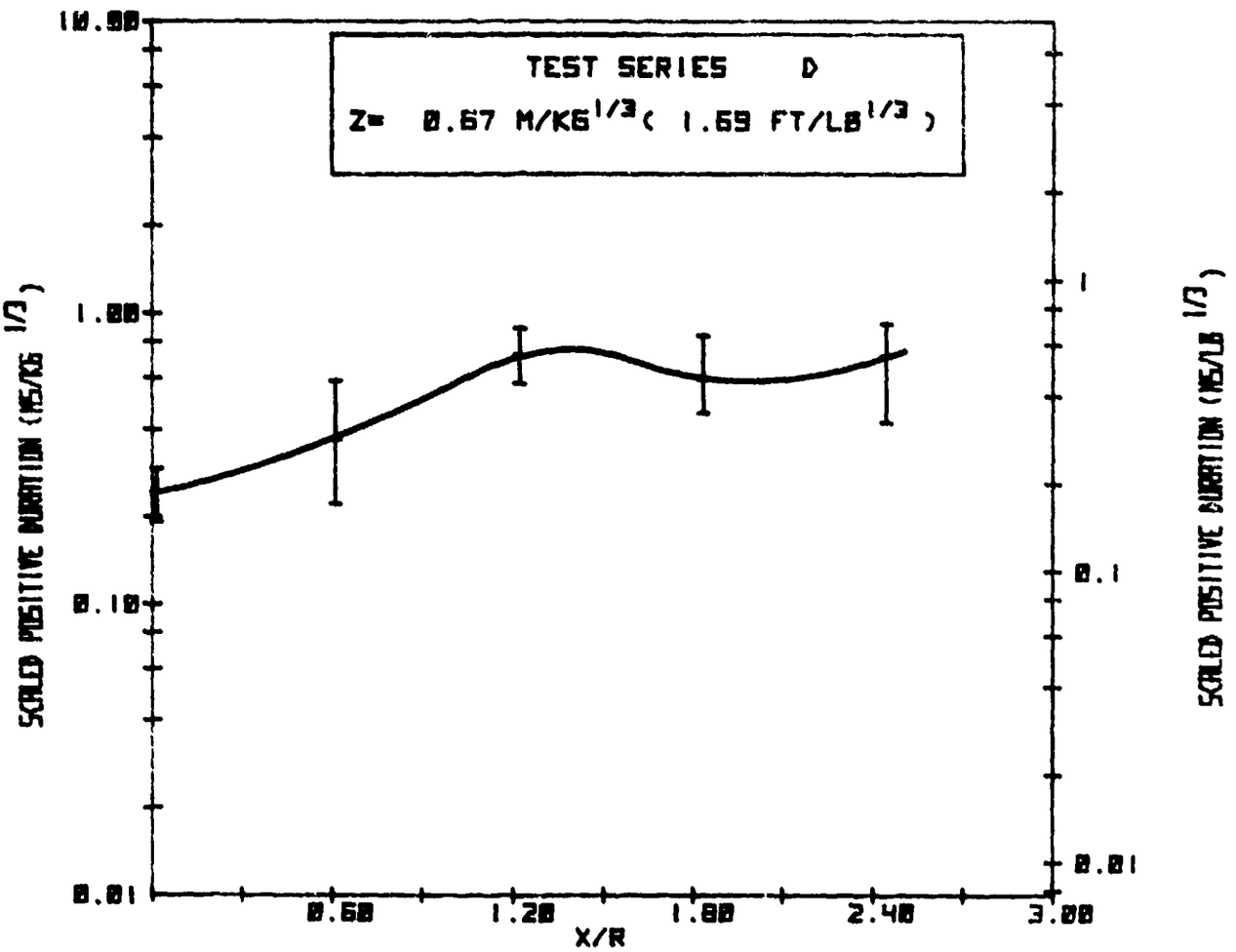

FIGURE 20. POSITIVE DURATION FOR SINGLE CHARGE TESTS (CONT'D)

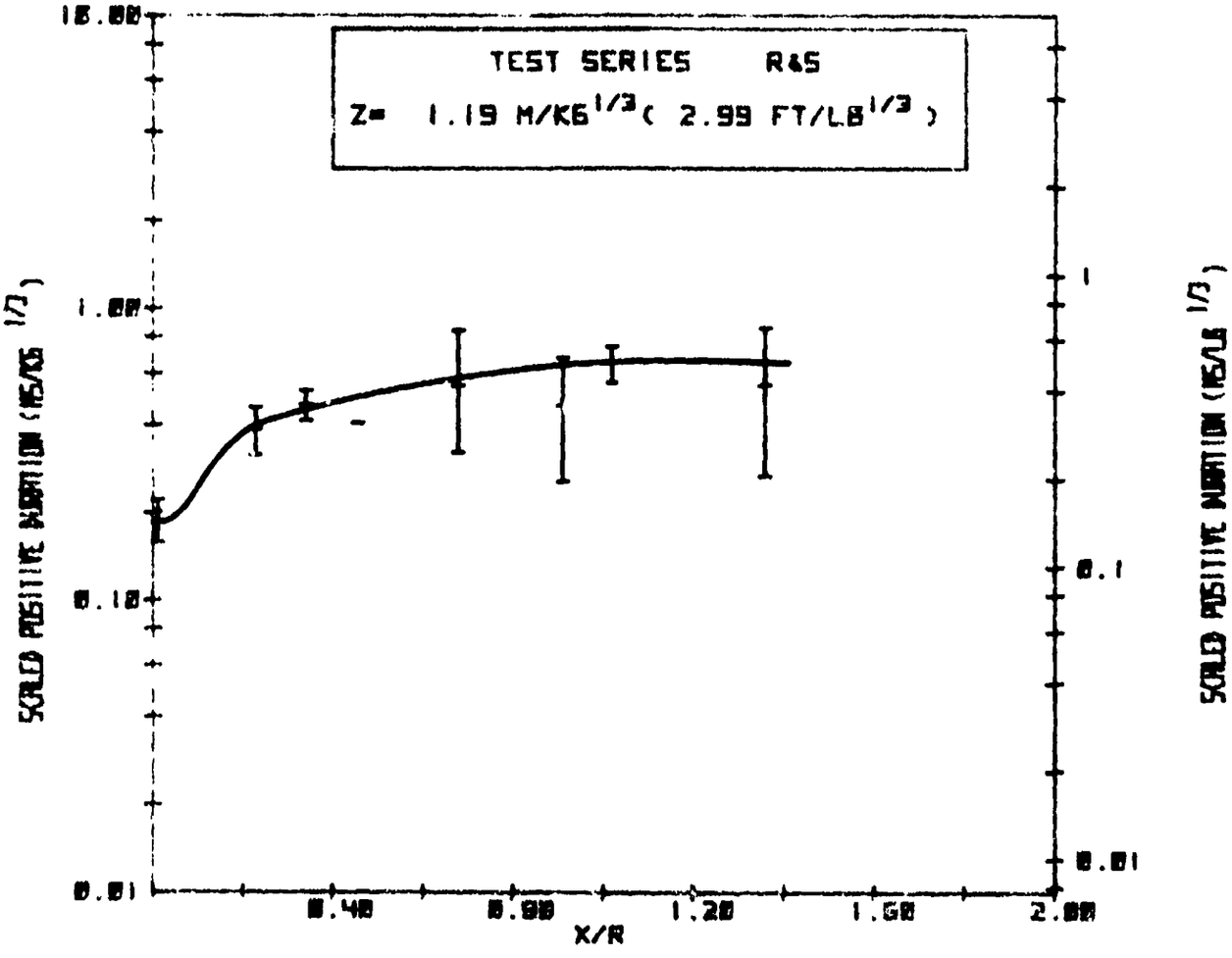

FIGURE 20. POSITIVE DURATION FOR SINGLE CHARGE TESTS (CONT'D)

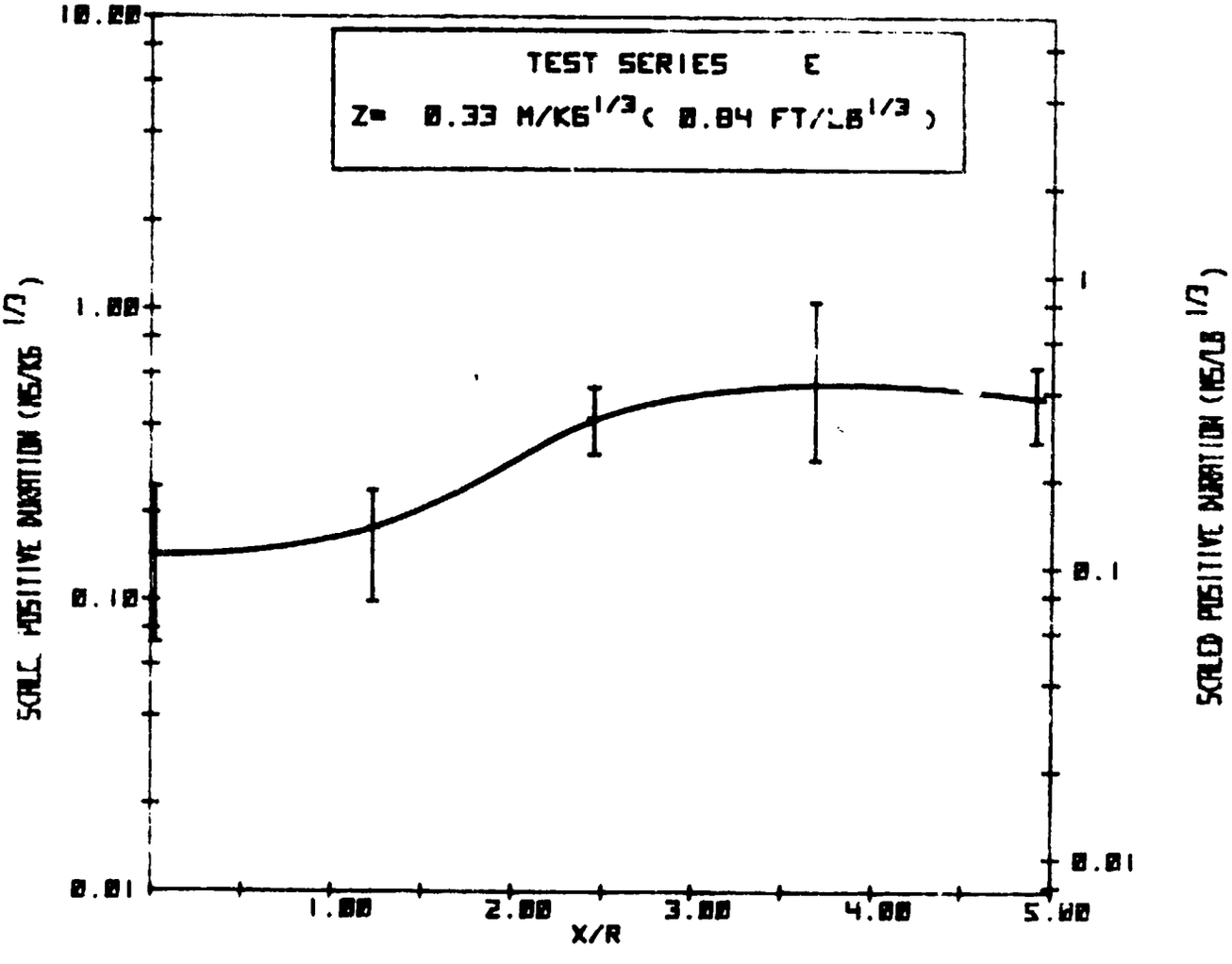

FIGURE 21. POSITIVE DURATION FOR GROUPED ARRAY TESTS

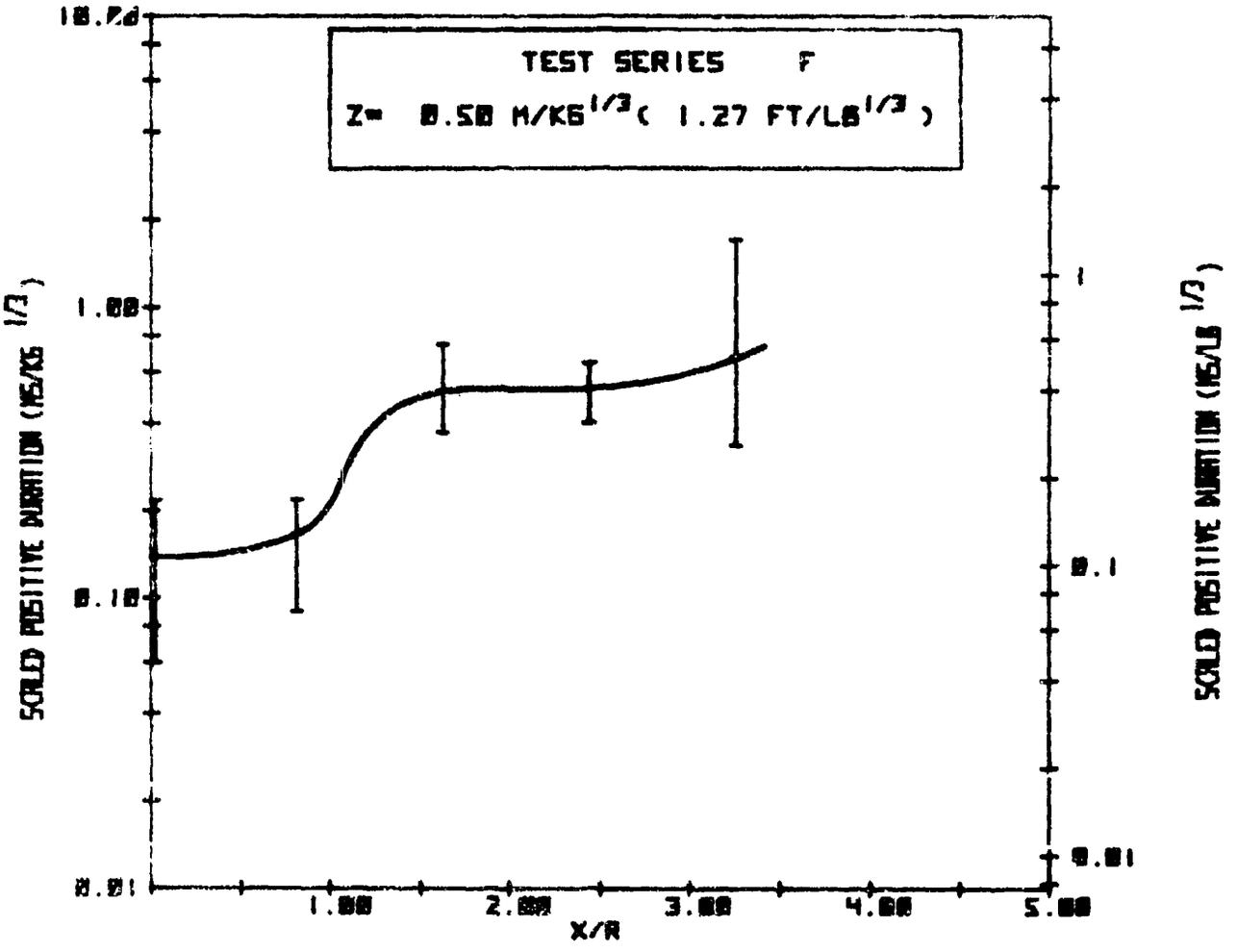

FIGURE 21. POSITIVE DURATION FOR GROUPED ARRAY TESTS (CONT'D)

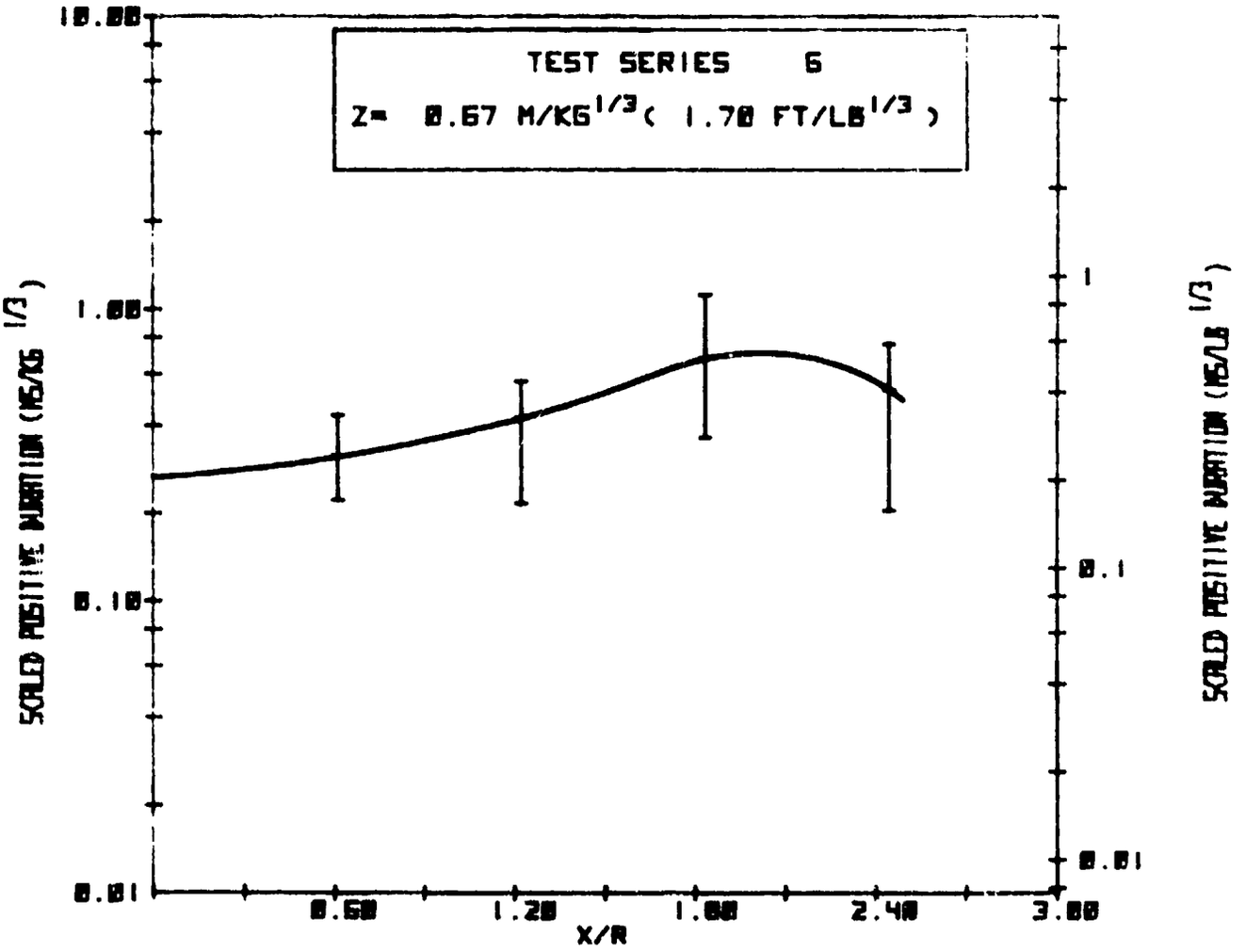

FIGURE 21. POSITIVE DURATION FOR GROUPED ARRAY TESTS (CONT'D)

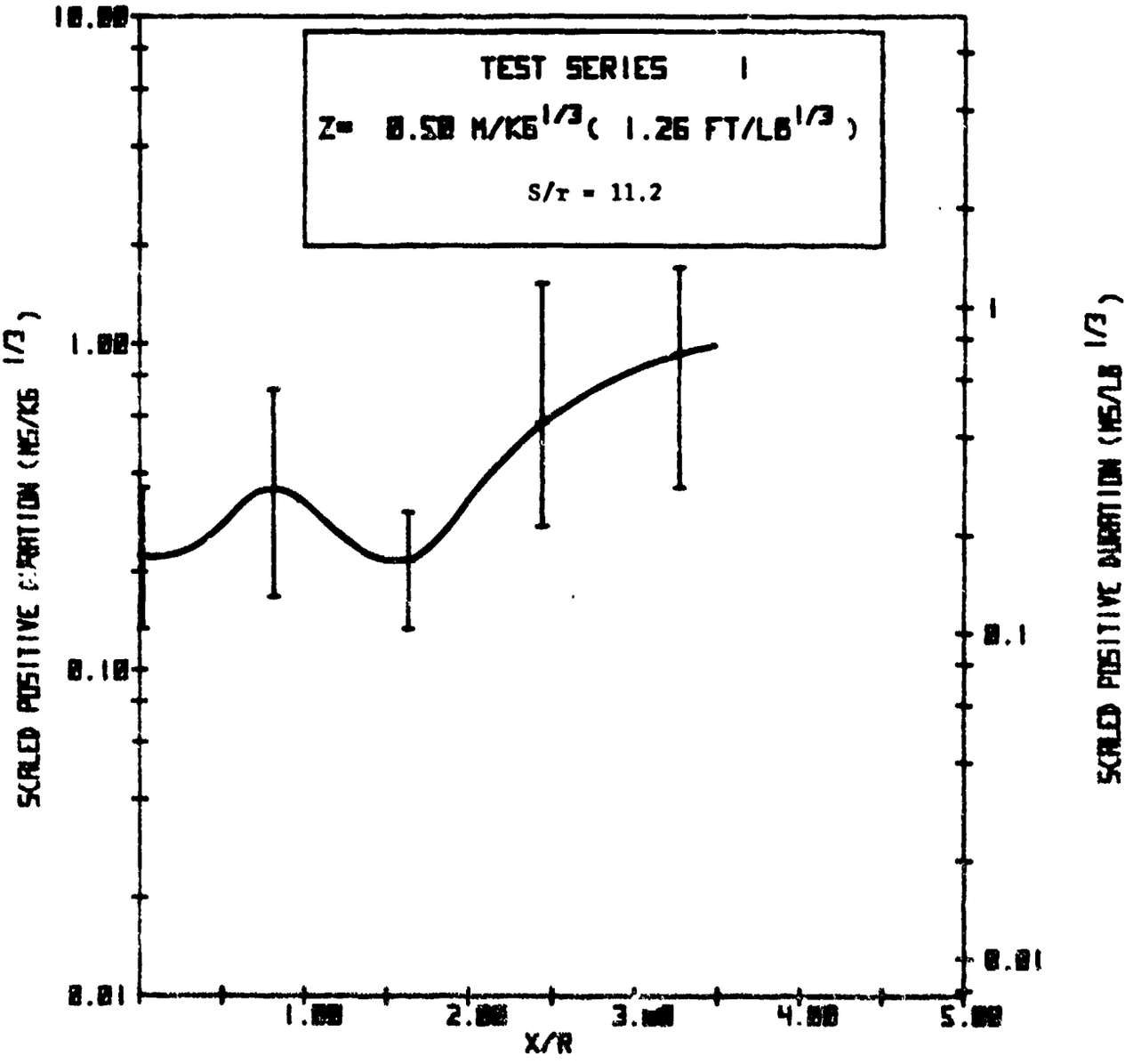

FIGURE 22. POSITIVE DURATION VARIATIONS DUE TO CHARGE STANDOFF FOR HORIZONTAL ARRAY TESTS

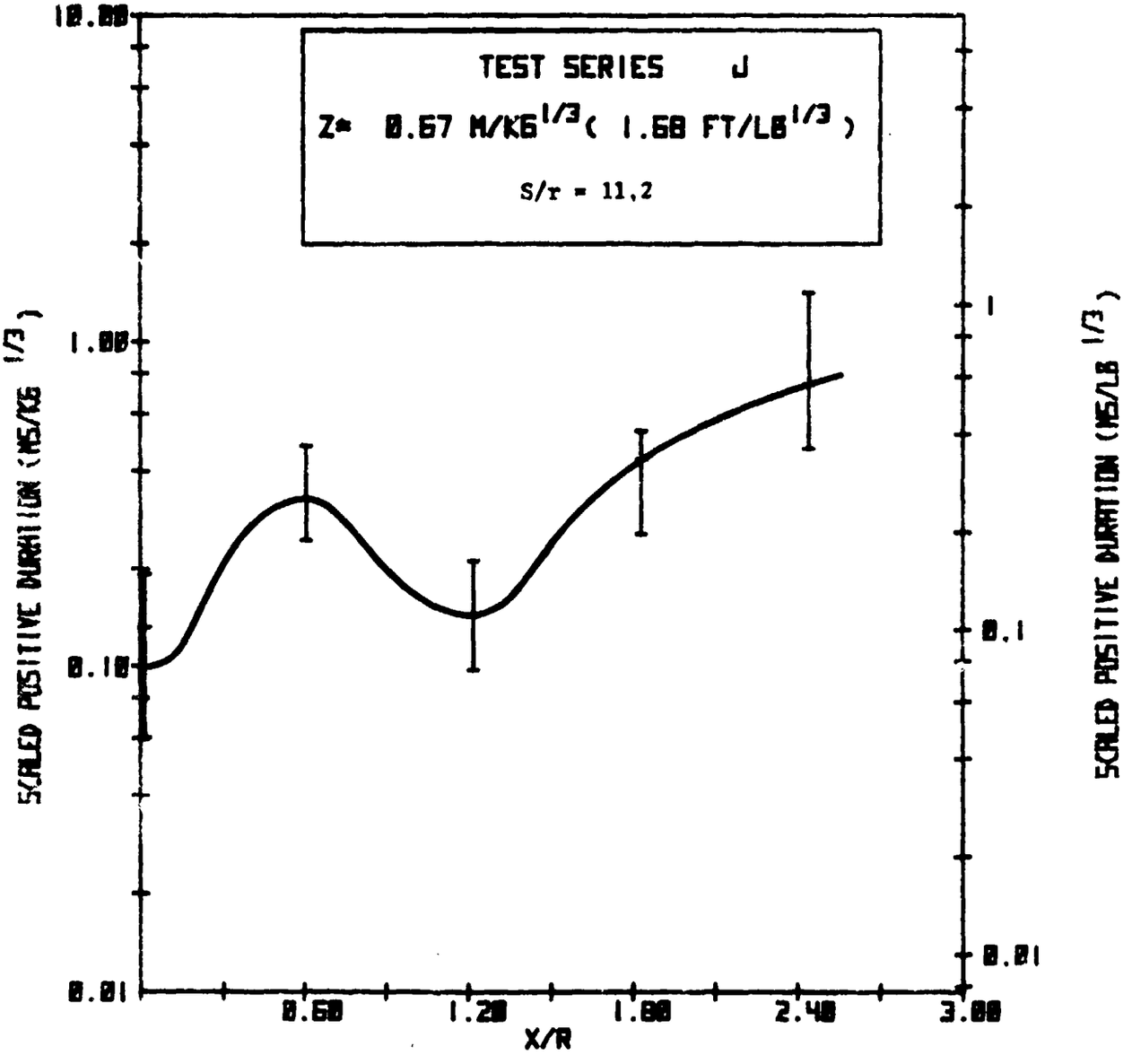

FIGURE 22. POSITIVE DURATION VARIATIONS DUE TO CHARGE STANDOFF FOR HORIZONTAL ARRAY TESTS (CONT'D)

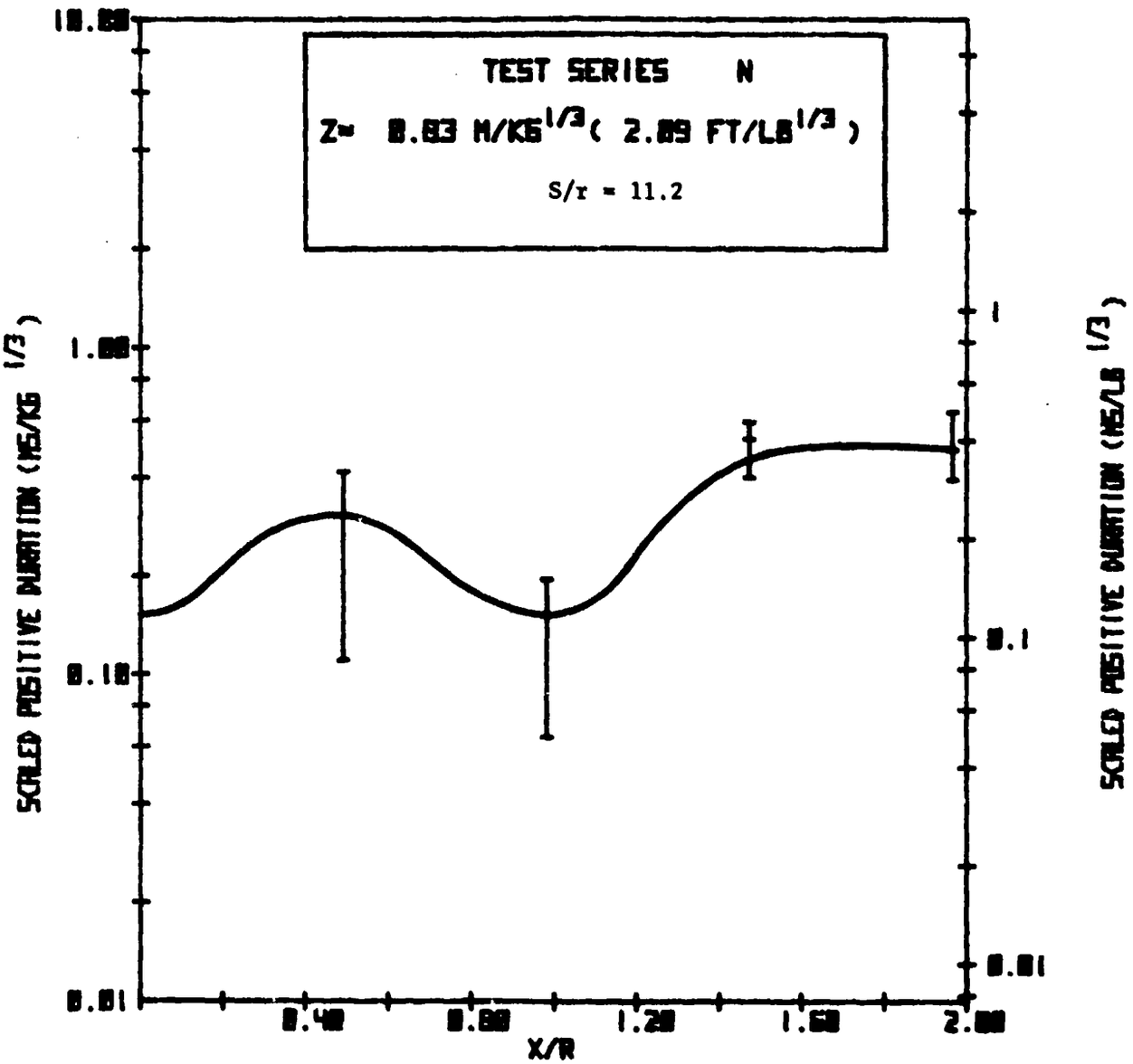

FIGURE 22. POSITIVE DURATION VARIATIONS DUE TO CHARGE STANDOFF FOR HORIZONTAL ARRAY TESTS(CONT'D)

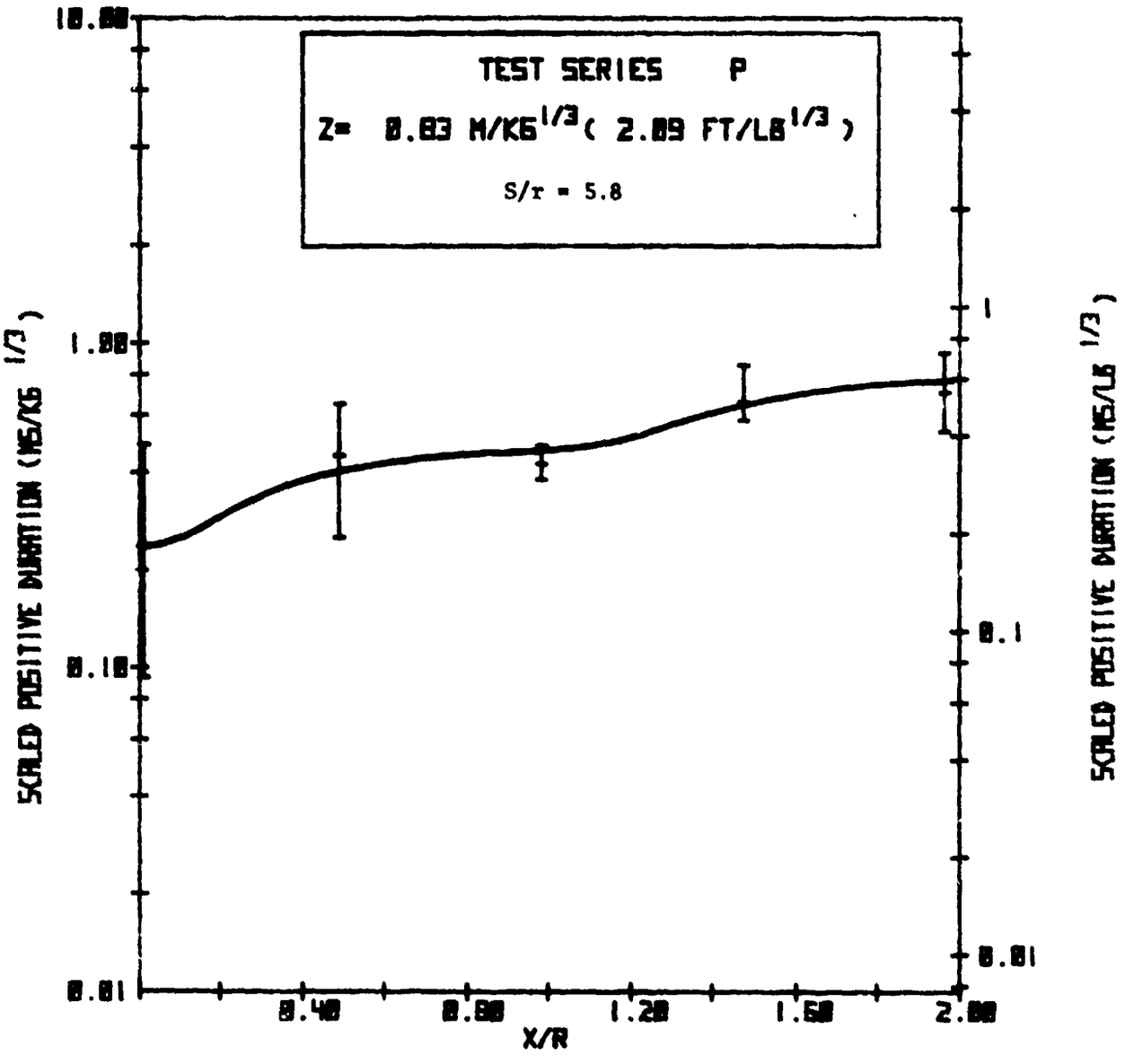

FIGURE 23. POSITIVE DURATION VARIATIONS DUE TO CHARGE SPACING FOR HORIZONTAL ARRAY TESTS

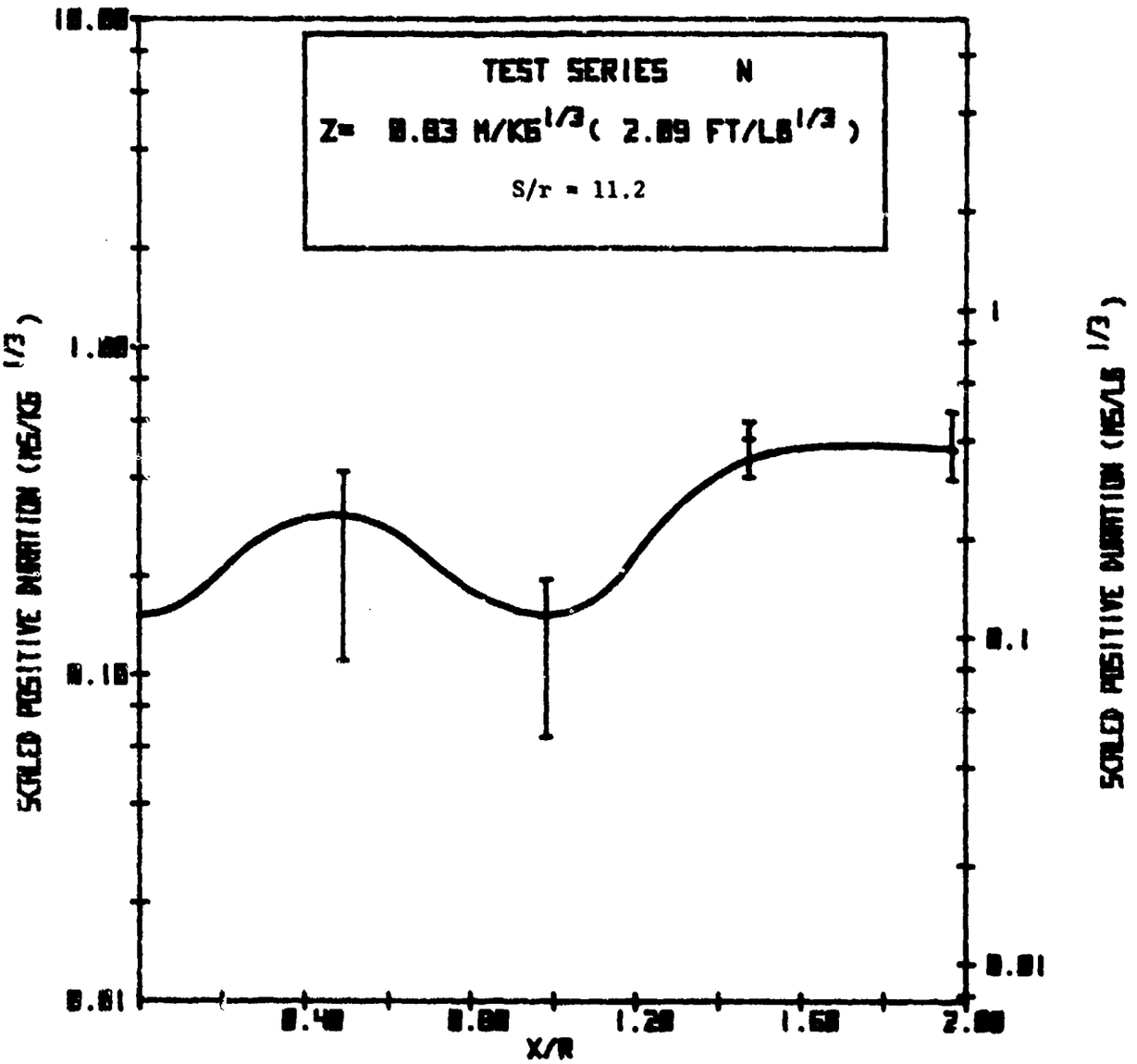

FIGURE 23. POSITIVE DURATION VARIATIONS DUE TO CHARGE SPACING FOR HORIZONTAL ARRAY TESTS (CONT'D)

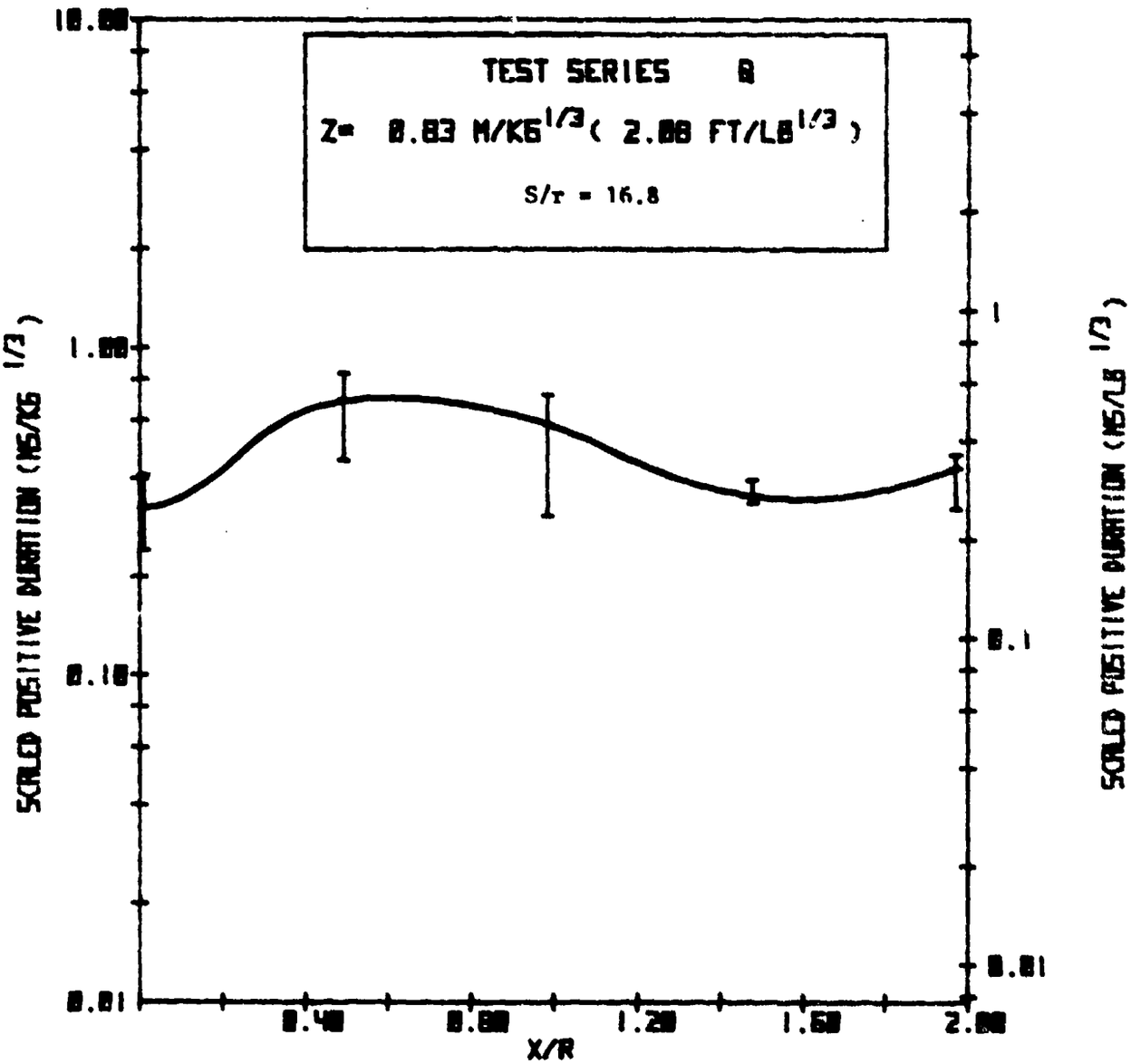

FIGURE 23. POSITIVE DURATION VARIATIONS DUE TO CHARGE SPACING FOR HORIZONTAL ARRAY TESTS (CONT'D)

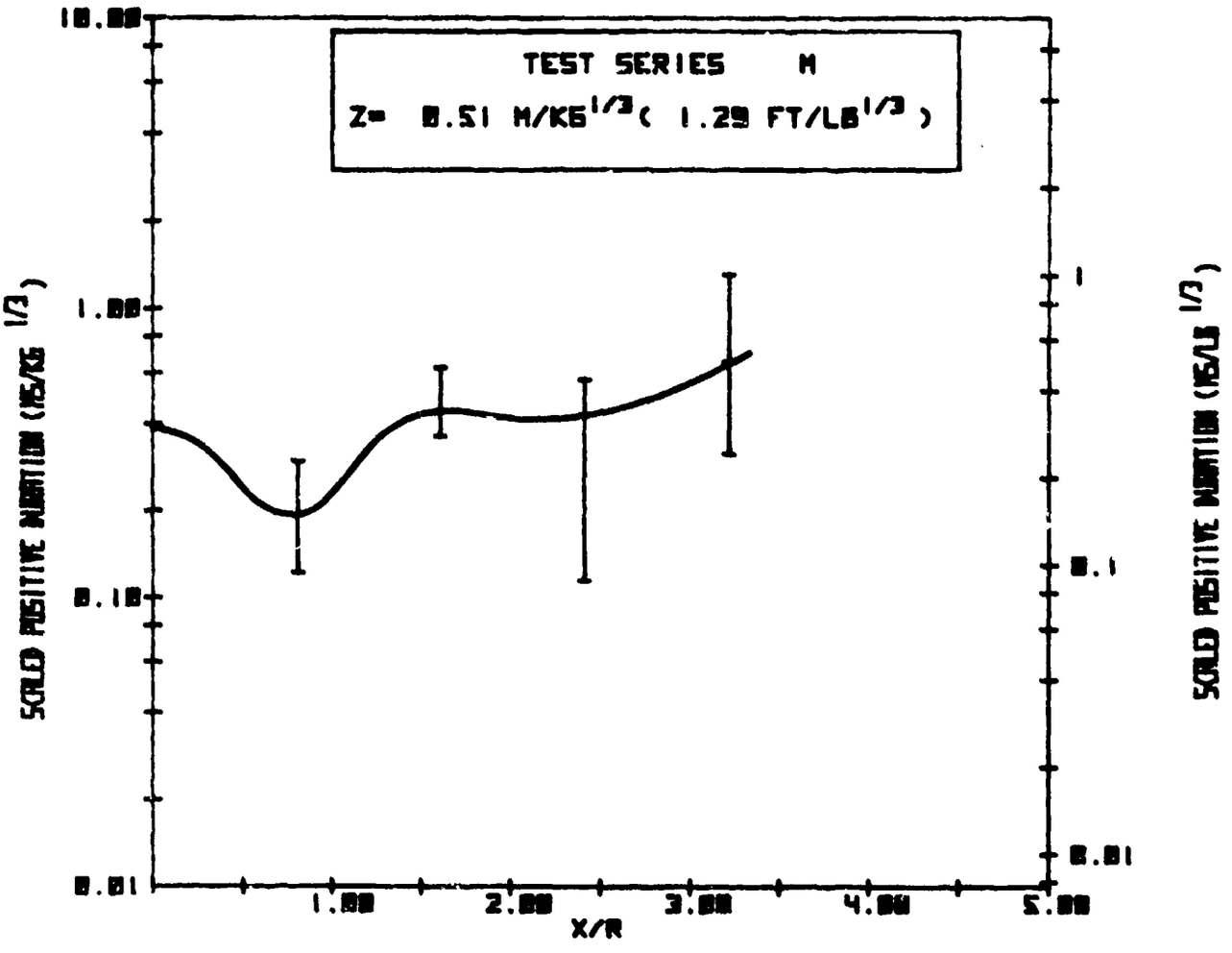

FIGURE 24. POSITIVE DURATION FOR VERTICAL ARRAY TESTS

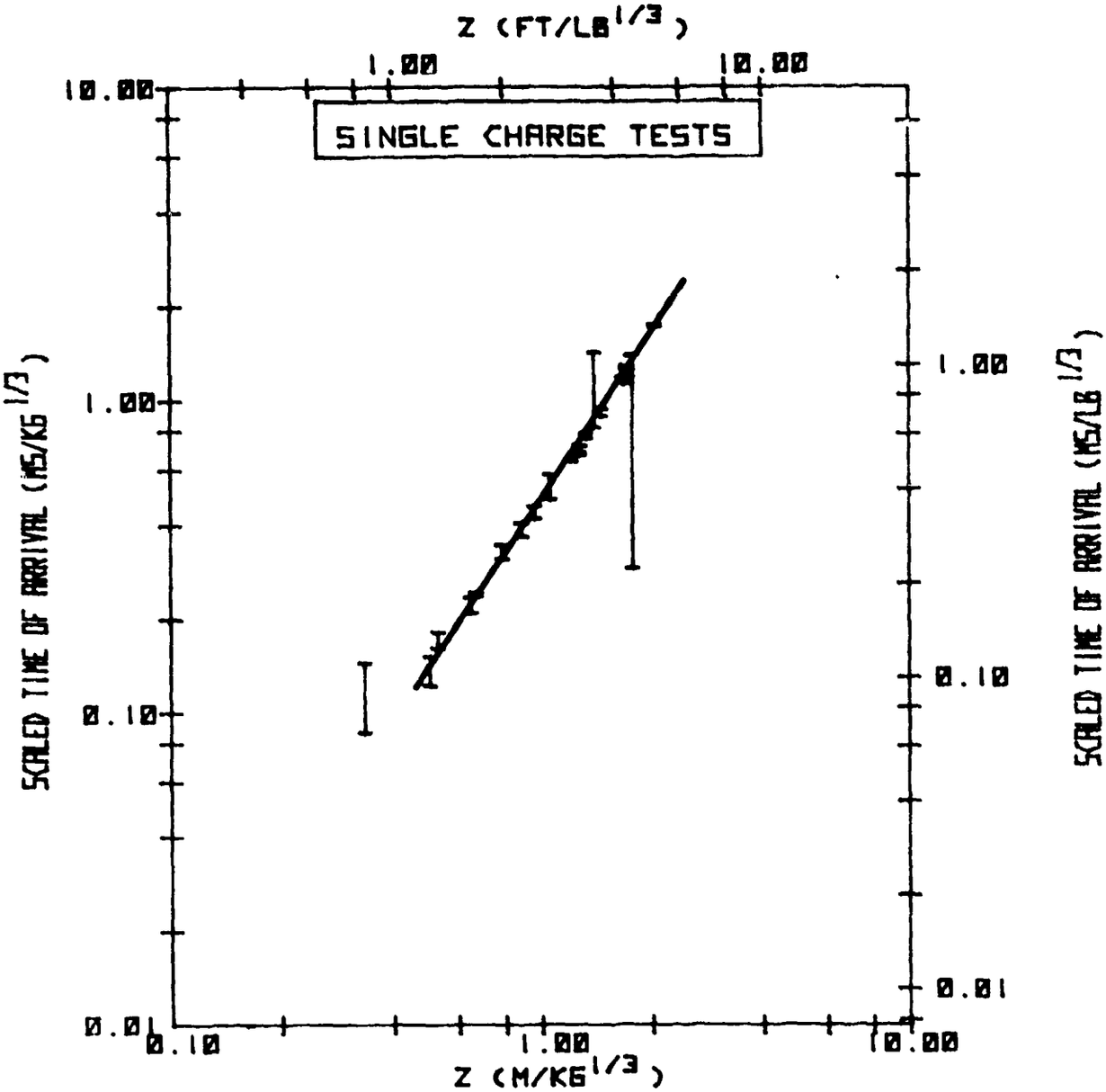

FIGURE 25a. ARRIVAL TIME OF INITIAL SHOCK FRONT FOR A SINGLE CHARGE TESTS

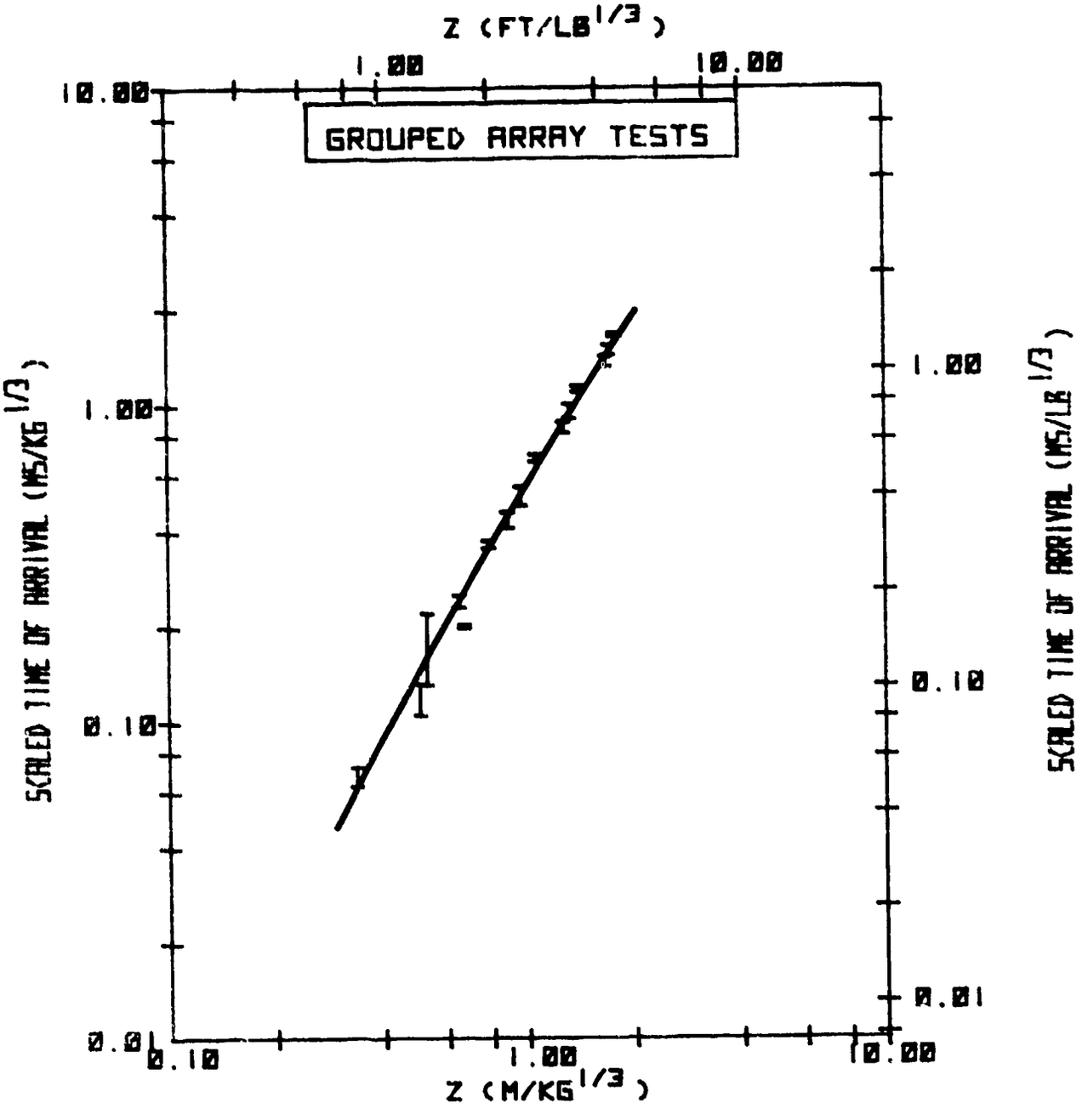

FIGURE 25b. ARRIVAL TIME OF INITIAL SHOCK FRONT FOR A GROUPED ARRAY TESTS

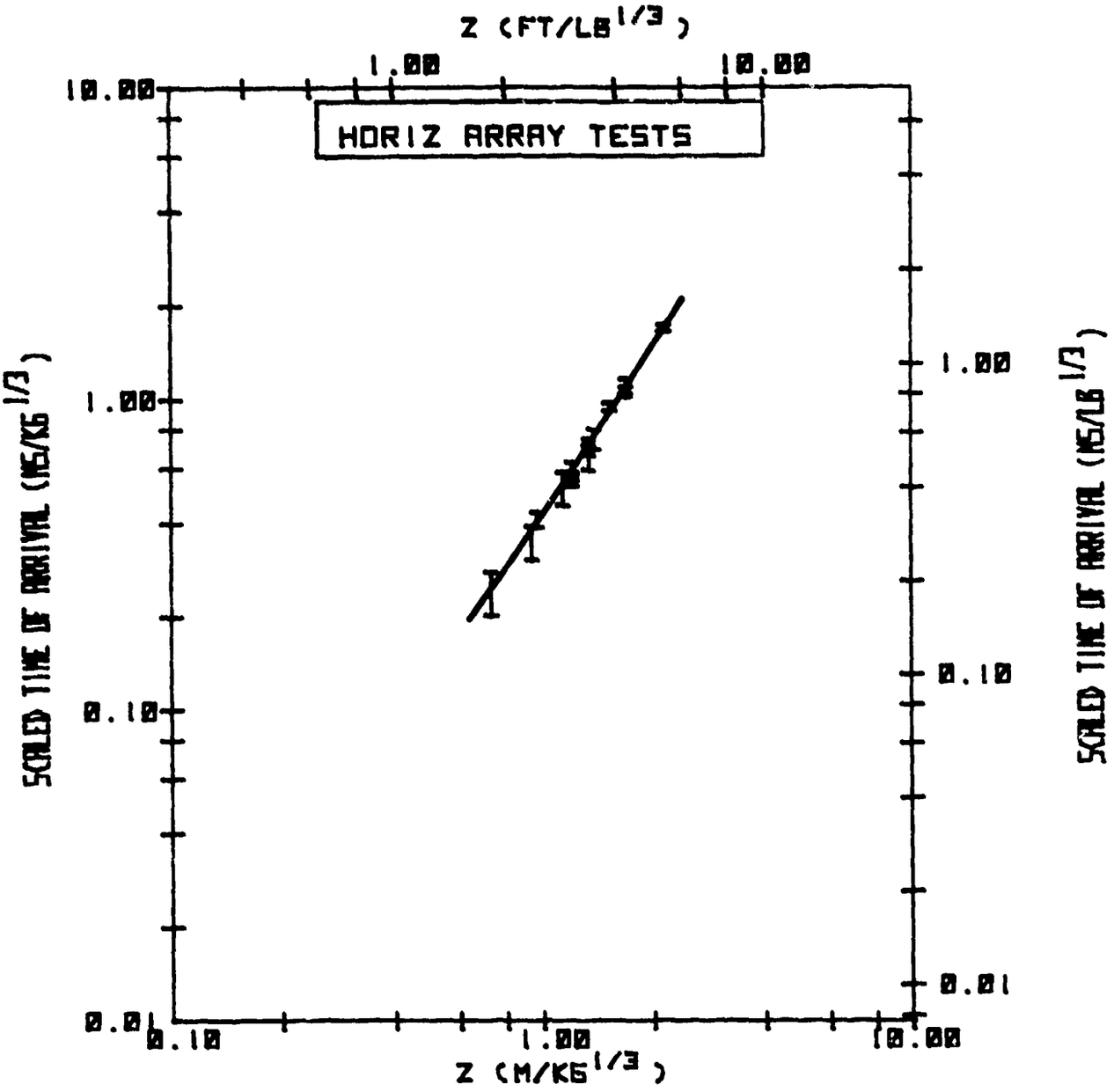

FIGURE 25c. ARRIVAL TIME OF INITIAL SHOCK FRONT FOR A HORIZONTAL ARRAY TESTS

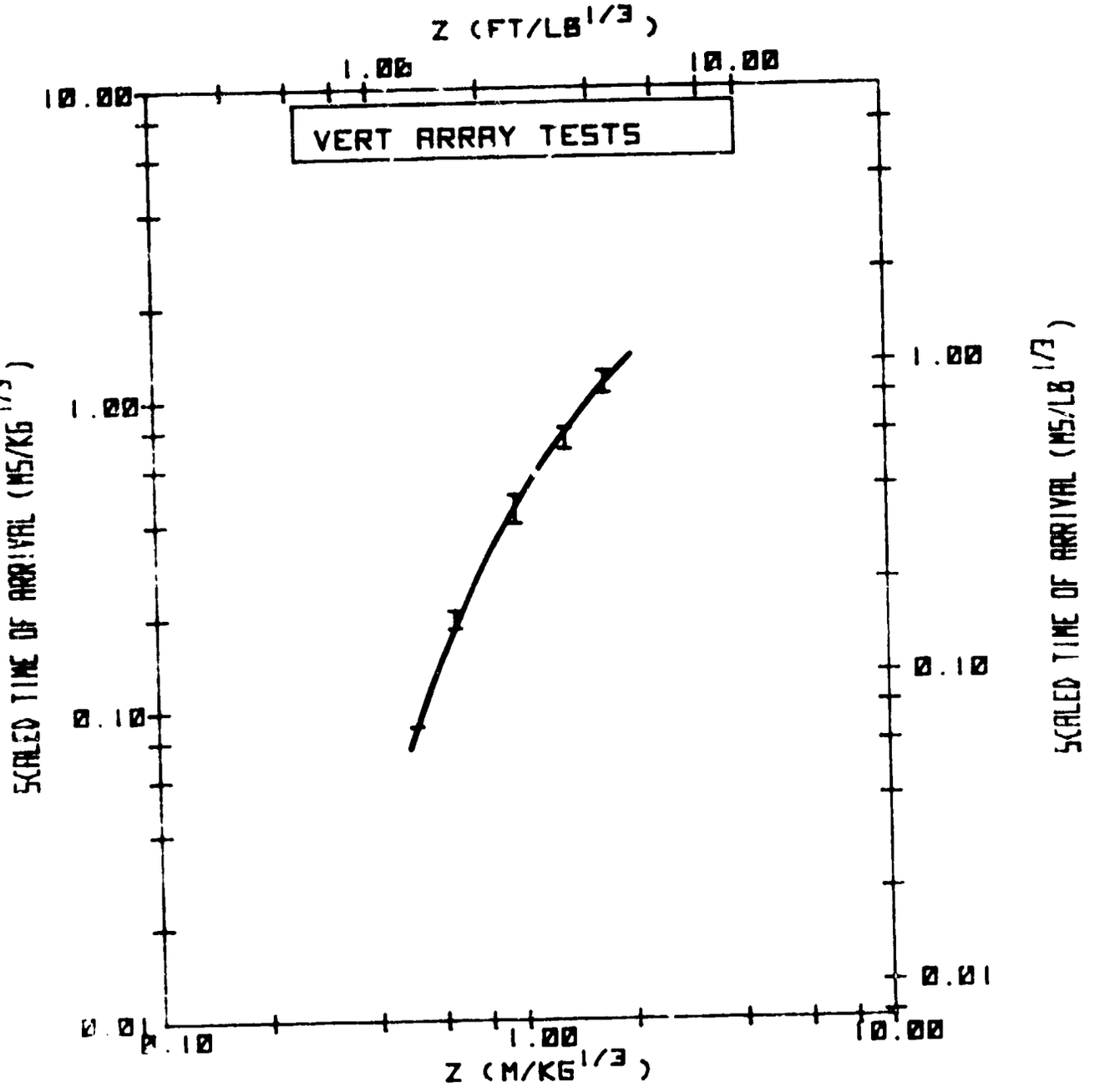

FIGURE 25d. ARRIVAL TIME OF INITIAL SHOCK FRONT FOR A VERTICAL ARRAY TESTS

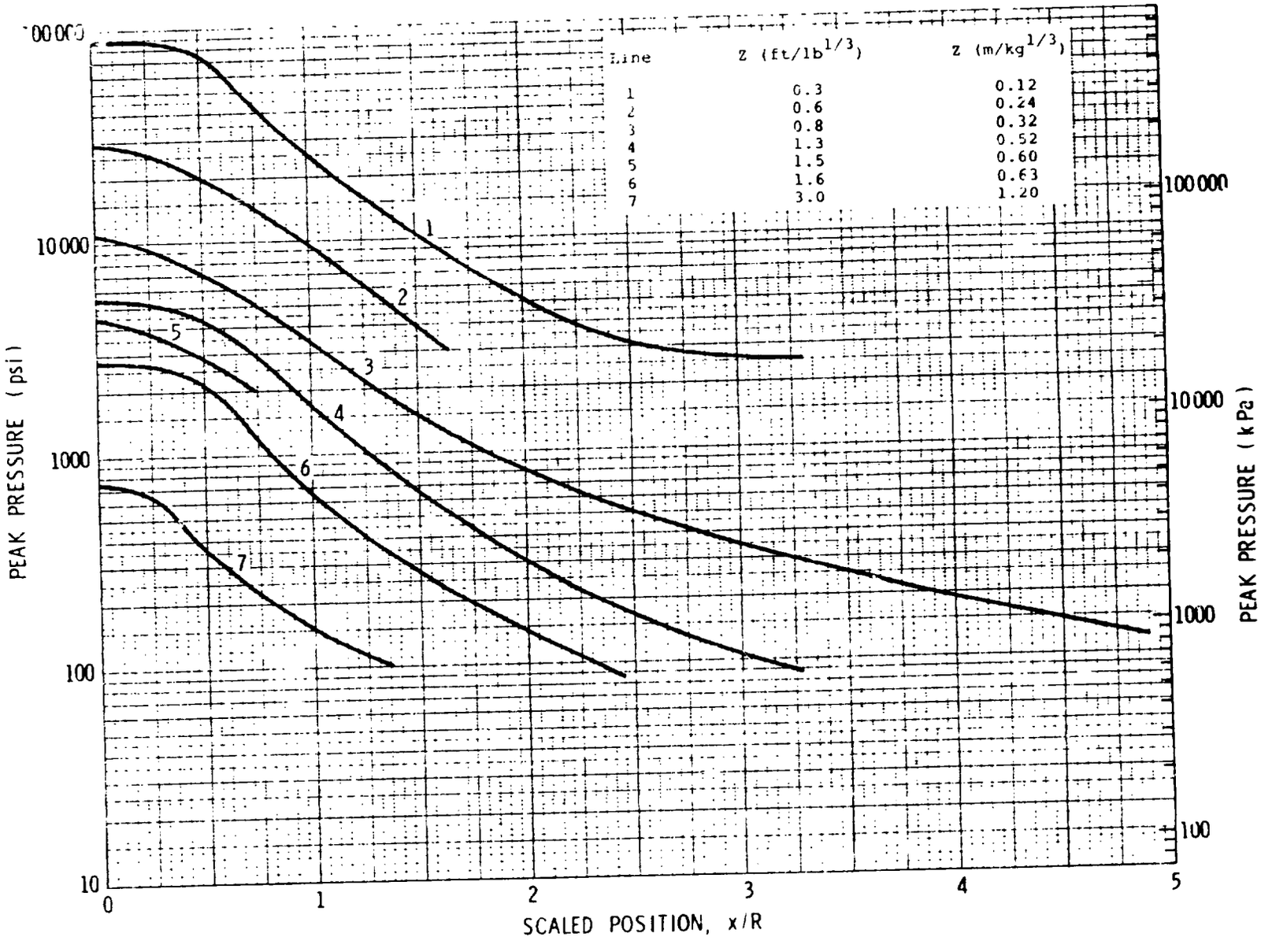

FIGURE 26. PEAK PRESSURE VS SCALED POSITION FOR DIFFERENT SCALED DISTANCES

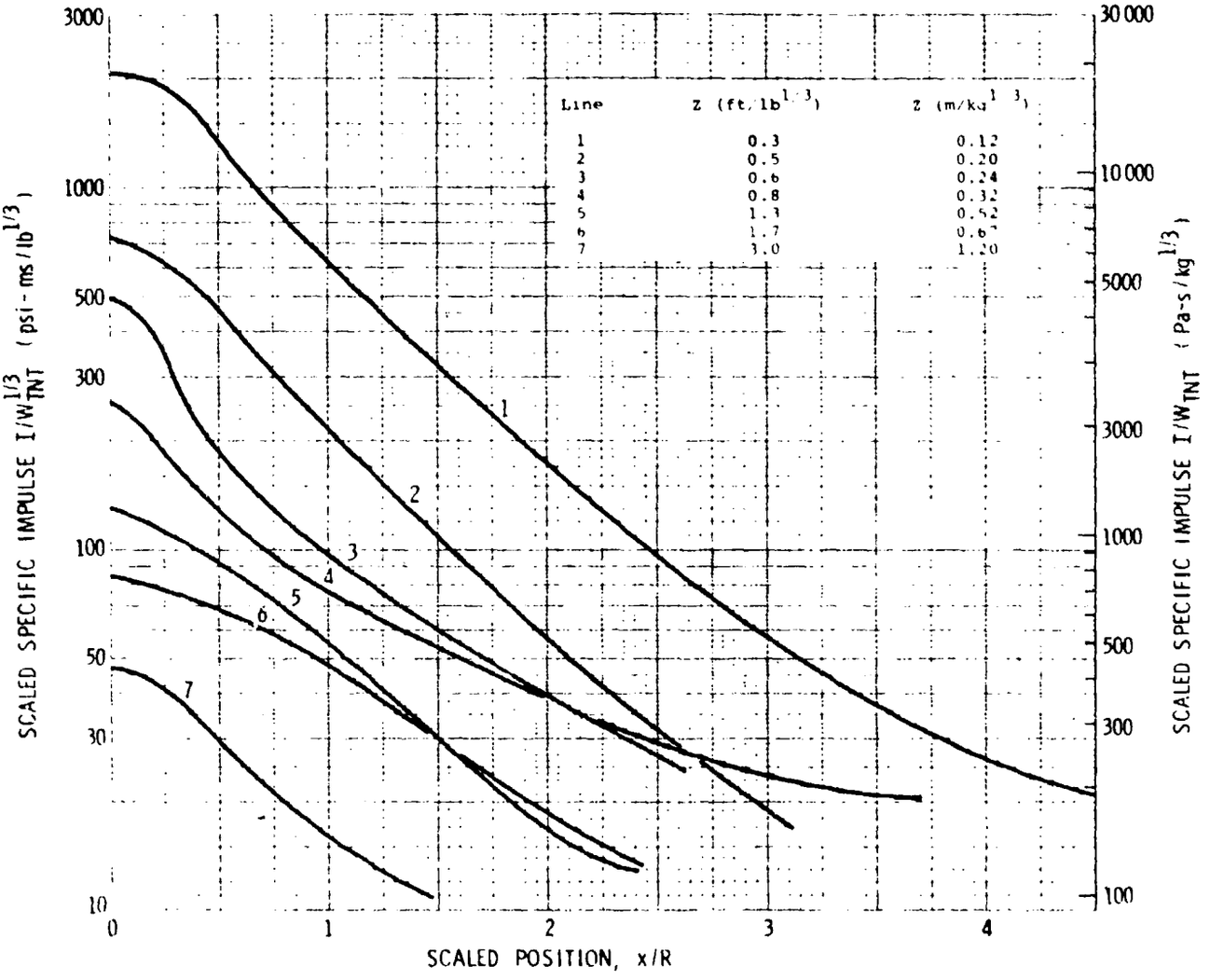

FIGURE 27. SCALED SPECIFIC IMPULSE VS SCALED POSITION FOR DIFFERENT SCALED DISTANCES

Table 1. List of symbols

Symbol	Definition	Units
E	Energy released by the explosive	FL
r	Radius of charge	L
γ_e	Explosive products specific heat ratio	-
ρ_e	Density of explosive	FT^2/L^4
a_e	Explosive detonation velocity	L/T
g	Effective limit for explosive detonation	L
P_a	Ambient air pressure	F/L^2
a_a	Sonic velocity in air	L/T
ρ_a	Ambient air density	FT^2/L^4
θ_a	Ambient air temperature	θ
γ_a	Specific heat ratio of air	-
S	Specific entropy	$L^2/T^2\theta$
U_i	Shock velocity	L/T
ρ_s	Gas density in shock wave	FT^2/L^4
u_s	Particle velocity in shock wave	L/T
θ_s	Shock front temperature	θ
R	Standoff distance	L
s_i	Charge spacing	L
Φ	Shock front encounter angle	-
P	Pressure	F/L^2
I	Specific Impulse	FT/L^2
t	Time	T
t_a	Arrival time of shock wave	T
t_d	Shock wave duration	T

$$\pi_1 = r/R$$
$$\pi_2 = z_1/R$$
$$\pi_3 = z/R$$
$$\pi_4 = \phi$$

geometric similarity

$$\pi_5 = \gamma_e$$

similar explosives

$$\pi_6 = \rho_e/\rho_a$$
$$\pi_7 = a_e/a_a$$

$$\pi_8 = U_i/a_a$$
$$\pi_9 = u_s/a_a$$

kinematic similarity

$$\pi_{10} = S\theta/a_a^2$$

$$\pi_{11} = \gamma_a$$

similar atmospheres

$$\pi_{12} = R\left(\frac{a_a^2 \rho_a}{E}\right)^{1/3}$$

modified Sach's scaling

$$\pi_{13} = \rho_s/\rho_a$$
$$\pi_{14} = \theta_s/\theta_a$$
$$\pi_{15} = P/P_a$$

similar shocks

$$\pi_{16} = \frac{P R^3}{E}$$

scaled pressure

$$\pi_{17} = \frac{I a_a}{\left(E P_a^2\right)^{1/3}}$$

scaled impulse

$$\pi_{18} = t_a a_a \left(\frac{P_a}{E}\right)^{1/3}$$
$$\pi_{19} = t_d a_a \left(\frac{P_a}{E}\right)^{1/3}$$

scaled time

$$\pi_{20} = \frac{a_a t}{R}$$

TABLE 3.
REPLICA SCALING LAW FCR MULTIPLE DETONATIONS

Quantity	Symbol	Scale Factor
Length	r, s_i, g, R	λ
Impulse	I	λ
Time	t, t_d, t_a	λ
Velocity	U_i, u_s, a_s	1.0
Specific Ht	γ_a, γ_e	1.0
Entropy	S	1.0
Density	ρ_a, ρ_e, ρ_s	1.0
Pressure	P_a, P_s	1.0
Temperature	θ_s, θ_a	1.0
Angle	Φ	1.0
Energy	E	λ^3

TABLE 4.
TEST PROGRAM

Designation	Test Series	No. Shots	Charge Weight K_g (lb)	No. Charges	Charge Separation m (ft)	Standoff m (ft)	Scaled Standoff $m/Kg^{1/3}$ $(ft/lb^{1/3})$
C	1	3	0.65 (1.43)	1	-	0.29 (0.95)	0.335 (0.84)
A	1	3	0.65 (1.43)	1	-	0.437 (1.43)	0.504 (1.27)
B	1A	3	2.29 (5.05)	1	-	0.652 (2.14)	0.495 (1.25)
D	1	3	0.65 (1.43)	1	-	0.582 (1.91)	0.672 (1.70)
R	1	2	0.65 (1.43)	1	-	1.05 (3.43)	1.21 (3.04)
S	1A	1	2.29 (5.05)	1	-	1.56 (5.13)	1.18 (2.99)
E	2	3	0.223 (0.492)	3	0	0.29 (0.95)	0.332 (0.834)*
F	2	3	0.223 (0.492)	3	0	0.436 (1.43)	0.499 (1.26)*
G	2	3	0.223 (0.492)	3	0	0.582 (1.91)	0.665 (1.68)*
I	3	3	0.223 (0.492)	3	0.71 (2.33)	0.436 (1.43)	0.495 (1.25)*
J	3	3	0.223 (0.492)	3	0.71 (2.33)	0.582 (1.91)	0.665 (1.68)*
P	3	3	0.223 (0.492)	3	0.366 (1.2)	0.724 (2.38)	0.821 (2.07)*
N	3	4	0.223 (0.492)	3	0.71 (2.33)	0.724 (2.38)	0.821 (2.07)*
Q	3	3	0.223 (0.492)	3	1.07 (3.5)	0.724 (2.38)	0.821 (2.07)*
M	4	4	0.223 (0.492)	3	0.145 (0.475)	0.437 (1.43)	0.504 (1.27)*

*For these tests, R is measured to the center of mass of the charges and W is the total weight of Composition B explosive.

APPENDIX
DATA SUMMARIES

- Table A.1 Metric Unit Summary

  Single Charge Tests
  Grouped Array Tests
  Horizontal Array Tests
  Vertical Array Tests

- Table A.2 English Unit Summary

  Single Charge Tests
  Grouped Array Tests
  Horizontal Array Tests
  Vertical Array Tests

TABLE A.1 METRIC UNIT SUMMARY

SUMMARY OF SINGLE CHARGE TEST DATA

TEST ID	CHARGE WEIGHT (KG)	STANDOFF DISTANCE (M)	GAGE NO	GAGE LOCATION (M)	CHARGE SPACING (M)	PEAK PRESSURE (KPA)	POSITIVE IMPULSE (PA-S)	POSITIVE DURATION (MS)	TIME OF ARRIVAL (MS)
1A	0.649	0.437	1	-1.443	0.000	617.8	86.6	0.437	1.073
1A	0.649	0.437	2	-1.082	0.000	1232.8	0.0	0.379	0.655
1A	0.649	0.437	3	-0.721	0.000	4596.7	328.5	0.203	0.384
1A	0.649	0.437	4	-0.361	0.000	17141.0	624.9	0.236	0.203
1A	0.649	0.437	5	0.000	0.000	31719.3	995.1	0.000	0.125
1A	0.649	0.437	6	0.361	0.000	20627.0	251.8	0.000	0.197
1A	0.649	0.437	7	0.721	0.000	4884.2	233.0	0.000	0.398
1A	0.649	0.437	8	1.082	0.000	932.2	170.7	0.000	0.682
1A	0.649	0.437	9	1.443	0.000	623.3	123.1	0.749	1.098
2A	0.649	0.437	1	-1.443	0.000	601.2	89.3	0.427	1.039
2A	0.649	0.437	2	-1.082	0.000	1167.3	138.9	0.432	0.655
2A	0.649	0.437	3	-0.721	0.000	2558.0	215.1	0.192	0.363
2A	0.649	0.437	4	-0.361	0.000	8994.2	657.9	0.357	0.181
2A	0.649	0.437	5	0.000	0.000	13652.3	1107.3	0.129	0.106
2A	0.649	0.437	6	0.361	0.000	21006.2	614.5	0.101	0.186
2A	0.649	0.437	7	0.721	0.000	2453.8	262.8	0.376	0.379
2A	0.649	0.437	8	1.082	0.000	1354.8	114.0	0.303	0.670
2A	0.649	0.437	9	1.443	0.000	550.9	0.0	7.487	1.073
3A	0.649	0.437	1	-1.443	0.000	643.6	73.7	0.351	1.039
3A	0.649	0.437	2	-1.082	0.000	1909.9	146.4	0.393	0.660
3A	0.649	0.437	3	-0.721	0.000	4003.6	320.6	0.277	0.382
3A	0.649	0.437	4	-0.361	0.000	14434.9	664.5	0.246	0.195
3A	0.649	0.437	5	0.000	0.000	18837.3	718.5	0.113	0.131
3A	0.649	0.437	6	0.361	0.000	17065.4	806.0	0.180	0.193
3A	0.649	0.437	7	0.721	0.000	4548.5	273.0	0.211	0.386
3A	0.649	0.437	8	1.082	0.000	1507.0	181.9	0.418	0.673
3A	0.649	0.437	9	1.443	0.000	0.0	0.0	0.000	0.000
20B	2.291	0.653	1	-1.443	0.000	1675.0	232.4	0.381	0.801
20B	2.291	0.653	2	-1.082	0.000	3813.6	378.3	0.378	0.521
20B	2.291	0.653	3	-0.721	0.000	10433.9	999.7	0.722	0.361
20B	2.291	0.653	4	-0.361	0.000	29913.5	1147.0	0.216	0.204
20B	2.291	0.653	5	0.000	0.000	62001.0	2750.5	0.260	0.125
20B	2.291	0.653	6	0.361	0.000	32257.4	1476.3	0.300	0.196
20B	2.291	0.653	7	0.721	0.000	9571.4	426.7	0.203	0.349
20B	2.291	0.653	8	1.082	0.000	4641.6	452.7	0.376	0.527
20B	2.291	0.653	9	1.443	0.000	1576.2	191.0	0.484	0.788
21B	2.291	0.653	1	-1.443	0.000	1665.4	234.1	0.482	0.788
21B	2.291	0.653	2	-1.082	0.000	3197.9	394.4	0.320	0.499
21B	2.291	0.653	3	-0.721	0.000	4904.0	686.0	0.442	0.313
21B	2.291	0.653	4	-0.361	0.000	22594.8	1503.6	0.250	0.188
21B	2.291	0.653	6	0.361	0.000	27036.8	2007.1	0.212	0.202
21B	2.291	0.653	7	0.721	0.000	12541.9	836.7	0.178	0.331
21B	2.291	0.653	8	1.082	0.000	4019.4	504.2	0.382	0.499
21B	2.291	0.653	9	1.443	0.000	1585.3	233.5	0.862	0.769

SUMMARY OF SINGLE CHARGE TEST DATA

TEST ID	CHARGE WEIGHT (KG)	STANDOFF DISTANCE (M)	GAGE NO	GAGE LOCATION (M)	CHARGE SPACING (M)	PEAK PRESSURE (KPA)	POSITIVE IMPULSE (PA-S)	POSITIVE DURATION (MS)	TIME OF ARRIVAL (MS)
22B	2.291	0.653	1	-1.443	0.000	1655.9	215.8	0.344	0.752
22B	2.291	0.653	2	-1.082	0.000	4008.2	402.0	0.315	0.503
22B	2.291	0.653	3	-0.721	0.000	8868.9	960.6	0.459	0.311
22B	2.291	0.653	4	-0.361	0.000	33401.0	1554.2	0.225	0.196
22B	2.291	0.653	6	0.361	0.000	35590.0	1839.3	0.240	0.183
22B	2.291	0.653	7	0.721	0.000	15786.9	1111.4	0.233	0.320
22B	2.291	0.653	8	1.082	0.000	4149.1	505.2	0.469	0.497
22B	2.291	0.653	9	1.443	0.000	1770.5	292.6	0.731	0.744
7C	0.649	0.290	1	-1.443	0.000	728.3	87.5	0.356	0.982
7C	0.649	0.290	2	-1.082	0.000	1228.5	169.1	0.448	0.580
7C	0.649	0.290	3	-0.721	0.000	3316.4	265.6	0.295	0.319
7C	0.649	0.290	4	-0.361	0.000	14416.9	753.9	0.196	0.146
7C	0.649	0.290	5	0.000	0.000	77684.6	1539.8	0.211	0.086
7C	0.649	0.290	6	0.361	0.000	15231.0	733.1	0.162	0.154
7C	0.649	0.290	7	0.721	0.000	3335.8	218.9	0.187	0.332
7C	0.649	0.290	8	1.082	0.000	1460.4	169.4	0.581	0.615
7C	0.649	0.290	9	1.443	0.000	0.0	0.0	0.000	0.000
8C	0.649	0.290	1	-1.443	0.000	867.8	116.4	0.384	0.982
8C	0.649	0.290	2	-1.082	0.000	1962.0	180.5	0.439	0.590
8C	0.649	0.290	3	-0.721	0.000	3735.1	276.5	0.312	0.328
8C	0.649	0.290	4	-0.361	0.000	15312.0	551.3	0.209	0.149
8C	0.649	0.290	5	0.000	0.000	77273.6	2003.8	0.295	0.075
8C	0.649	0.290	6	0.361	0.000	26805.9	527.4	0.233	0.140
8C	0.649	0.290	7	0.721	0.000	4362.4	338.3	0.785	0.352
8C	0.649	0.290	8	1.082	0.000	1764.6	224.5	0.518	0.620
8C	0.649	0.290	9	1.443	0.000	971.4	159.0	1.863	1.023
9C	0.649	0.290	1	-1.443	0.000	886.8	115.1	0.385	1.010
9C	0.649	0.290	2	-1.082	0.000	1774.1	186.1	0.505	0.611
9C	0.649	0.290	3	-0.721	0.000	3301.4	303.5	0.372	0.331
9C	0.649	0.290	4	-0.361	0.000	8833.9	346.6	0.142	0.158
9C	0.649	0.290	5	0.000	0.000	77421.9	2848.9	0.336	0.125
9C	0.649	0.290	6	0.361	0.000	18000.7	558.5	0.119	0.145
9C	0.649	0.290	7	0.721	0.000	3467.4	249.6	0.251	0.332
9C	0.649	0.290	8	1.082	0.000	1924.4	209.8	0.456	0.611
9C	0.649	0.290	9	1.443	0.000	0.0	0.0	0.000	0.000
4D	0.649	0.582	1	-1.443	0.000	571.2	112.2	0.000	1.211
4D	0.649	0.582	2	-1.082	0.000	1605.1	181.6	0.436	0.781
4D	0.649	0.582	3	-0.721	0.000	2330.4	346.8	0.000	0.473
4D	0.649	0.582	4	-0.361	0.000	12089.7	783.2	0.288	0.270
4D	0.649	0.582	6	0.361	0.000	13382.1	829.3	0.000	0.276
4D	0.649	0.582	7	0.721	0.000	3192.7	295.8	0.000	0.494
4D	0.649	0.582	8	1.082	0.000	1660.9	252.6	0.728	0.711
4D	0.649	0.582	9	1.443	0.000	626.0	136.6	0.000	1.213
5D	0.649	0.582	1	-1.443	0.000	0.0	0.0	0.000	0.000

SUMMARY OF SINGLE CHARGE TEST DATA

TEST ID	CHARGE WEIGHT (KG)	STANDOFF DISTANCE (M)	GAGE NO	GAGE LOCATION (M)	CHARGE SPACING (M)	PEAK PRESSURE (KPA)	POSITIVE IMPULSE (PA-S)	POSITIVE DURATION (MS)	TIME OF ARRIVAL (MS)
5D	0.649	0.582	2	-1.082	0.000	1970.9	314.4	0.395	1.231
5D	0.649	0.582	3	-0.721	0.000	2832.7	248.2	0.640	0.501
5D	0.649	0.582	4	-0.361	0.000	11734.0	811.6	0.508	0.298
5D	0.649	0.582	5	0.000	0.000	17335.2	602.0	0.254	0.210
5D	0.649	0.582	6	0.361	0.000	14248.4	618.0	0.192	0.272
5D	0.649	0.582	7	0.721	0.000	3531.2	323.3	0.582	0.468
5D	0.649	0.582	8	1.082	0.000	1840.0	257.6	0.674	0.751
5D	0.649	0.582	9	1.443	0.000	588.6	151.8	0.691	1.148
6D	0.649	0.582	1	-1.443	0.000	664.1	93.4	0.366	1.140
6D	0.649	0.582	2	-1.082	0.000	1208.4	165.3	0.414	0.742
6D	0.649	0.582	3	-0.721	0.000	2073.7	551.6	0.768	0.419
6D	0.649	0.582	4	-0.361	0.000	13604.1	670.0	0.377	0.272
6D	0.649	0.582	5	0.000	0.000	19811.6	717.2	0.166	0.205
6D	0.649	0.582	6	0.361	0.000	12073.1	798.8	0.236	0.274
6D	0.649	0.582	7	0.721	0.000	3621.5	354.2	0.499	0.473
6D	0.649	0.582	8	1.082	0.000	1509.4	170.2	0.449	0.778
6D	0.649	0.582	9	1.443	0.000	556.2	128.1	0.798	0.251
38R	0.649	1.046	1	-1.443	0.000	711.1	62.9	0.232	1.510
38R	0.649	1.046	2	-1.082	0.000	1297.7	201.1	0.575	1.118
38R	0.649	1.046	3	-0.721	0.000	2220.8	308.2	0.731	0.813
38R	0.649	1.046	4	-0.361	0.000	4521.1	374.4	0.428	0.621
38R	0.649	1.046	5	0.000	0.000	0.0	512.5	0.152	0.560
38R	0.649	1.046	6	0.361	0.000	3701.6	260.6	0.360	0.623
38R	0.649	1.046	7	0.721	0.000	1411.7	191.7	0.311	0.813
38R	0.649	1.046	8	1.082	0.000	1318.6	192.4	0.585	1.111
38R	0.649	1.046	9	1.443	0.000	788.3	198.8	0.745	1.489
40R	0.649	1.046	1	-1.443	0.000	558.9	82.7	0.357	1.514
40R	0.649	1.046	2	-1.082	0.000	1299.5	214.6	0.483	1.095
40R	0.649	1.046	3	-0.721	0.000	1322.4	202.7	0.648	0.773
40R	0.649	1.046	4	-0.361	0.000	4604.9	424.0	0.456	0.592
40R	0.649	1.046	5	0.000	0.000	4885.8	238.6	0.137	0.553
40R	0.649	1.046	6	0.361	0.000	4783.6	334.4	0.389	0.592
40R	0.649	1.046	7	0.721	0.000	1681.4	258.6	0.405	0.778
40R	0.649	1.046	8	1.082	0.000	1291.2	235.6	0.642	1.085
40R	0.649	1.046	9	1.443	0.000	764.4	180.1	0.566	1.508
39S	2.291	1.562	1	-1.443	0.000	0.0	0.0	0.337	1.454
39S	2.291	1.562	2	-1.082	0.000	1674.3	313.7	0.424	1.190
39S	2.291	1.562	3	-0.721	0.000	0.0	0.0	0.000	0.000
39S	2.291	1.562	4	-0.361	0.000	5635.9	642.6	0.606	0.865
39S	2.291	1.562	5	0.000	0.000	7927.7	783.8	0.291	0.837
39S	2.291	1.562	6	0.361	0.000	4368.7	654.3	0.417	0.870
39S	2.291	1.562	7	0.721	0.000	2606.2	334.9	0.537	0.998
39S	2.291	1.562	8	1.082	0.000	2040.7	362.5	0.689	1.213
39S	2.291	1.562	9	1.443	0.000	1057.6	290.3	0.896	1.494

SUMMARY OF GROUPED ARRAY TESTS

TEST ID	CHARGE WEIGHT (KG)	STANDOFF DISTANCE (M)	GAGE NO	GAGE LOCATION (M)	CHARGE SPACING (M)	PEAK PRESSURE (KPA)	POSITIVE IMPULSE (PA-S)	POSITIVE DURATION (MS)	TIME OF ARRIVAL (MS)
16E	0.222	0.290	1	-1.443	0.000	623.7	82.0	0.305	1.147
16E	0.222	0.290	2	-1.082	0.000	1148.0	111.7	0.310	0.708
16E	0.222	0.290	3	-0.721	0.000	1361.1	0.0	0.402	0.365
16E	0.222	0.290	4	-0.361	0.000	0.0	276.5	0.000	0.000
16E	0.222	0.290	5	0.000	0.000	51715.2	0.0	0.062	0.054
16E	0.222	0.290	6	0.361	0.000	5650.9	0.0	0.160	0.114
16E	0.222	0.290	7	0.721	0.000	1874.3	236.0	0.462	0.356
16E	0.222	0.290	8	1.082	0.000	0.0	0.0	0.000	0.000
16E	0.222	0.290	9	1.443	0.000	697.0	109.7	0.433	1.145
17E	0.222	0.290	1	-1.443	0.000	678.0	122.7	0.358	1.145
17E	0.222	0.290	2	-1.082	0.000	1036.2	137.9	0.264	0.716
17E	0.222	0.290	3	-0.721	0.000	2857.3	218.6	0.299	0.384
17E	0.222	0.290	4	-0.361	0.000	7144.8	380.6	0.160	0.150
17E	0.222	0.290	5	0.000	0.000	40217.8	3388.8	0.213	0.062
17E	0.222	0.290	6	0.361	0.000	8241.0	293.0	0.086	0.161
17E	0.222	0.290	7	0.721	0.000	1543.2	235.2	0.469	0.394
17E	0.222	0.290	8	1.082	0.000	1045.7	293.7	0.917	0.765
17E	0.222	0.290	9	1.443	0.000	694.2	119.3	0.440	1.229
18E	0.222	0.290	1	-1.443	0.000	659.7	111.7	0.550	1.183
18E	0.222	0.290	2	-1.082	0.000	0.0	0.0	0.000	0.000
18E	0.222	0.290	3	-0.721	0.000	2109.4	273.9	0.276	0.398
18E	0.222	0.290	4	-0.361	0.000	0.0	0.0	0.207	0.191
18E	0.222	0.290	5	0.000	0.000	30936.7	890.8	0.098	0.059
18E	0.222	0.290	6	0.361	0.000	10006.8	413.7	0.152	0.145
18E	0.222	0.290	7	0.721	0.000	1948.0	234.4	0.295	0.368
18E	0.222	0.290	9	1.443	0.000	0.0	136.5	0.531	1.153
13F	0.222	0.437	1	-1.443	0.000	625.2	65.2	0.291	1.247
13F	0.222	0.437	2	-1.082	0.000	1088.6	151.7	0.421	0.784
13F	0.222	0.437	3	-0.721	0.000	1997.5	219.2	0.556	0.449
13F	0.222	0.437	4	-0.361	0.000	9159.9	395.2	0.174	0.210
13F	0.222	0.437	5	0.000	0.000	0.0	0.0	0.000	0.000
13F	0.222	0.437	6	0.361	0.000	11410.5	557.8	0.190	0.200
13F	0.222	0.437	7	0.721	0.000	1530.4	275.8	0.649	0.478
13F	0.222	0.437	8	1.082	0.000	1010.2	220.6	0.518	0.848
13F	0.222	0.437	9	1.443	0.000	574.3	89.6	0.460	1.338
14F	0.222	0.437	1	-1.443	0.000	677.2	75.8	0.380	1.268
14F	0.222	0.437	2	-1.082	0.000	922.5	168.2	0.488	0.833
14F	0.222	0.437	3	-0.721	0.000	1594.5	221.3	0.454	0.418
14F	0.222	0.437	4	-0.361	0.000	11625.4	524.7	0.157	0.215
14F	0.222	0.437	6	0.361	0.000	0.0	289.6	0.174	0.208
14F	0.222	0.437	7	0.721	0.000	1327.9	188.3	0.351	0.479
14F	0.222	0.437	8	1.082	0.000	992.1	247.4	0.562	0.869
14F	0.222	0.437	9	1.443	0.000	504.9	122.1	0.565	1.299
15F	0.222	0.437	1	-1.443	0.000	650.9	64.4	0.329	1.282

SUMMARY OF GROUPED ARRAY TESTS

TEST ID	CHARGE WEIGHT (KG)	STANDOFF DISTANCE (M)	GAGE NO	GAGE LOCATION (M)	CHARGE SPACING (M)	PEAK PRESSURE (KPA)	POSITIVE IMPULSE (PA-S)	POSITIVE DURATION (MS)	TIME OF ARRIVAL (MS)
15F	0.222	0.437	2	-1.082	0.000	1067.6	124.1	0.350	0.841
15F	0.222	0.437	3	-0.721	0.000	1763.6	151.0	0.322	0.460
15F	0.222	0.437	4	-0.361	0.000	9401.0	355.9	0.078	0.216
15F	0.222	0.437	6	0.361	0.000	9108.4	325.7	0.091	0.218
15F	0.222	0.437	7	0.721	0.000	1719.2	205.1	0.351	0.427
15F	0.222	0.437	8	1.082	0.000	938.4	220.6	0.421	0.806
15F	0.222	0.437	9	1.443	0.000	615.4	129.6	1.484	1.284
10G	0.222	0.582	1	-1.443	0.000	492.1	96.5	0.452	1.455
10G	0.222	0.582	2	-1.082	0.000	813.2	283.0	0.972	0.992
10G	0.222	0.582	3	-0.721	0.000	1322.7	222.5	0.492	0.594
10G	0.222	0.582	4	-0.361	0.000	5526.9	0.0	0.000	0.325
10G	0.222	0.582	5	0.000	0.000	17381.8	797.6	0.232	0.172
10G	0.222	0.582	6	0.361	0.000	6703.8	376.7	0.273	0.307
10G	0.222	0.582	7	0.721	0.000	1187.0	224.8	0.466	0.575
10G	0.222	0.582	8	1.082	0.000	880.6	299.0	0.790	0.953
10G	0.222	0.582	9	1.443	0.000	616.0	114.5	0.661	1.420
11G	0.222	0.582	1	-1.443	0.000	724.1	70.5	0.460	1.452
11G	0.222	0.582	2	-1.082	0.000	0.0	0.0	0.000	0.000
11G	0.222	0.582	3	-0.721	0.000	1259.7	210.4	0.406	0.578
11G	0.222	0.582	4	-0.361	0.000	5937.0	556.6	0.193	0.307
11G	0.222	0.582	5	0.000	0.000	0.0	0.0	0.000	0.176
11G	0.222	0.582	6	0.361	0.000	8874.9	423.3	0.295	0.323
11G	0.222	0.582	7	0.721	0.000	2016.9	243.4	0.400	0.605
11G	0.222	0.582	8	1.082	0.000	1110.5	202.1	0.384	0.995
11G	0.222	0.582	9	1.443	0.000	755.7	122.9	0.457	1.433
12G	0.222	0.582	1	-1.443	0.000	692.5	133.8	0.117	1.430
12G	0.222	0.582	2	-1.082	0.000	1353.0	105.5	0.316	0.995
12G	0.222	0.582	3	-0.721	0.000	1484.9	131.0	0.187	0.582
12G	0.222	0.582	4	-0.361	0.000	6014.1	513.0	0.377	0.314
12G	0.222	0.582	6	0.361	0.000	8784.3	318.8	0.231	0.325
12G	0.222	0.582	7	0.721	0.000	1424.5	190.5	0.251	0.588
12G	0.222	0.582	8	1.082	0.000	1243.5	289.6	0.497	0.984
12G	0.222	0.582	9	1.443	0.000	647.7	206.2	0.548	1.418

SUMMARY OF HORIZONTAL ARRAY TESTS

TEST ID	CHARGE WEIGHT (KG)	STANDOFF DISTANCE (M)	GAGE NO	GAGE LOCATION (M)	CHARGE SPACING (M)	PEAK PRESSURE (KPA)	POSITIVE IMPULSE (PA-S)	POSITIVE DURATION (MS)	TIME OF ARRIVAL (MS)
28I	0.222	0.436	1	-1.443	0.724	1384.5	143.4	0.708	0.499
28I	0.222	0.436	2	-1.082	0.724	4567.2	325.5	1.340	0.249
28I	0.222	0.436	3	-0.721	0.724	3972.5	394.4	0.203	0.164
28I	0.222	0.436	4	-0.361	0.724	29784.0	1150.1	0.372	0.252
28I	0.222	0.436	5	0.000	0.724	19829.2	629.4	0.317	0.184
28I	0.222	0.436	6	0.361	0.724	26930.2	1322.4	0.636	0.251
28I	0.222	0.436	7	0.721	0.724	20711.7	448.8	0.186	0.145
28I	0.222	0.436	8	1.082	0.724	6140.7	517.1	0.422	0.259
28I	0.222	0.436	9	1.443	0.724	2967.5	276.0	1.310	0.532
29I	0.222	0.436	1	-1.443	0.724	1330.5	151.0	0.318	0.488
29I	0.222	0.436	2	-1.082	0.724	7848.0	346.8	0.348	0.245
29I	0.222	0.436	3	-0.721	0.724	29923.1	677.1	0.000	0.161
29I	0.222	0.436	4	-0.361	0.724	28489.0	1027.6	0.147	0.236
29I	0.222	0.436	5	0.000	0.724	20663.2	861.8	0.154	0.159
29I	0.222	0.436	6	0.361	0.724	22408.8	1491.7	0.259	0.229
29I	0.222	0.436	7	0.721	0.724	20893.3	478.5	0.117	0.154
29I	0.222	0.436	8	1.082	0.724	9632.9	377.8	0.241	0.227
29I	0.222	0.436	9	1.443	0.724	2082.4	195.4	0.500	0.478
30I	0.222	0.436	1	-1.443	0.724	1560.4	168.1	1.501	0.460
30I	0.222	0.436	2	-1.082	0.724	10676.1	374.4	0.328	0.219
30I	0.222	0.436	3	-0.721	0.724	11351.5	438.0	0.178	0.156
30I	0.222	0.436	4	-0.361	0.724	7423.2	968.0	0.240	0.227
30I	0.222	0.436	5	0.000	0.724	18980.3	648.8	0.117	0.134
30I	0.222	0.436	6	0.361	0.724	29064.0	1500.0	0.232	0.202
30I	0.222	0.436	7	0.721	0.724	16997.9	536.3	0.267	0.141
30I	0.222	0.436	8	1.082	0.724	8420.6	453.7	0.326	0.222
30I	0.222	0.436	9	1.443	0.724	1819.0	200.3	0.560	0.489
25J	0.222	0.582	1	-1.443	0.724	1342.6	120.7	1.239	0.632
25J	0.222	0.582	2	-1.082	0.724	4796.0	275.1	0.466	0.358
25J	0.222	0.582	3	-0.721	0.724	0.0	0.0	0.000	0.000
25J	0.222	0.582	4	-0.361	0.724	0.0	638.6	0.214	0.324
25J	0.222	0.582	6	0.361	0.724	16210.1	1348.6	0.336	0.311
25J	0.222	0.582	7	0.721	0.724	0.0	0.0	0.000	0.000
25J	0.222	0.582	8	1.082	0.724	6736.5	322.0	0.225	0.355
25J	0.222	0.582	9	1.443	0.724	1554.9	186.5	0.594	0.633
26J	0.222	0.582	1	-1.443	0.724	1481.2	158.6	0.418	0.645
26J	0.222	0.582	2	-1.082	0.724	4320.3	254.4	0.458	0.376
26J	0.222	0.582	3	-0.721	0.724	0.0	44.8	0.110	0.208
26J	0.222	0.582	4	-0.361	0.724	15384.0	663.7	0.223	0.303
26J	0.222	0.582	5	0.000	0.724	11591.5	1432.5	0.169	0.258
26J	0.222	0.582	6	0.361	0.724	17025.2	1439.6	0.420	0.339
26J	0.222	0.582	7	0.721	0.724	0.0	0.0	0.000	0.000
26J	0.222	0.582	8	1.082	0.724	4214.5	340.6	0.415	0.385
26J	0.222	0.582	9	1.443	0.724	1649.7	177.6	0.411	0.647

SUMMARY OF HORIZONTAL ARRAY TESTS

TEST ID	CHARGE WEIGHT (KG)	STANDOFF DISTANCE (M)	GAGE NO	GAGE LOCATION (M)	CHARGE SPACING (M)	PEAK PRESSURE (KPA)	POSITIVE IMPULSE (PA-S)	POSITIVE DURATION (MS)	TIME OF ARRIVAL (MS)
27J	0.222	0.582	1	-1.443	0.724	1558.1	196.8	0.720	0.611
27J	0.222	0.582	2	-1.082	0.724	0.0	702.7	0.365	0.365
27J	0.222	0.582	3	-0.721	0.724	9170.6	357.1	0.186	0.267
27J	0.222	0.582	4	-0.361	0.724	18367.9	878.[illegible]	0.246	0.345
27J	0.222	0.582	5	0.000	0.724	12013.0	0.0	0.126	0.279
27J	0.222	0.582	6	0.361	0.724	18750.8	711.8	0.233	0.347
27J	0.222	0.582	7	0.721	0.724	10826.5	345.5	0.086	0.267
27J	0.222	0.582	8	1.082	0.724	5950.8	428.2	0.357	0.369
27J	0.222	0.582	9	1.443	0.724	2193.2	254.5	0.505	0.629
31N	0.222	0.724	1	-1.443	0.724	971.6	135.8	0.441	0.732
31N	0.222	0.724	2	-1.082	0.724	2321.5	440.6	0.515	0.420
31N	0.222	0.724	3	-0.721	0.724	1126.1	304.2	0.171	0.378
31N	0.222	0.724	4	-0.361	0.724	13951.8	797.8	0.365	0.411
31N	0.222	0.724	5	0.000	0.724	7312.3	1019.5	0.000	0.366
31N	0.222	0.724	6	0.361	0.724	8213.7	455.2	0.096	0.393
31N	0.222	0.724	7	0.721	0.724	5014.4	123.5	0.056	0.383
31N	0.222	0.724	8	1.082	0.724	3785.0	250.6	0.518	0.460
31N	0.222	0.724	9	1.443	0.724	1370.8	146.9	0.444	0.727
32N	0.222	0.724	1	-1.443	0.724	1338.9	161.9	0.345	0.771
32N	0.222	0.724	2	-1.082	0.724	4667.6	371.6	0.513	0.462
32N	0.222	0.724	3	-0.721	0.724	4880.1	317.2	0.147	0.388
32N	0.222	0.724	4	-0.361	0.724	0.0	0.0	0.000	0.000
32N	0.222	0.724	5	0.000	0.724	0.0	0.0	0.000	0.000
32N	0.222	0.724	6	0.361	0.724	0.0	0.0	0.000	0.000
32N	0.222	0.724	7	0.721	0.724	3718.3	186.8	0.000	0.372
32N	0.222	0.724	8	1.082	0.724	3895.3	355.0	0.415	0.454
32N	0.222	0.724	9	1.443	0.724	1838.8	223.2	0.367	0.717
33N	0.222	0.724	1	-1.443	0.724	1230.7	126.9	0.444	0.722
33N	0.222	0.724	2	-1.082	0.724	4695.1	286.1	0.504	0.470
33N	0.222	0.724	3	-0.721	0.724	0.0	0.0	0.000	0.000
33N	0.222	0.724	4	-0.361	0.724	0.0	0.0	0.000	0.000
33N	0.222	0.724	5	0.000	0.724	0.0	0.0	0.000	0.000
33N	0.222	0.724	6	0.361	0.724	55514.8	5535.8	0.334	0.421
33N	0.222	0.724	7	0.721	0.724	0.0	0.0	0.000	0.000
33N	0.222	0.724	8	1.082	0.724	4577.4	342.1	0.401	0.452
33N	0.222	0.724	9	1.443	0.724	1409.0	205.5	0.557	0.672
34N	0.222	0.724	1	-1.443	0.724	1243.1	131.9	0.383	0.712
34N	0.222	0.724	2	-1.082	0.724	5095.9	144.8	0.351	0.446
34N	0.222	0.724	3	-0.721	0.724	6853.4	278.5	0.153	0.365
34N	0.222	0.724	4	-0.361	0.724	12512.0	784.6	0.000	0.407
34N	0.222	0.724	5	0.000	0.724	6714.9	396.6	0.133	0.372
34N	0.222	0.724	6	0.361	0.724	0.0	0.0	0.000	0.000
34N	0.222	0.724	9	1.443	0.724	0.0	0.0	0.000	0.000
35P	0.222	0.724	1	-1.443	0.361	5993.0	1005.3	0.820	1.141

SUMMARY OF HORIZONTAL ARRAY TESTS

TEST ID	CHARGE WEIGHT (KG)	STANDOFF DISTANCE (M)	GAGE NO	GAGE LOCATION (M)	CHARGE SPACING (M)	PEAK PRESSURE (KPA)	POSITIVE IMPULSE (PA-S)	POSITIVE DURATION (MS)	TIME OF ARRIVAL (MS)
35P	0.222	0.724	2	-1.082	0.361	1215.6	144.8	0.517	0.716
35P	0.222	0.724	3	-0.721	0.361	3158.2	299.9	0.360	0.460
35P	0.222	0.724	4	-0.361	0.361	10588.8	732.9	0.458	0.362
35P	0.222	0.724	5	0.000	0.361	17396.7	631.9	0.082	0.350
35P	0.222	0.724	6	0.361	0.361	6763.8	439.9	0.381	0.381
35P	0.222	0.724	7	0.721	0.361	2218.8	156.5	0.407	0.474
35P	0.222	0.724	8	1.082	0.361	14820.1	2193.8	0.609	0.726
35P	0.222	0.724	9	1.443	0.361	6958.7	1376.5	0.608	1.156
36P	0.222	0.724	1	-1.443	0.361	563.4	111.7	0.516	1.140
36P	0.222	0.724	2	-1.082	0.361	1564.2	171.5	0.537	0.691
36P	0.222	0.724	3	-0.721	0.361	3275.1	285.4	0.340	0.475
36P	0.222	0.724	4	-0.361	0.361	11395.5	754.3	0.460	0.353
36P	0.222	0.724	5	0.000	0.361	14990.0	1031.4	0.111	0.373
36P	0.222	0.724	6	0.361	0.361	9914.9	701.9	0.571	0.357
36P	0.222	0.724	7	0.721	0.361	1748.9	137.2	0.377	0.473
36P	0.222	0.724	8	1.082	0.361	1375.4	281.7	0.507	0.712
36P	0.222	0.724	9	1.443	0.361	581.5	156.5	0.697	1.153
37P	0.222	0.724	1	-1.443	0.361	583.0	95.7	0.471	1.100
37P	0.222	0.724	2	-1.082	0.361	1761.6	189.0	0.752	0.675
37P	0.222	0.724	3	-0.721	0.361	2012.3	282.0	0.425	0.437
37P	0.222	0.724	4	-0.361	0.361	13478.6	434.9	0.221	0.360
37P	0.222	0.724	5	0.000	0.361	14168.6	1135.5	0.427	0.356
37P	0.222	0.724	6	0.361	0.361	9290.6	590.2	0.284	0.362
37P	0.222	0.724	7	0.721	0.361	2420.0	155.7	0.334	0.472
37P	0.222	0.724	8	1.082	0.361	2057.0	176.7	0.546	0.702
37P	0.222	0.724	9	1.443	0.361	678.6	141.3	0.611	1.136
41G	0.222	0.724	1	-1.443	1.082	0.0	0.0	0.000	0.000
41G	0.222	0.724	2	-1.082	1.082	0.0	0.0	0.000	0.000
41G	0.222	0.724	3	-0.721	1.082	3145.0	410.4	0.581	0.463
41G	0.222	0.724	4	-0.361	1.082	3794.0	472.4	0.633	0.478
41G	0.222	0.724	6	0.361	1.082	3764.5	466.2	0.609	0.478
41G	0.222	0.724	7	0.721	1.082	2354.0	229.8	0.498	0.461
41G	0.222	0.724	9	1.443	1.082	4138.9	300.9	0.414	0.465
42G	0.222	0.724	1	-1.443	1.082	3265.9	219.9	0.282	0.453
42G	0.222	0.724	2	-1.082	1.082	6449.0	365.3	0.347	0.393
42G	0.222	0.724	3	-0.721	1.082	2987.9	375.2	0.269	0.467
42G	0.222	0.724	4	-0.361	1.082	3071.2	445.9	0.731	0.454
42G	0.222	0.724	5	0.000	1.082	3480.9	595.7	0.358	0.417
42G	0.222	0.724	6	0.361	1.082	4880.9	493.3	0.665	0.443
42G	0.222	0.724	7	0.721	1.082	2466.6	333.8	0.580	0.488
42G	0.222	0.724	8	1.082	1.082	5659.6	324.7	0.300	0.304
42G	0.222	0.724	9	1.443	1.082	4761.7	404.8	0.404	0.457
43G	0.222	0.724	1	-1.443	1.082	3186.2	265.8	0.379	0.465
43G	0.222	0.724	2	-1.082	1.082	6899.7	351.6	0.294	0.396

SUMMARY OF VERTICAL ARRAY TESTS

TEST ID	CHARGE WEIGHT (KG)	STANDOFF DISTANCE (M)	GAGE NO	GAGE LOCATION (M)	CHARGE SPACING (M)	PEAK PRESSURE (KPA)	POSITIVE IMPULSE (PA-S)	POSITIVE DURATION (MS)	TIME OF ARRIVAL (MS)
19M	0.222	0.442	1	-1.443	0.145	843.0	153.8	0.424	1.029
19M	0.222	0.442	2	-1.082	0.145	1776.8	239.9	0.417	0.669
19M	0.222	0.442	3	-0.721	0.145	0.0	0.0	0.000	0.000
19M	0.222	0.442	4	-0.361	0.145	958.5	44.1	0.177	0.182
19M	0.222	0.442	6	0.361	0.145	5410.2	362.5	0.123	0.175
19M	0.222	0.442	7	0.721	0.145	2637.6	341.1	0.366	0.418
19M	0.222	0.442	8	1.082	0.145	1980.5	301.1	0.406	0.699
19M	0.222	0.442	9	1.443	0.145	1442.9	105.4	0.273	1.062
23M	0.222	0.442	1	-1.443	0.145	1122.7	204.8	0.484	1.041
23M	0.222	0.442	2	-1.082	0.145	1923.1	271.0	0.352	0.648
23M	0.222	0.442	3	-0.721	0.145	2263.4	293.7	0.332	0.409
23M	0.222	0.442	4	-0.361	0.145	10401.1	334.4	0.106	0.178
23M	0.222	0.442	5	0.000	0.145	0.0	0.0	0.000	0.000
23M	0.222	0.442	6	0.361	0.145	2153.6	0.0	0.000	0.167
23M	0.222	0.442	7	0.721	0.145	0.0	0.0	0.000	0.000
23M	0.222	0.442	8	1.082	0.145	2064.6	354.3	0.493	0.679
23M	0.222	0.442	9	1.443	0.145	1116.9	192.9	0.687	1.028
24M	0.222	0.442	1	-1.443	0.145	856.1	110.3	0.419	1.043
24M	0.222	0.442	2	-1.082	0.145	0.0	0.0	0.000	0.000
24M	0.222	0.442	3	-0.721	0.145	3679.4	286.8	0.414	0.399
24M	0.222	0.442	4	-0.361	0.145	8407.9	0.0	0.000	0.172
24M	0.222	0.442	5	0.000	0.145	0.0	0.0	0.000	0.000
24M	0.222	0.442	6	0.361	0.145	6116.1	575.8	0.258	0.172
24M	0.222	0.442	7	0.721	0.145	4606.7	575.0	0.543	0.427
24M	0.222	0.442	8	1.082	0.145	2091.4	319.2	0.402	0.684
24M	0.222	0.442	9	1.443	0.145	1388.1	243.4	0.509	1.061
44M	0.222	0.442	1	-1.443	0.145	1007.7	144.1	0.604	0.904
44M	0.222	0.442	2	-1.082	0.145	2814.3	339.7	0.435	0.600
44M	0.222	0.442	3	-0.721	0.145	3662.4	288.6	0.314	0.348
44M	0.222	0.442	4	-0.361	0.145	8388.4	292.6	0.171	0.163
44M	0.222	0.442	5	0.000	0.145	49384.3	1414.3	0.335	0.077
44M	0.222	0.442	6	0.361	0.145	11259.1	368.9	0.176	0.139
44M	0.222	0.442	7	0.721	0.145	2369.0	198.2	0.349	0.358
44M	0.222	0.442	8	1.082	0.145	2977.8	364.9	0.099	0.600
44M	0.222	0.442	9	1.443	0.145	1380.3	225.2	1.136	0.909

TABLE A.2 ENGLISH UNIT SUMMARY

SUMMARY OF SINGLE CHARGE TEST DATA

TEST ID	CHARGE WEIGHT (LBS)	STANDOFF DISTANCE (IN)	GAGE NO	GAGE LOCATION (IN)	CHARGE SPACING (IN)	PEAK PRESSURE (PSI)	POSITIVE IMPULSE (PSI-MS)	POSITIVE DURATION (MS)	TIME OF ARRIVAL (MS)
1A	1.430	17.20	1	-56.800	0.000	89.6	12.6	0.437	1.073
1A	1.430	17.20	2	-42.600	0.000	178.8	0.0	0.379	0.655
1A	1.430	17.20	3	-28.400	0.000	666.7	47.6	0.203	0.384
1A	1.430	17.20	4	-14.200	0.000	2486.1	90.6	0.236	0.203
1A	1.430	17.20	5	0.000	0.000	4600.5	144.3	0.000	0.125
1A	1.430	17.20	6	14.200	0.000	2991.7	36.5	0.000	0.197
1A	1.430	17.20	7	28.400	0.000	708.4	33.8	0.000	0.398
1A	1.430	17.20	8	42.600	0.000	135.2	24.8	0.000	0.682
1A	1.430	17.20	9	56.800	0.000	90.4	17.9	0.749	1.098
2A	1.430	17.20	1	-56.800	0.000	87.2	13.0	0.427	1.039
2A	1.430	17.20	2	-42.600	0.000	169.3	20.2	0.432	0.655
2A	1.430	17.20	3	-28.400	0.000	371.0	31.2	0.192	0.363
2A	1.430	17.20	4	-14.200	0.000	1304.5	95.4	0.357	0.181
2A	1.430	17.20	5	0.000	0.000	1980.1	160.6	0.129	0.106
2A	1.430	17.20	6	14.200	0.000	3046.7	69.1	0.101	0.186
2A	1.430	17.20	7	28.400	0.000	355.9	38.1	0.376	0.379
2A	1.430	17.20	8	42.600	0.000	196.5	16.5	0.303	0.670
2A	1.430	17.20	9	56.800	0.000	79.9	0.0	7.487	1.073
3A	1.430	17.20	1	-56.800	0.000	93.4	10.7	0.351	1.039
3A	1.430	17.20	2	-42.600	0.000	277.0	21.2	0.393	0.660
3A	1.430	17.20	3	-28.400	0.000	580.7	46.5	0.277	0.382
3A	1.430	17.20	4	-14.200	0.000	2093.6	96.4	0.246	0.195
3A	1.430	17.20	5	0.000	0.000	2732.1	104.2	0.113	0.131
3A	1.430	17.20	6	14.200	0.000	2475.1	116.9	0.180	0.193
3A	1.430	17.20	7	28.400	0.000	659.7	39.6	0.211	0.396
3A	1.430	17.20	8	42.600	0.000	218.6	26.4	0.418	0.673
3A	1.430	17.20	9	56.800	0.000	0.0	0.0	0.000	0.000
20B	5.050	25.70	1	-56.800	0.000	242.9	33.7	0.381	0.801
20B	5.050	25.70	2	-42.600	0.000	553.1	54.9	0.378	0.521
20B	5.050	25.70	3	-28.400	0.000	1513.3	145.0	0.722	0.361
20B	5.050	25.70	4	-14.200	0.000	4338.6	166.4	0.216	0.204
20B	5.050	25.70	5	0.000	0.000	8992.5	398.9	0.260	0.125
20B	5.050	25.70	6	14.200	0.000	4678.6	214.1	0.309	0.196
20B	5.050	25.70	7	28.400	0.000	1388.2	61.9	0.203	0.349
20B	5.050	25.70	8	42.600	0.000	673.2	65.7	0.376	0.527
20B	5.050	25.70	9	56.800	0.000	228.6	27.7	0.484	0.738
21B	5.050	25.70	1	-56.800	0.000	241.6	34.0	0.492	0.738
21B	5.050	25.70	2	-42.600	0.000	463.8	57.2	0.330	0.499
21B	5.050	25.70	3	-28.400	0.000	711.3	99.5	0.442	0.313
21B	5.050	25.70	4	-14.200	0.000	3277.1	218.1	0.250	0.188
21B	5.050	25.70	6	14.200	0.000	3921.4	291.1	0.212	0.202
21B	5.050	25.70	7	28.400	0.000	1819.1	121.4	0.178	0.331
21B	5.050	25.70	8	42.600	0.000	583.0	73.1	0.382	0.499
21B	5.050	25.70	9	56.800	0.000	229.9	33.9	0.862	0.769

SUMMARY OF SINGLE CHARGE TEST DATA

TEST ID	CHARGE WEIGHT (LBS)	STANDOFF DISTANCE (IN)	GAGE NO	GAGE LOCATION (IN)	CHARGE SPACING (IN)	PEAK PRESSURE (PSI)	POSITIVE IMPULSE (PSI-MS)	POSITIVE DURATION (MS)	TIME OF ARRIVAL (MS)
2B	5.050	25.70	1	-56.800	0.000	240.2	31.3	0.344	0.752
2B	5.050	25.70	2	-42.600	0.000	581.3	58.3	0.315	0.503
2B	5.050	25.70	3	-28.400	0.000	1286.3	139.3	0.459	0.314
2B	5.050	25.70	4	-14.200	0.000	4844.4	225.4	0.225	0.196
2B	5.050	25.70	6	14.200	0.000	5161.9	266.8	0.240	0.183
2B	5.050	25.70	7	28.400	0.000	2289.7	161.2	0.233	0.320
2B	5.050	25.70	8	42.600	0.000	601.8	73.3	0.469	0.497
2B	5.050	25.70	9	56.800	0.000	256.8	42.4	0.731	0.744
7C	1.430	11.40	1	-56.800	0.000	105.6	12.7	0.356	0.982
7C	1.430	11.40	2	-42.600	0.000	178.2	24.5	0.448	0.580
7C	1.430	11.40	3	-28.400	0.000	481.0	38.5	0.295	0.319
7C	1.430	11.40	4	-14.200	0.000	2091.0	109.4	0.196	0.146
7C	1.430	11.40	5	0.000	0.000	11267.2	223.3	0.211	0.086
7C	1.430	11.40	6	14.200	0.000	2209.1	106.3	0.162	0.154
7C	1.430	11.40	7	28.400	0.000	483.8	31.8	0.187	0.332
7C	1.430	11.40	8	42.600	0.000	211.8	24.6	0.581	0.615
7C	1.430	11.40	9	56.800	0.000	0.0	0.0	0.000	0.000
8C	1.430	11.40	1	-56.800	0.000	125.9	16.9	0.384	0.982
8C	1.430	11.40	2	-42.600	0.000	284.6	26.2	0.439	0.590
8C	1.430	11.40	3	-28.400	0.000	541.7	40.1	0.312	0.328
8C	1.430	11.40	4	-14.200	0.000	2220.8	80.0	0.209	0.149
8C	1.430	11.40	5	0.000	0.000	11207.6	290.6	0.295	0.075
8C	1.430	11.40	6	14.200	0.000	3887.9	76.5	0.233	0.140
8C	1.430	11.40	7	28.400	0.000	632.7	49.1	0.785	0.352
8C	1.430	11.40	8	42.600	0.000	255.9	32.6	0.518	0.620
8C	1.430	11.40	9	56.800	0.000	140.9	23.1	1.863	1.023
9C	1.430	11.40	1	-56.800	0.000	128.6	16.7	0.385	1.010
9C	1.430	11.40	2	-42.600	0.000	257.3	27.0	0.505	0.611
9C	1.430	11.40	3	-28.400	0.000	478.8	44.0	0.372	0.331
9C	1.430	11.40	4	-14.200	0.000	1281.3	50.3	0.142	0.158
9C	1.430	11.40	5	0.000	0.000	11229.1	413.2	0.336	0.125
9C	1.430	11.40	6	14.200	0.000	2610.8	81.0	0.119	0.145
9C	1.430	11.40	7	28.400	0.000	502.9	36.2	0.251	0.332
9C	1.430	11.40	8	42.600	0.000	279.1	30.4	0.456	0.611
9C	1.430	11.40	9	56.800	0.000	0.0	0.0	0.000	0.000
4D	1.430	22.90	1	-56.800	0.000	82.8	16.3	0.000	1.211
4D	1.430	22.90	2	-42.600	0.000	232.8	26.3	0.436	0.781
4D	1.430	22.90	3	-28.400	0.000	338.0	50.3	0.000	0.473
4D	1.430	22.90	4	-14.200	0.000	1753.5	113.6	0.288	0.270
4D	1.430	22.90	6	14.200	0.000	1940.9	120.3	0.000	0.276
4D	1.430	22.90	7	28.400	0.000	463.1	42.9	0.000	0.494
4D	1.430	22.90	8	42.600	0.000	240.9	36.6	0.728	0.711
4D	1.430	22.90	9	56.800	0.000	90.8	19.8	0.000	1.213
5D	1.430	22.90	1	-56.800	0.000	0.0	0.0	0.000	0.000

SUMMARY OF SINGLE CHARGE TEST DATA

TEST ID	CHARGE WEIGHT (LBS)	STANDOFF DISTANCE (IN)	GAGE NO	GAGE LOCATION (IN)	CHARGE SPACING (IN)	PEAK PRESSURE (PSI)	POSITIVE IMPULSE (PSI-MS)	POSITIVE DURATION (MS)	TIME OF ARRIVAL (MS)
5D	1.430	22.90	2	-42.600	0.000	285.8	45.6	0.395	1.231
5D	1.430	22.90	3	-28.400	0.000	410.8	36.0	0.640	0.501
5D	1.430	22.90	4	-14.200	0.000	1701.9	117.7	0.508	0.298
5D	1.430	22.90	5	0.000	0.000	2514.3	116.3	0.254	0.210
5D	1.430	22.90	6	14.200	0.000	2066.6	89.6	0.192	0.272
5D	1.430	22.90	7	28.400	0.000	512.2	46.9	0.582	0.468
5D	1.430	22.90	8	42.600	0.000	266.9	37.4	0.674	0.751
5D	1.430	22.90	9	56.800	0.000	85.4	22.0	0.691	1.148
6D	1.430	22.90	1	-56.800	0.000	93.3	13.5	0.366	1.140
6D	1.430	22.90	2	-42.600	0.000	175.3	24.0	0.414	0.742
6D	1.430	22.90	3	-28.400	0.000	300.8	80.0	0.768	0.419
6D	1.430	22.90	4	-14.200	0.000	1973.1	97.2	0.377	0.272
6D	1.430	22.90	5	0.000	0.000	2873.4	104.0	0.166	0.205
6D	1.430	22.90	6	14.200	0.000	1751.1	115.9	0.238	0.274
6D	1.430	22.90	7	28.400	0.000	525.3	51.4	0.499	0.473
6D	1.430	22.90	8	42.600	0.000	218.9	24.7	0.449	0.778
6D	1.430	22.90	9	56.800	0.000	80.7	18.6	0.798	0.251
38R	1.430	41.20	1	-56.800	0.000	103.1	9.1	0.232	1.510
38R	1.430	41.20	2	-42.600	0.000	188.2	29.2	0.575	1.118
38R	1.430	41.20	3	-28.400	0.000	322.1	44.7	0.731	0.813
38R	1.430	41.20	4	-14.200	0.000	655.7	54.3	0.428	0.621
38R	1.430	41.20	5	0.000	0.000	0.0	74.3	0.152	0.560
38R	1.430	41.20	6	14.200	0.000	536.9	37.8	0.360	0.623
38R	1.430	41.20	7	28.400	0.000	204.7	27.8	0.311	0.813
38R	1.430	41.20	8	42.600	0.000	191.2	27.9	0.585	1.111
38R	1.430	41.20	9	56.800	0.000	114.3	28.8	0.745	1.489
40R	1.430	41.20	1	-56.800	0.000	81.1	12.0	0.357	1.514
40R	1.430	41.20	2	-42.600	0.000	188.5	31.1	0.483	1.095
40R	1.430	41.20	3	-28.400	0.000	191.8	29.4	0.640	0.773
40R	1.430	41.20	4	-14.200	0.000	667.9	61.5	0.456	0.592
40R	1.430	41.20	5	0.000	0.000	708.6	34.6	0.137	0.553
40R	1.430	41.20	6	14.200	0.000	693.8	48.5	0.389	0.592
40R	1.430	41.20	7	28.400	0.000	243.9	37.5	0.405	0.778
40R	1.430	41.20	8	42.600	0.000	187.3	34.2	0.642	1.085
40R	1.430	41.20	9	56.800	0.000	110.9	26.1	0.566	1.508
39S	5.050	61.50	1	-56.800	0.000	0.0	0.0	0.337	1.454
39S	5.050	61.50	2	-42.600	0.000	242.8	45.5	0.424	1.190
39S	5.050	61.50	3	-28.400	0.000	0.0	0.0	0.000	0.000
39S	5.050	61.50	4	-14.200	0.000	817.4	93.2	0.606	0.865
39S	5.050	61.50	5	0.000	0.000	1149.8	113.7	0.291	0.837
39S	5.050	61.50	6	14.200	0.000	633.6	94.9	0.417	0.870
39S	5.050	61.50	7	28.400	0.000	378.0	48.6	0.567	0.998
39S	5.050	61.50	8	42.600	0.000	296.0	52.6	0.689	1.213
39S	5.050	61.50	9	56.800	0.000	153.4	42.1	0.896	1.494

SUMMARY OF GROUPED ARRAY TESTS

TEST ID	CHARGE WEIGHT (LBS)	STANDOFF DISTANCE (IN)	GAGE NO	GAGE LOCATION (IN)	CHARGE SPACING (IN)	PEAK PRESSURE (PSI)	POSITIVE IMPULSE (PSI-MS)	POSITIVE DURATION (MS)	TIME OF ARRIVAL (MS)
16E	0.490	11.40	1	-56.800	0.000	90.5	11.9	0.305	1.147
16E	0.490	11.40	2	-42.600	0.000	166.5	16.2	0.310	0.708
16E	0.490	11.40	3	-28.400	0.000	197.4	0.0	0.402	0.365
16E	0.490	11.40	4	-14.200	0.000	0.0	40.1	0.000	0.000
16E	0.490	11.40	5	0.000	0.000	7500.7	0.0	0.062	0.054
16E	0.490	11.40	6	14.200	0.000	819.6	0.0	0.160	0.114
16E	0.490	11.40	7	28.400	0.000	271.8	34.2	0.462	0.356
16E	0.490	11.40	8	42.600	0.000	0.0	0.0	0.000	0.000
16E	0.490	11.40	9	56.800	0.000	101.1	15.9	0.433	1.145
17E	0.490	11.40	1	-56.800	0.000	98.3	17.8	0.358	1.145
17E	0.490	11.40	2	-42.600	0.000	150.3	20.0	0.264	0.716
17E	0.490	11.40	3	-28.400	0.000	414.4	31.7	0.299	0.384
17E	0.490	11.40	4	-14.200	0.000	1036.3	55.2	0.160	0.150
17E	0.490	11.40	5	0.000	0.000	5833.1	491.5	0.213	0.062
17E	0.490	11.40	6	14.200	0.000	1195.3	42.5	0.086	0.161
17E	0.490	11.40	7	28.400	0.000	223.8	34.1	0.469	0.394
17E	0.490	11.40	8	42.600	0.000	151.7	42.6	0.917	0.765
17E	0.490	11.40	9	56.800	0.000	100.7	17.3	0.440	1.229
18E	0.490	11.40	1	-56.800	0.000	95.7	16.2	0.550	1.183
18E	0.490	11.40	2	-42.600	0.000	0.0	0.0	0.000	0.000
18E	0.490	11.40	3	-28.400	0.000	305.9	39.7	0.276	0.398
18E	0.490	11.40	4	-14.200	0.000	0.0	0.0	0.207	0.191
18E	0.490	11.40	5	0.000	0.000	4487.0	129.2	0.098	0.059
18E	0.490	11.40	6	14.200	0.000	1451.4	60.0	0.152	0.145
18E	0.490	11.40	7	28.400	0.000	282.5	34.0	0.295	0.34[illegible]
18E	0.490	11.40	9	56.800	0.000	0.0	19.8	0.531	1.153
13F	0.490	17.20	1	-56.800	0.000	90.7	9.5	0.291	1.247
13F	0.490	17.20	2	-42.600	0.000	157.9	22.0	0.421	0.784
13F	0.490	17.20	3	-28.400	0.000	289.7	31.8	0.556	0.449
13F	0.490	17.20	4	-14.200	0.000	1328.5	57.3	0.174	0.210
13F	0.490	17.20	5	0.000	0.000	0.0	0.0	0.000	0.000
13F	0.490	17.20	6	14.200	0.000	1655.0	80.9	0.190	0.200
13F	0.490	17.20	7	28.400	0.000	222.0	40.0	0.649	0.478
13F	0.490	17.20	8	42.600	0.000	146.5	32.0	0.518	0.818
13F	0.490	17.20	9	56.800	0.000	83.3	13.0	0.460	1.338
14F	0.490	17.20	1	-56.800	0.000	98.2	11.0	0.380	1.268
14F	0.490	17.20	2	-42.600	0.000	133.8	24.4	0.488	0.833
14F	0.490	17.20	3	-28.400	0.000	231.3	32.1	0.454	0.418
14F	0.490	17.20	4	-14.200	0.000	1686.1	76.1	0.157	0.215
14F	0.490	17.20	6	14.200	0.000	0.0	42.0	0.174	0.208
14F	0.490	17.20	7	28.400	0.000	192.6	27.3	0.351	0.479
14F	0.490	17.20	8	42.600	0.000	143.9	35.9	0.562	0.869
14F	0.490	17.20	9	56.800	0.000	73.2	17.7	0.565	1.299
15F	0.490	17.20	1	-56.800	0.000	94.4	9.3	0.329	1.282

SUMMARY OF GROUPED ARRAY TESTS

TEST ID	CHARGE WEIGHT (LBS)	STANDOFF DISTANCE (IN)	GAGE NO	GAGE LOCATION (IN)	CHARGE SPACING (IN)	PEAK PRESSURE (PSI)	POSITIVE IMPULSE (PSI-MS)	POSITIVE DURATION (MS)	TIME OF ARRIVAL (MS)
15F	0.490	17.20	2	-42.600	0.000	157.7	18.0	0.350	0.841
15F	0.490	17.20	3	-28.400	0.000	255.8	21.9	0.322	0.460
15F	0.490	17.20	4	-14.200	0.000	1363.5	51.6	0.078	0.216
15F	0.490	17.20	6	14.200	0.000	1321.1	47.2	0.091	0.218
15F	0.490	17.20	7	28.400	0.000	249.3	29.7	0.351	0.427
15F	0.490	17.20	8	42.600	0.000	136.1	32.0	0.421	0.806
15F	0.490	17.20	9	56.800	0.000	89.2	18.8	1.404	1.284
10G	0.490	22.92	1	-56.800	0.000	71.4	14.0	0.452	1.455
10G	0.490	22.92	2	-42.600	0.000	117.9	41.0	0.972	0.992
10G	0.490	22.92	3	-28.400	0.000	191.8	32.3	0.492	0.594
10G	0.490	22.92	4	-14.200	0.000	801.6	0.0	0.000	0.325
10G	0.490	22.92	5	0.000	0.000	2521.0	115.7	0.232	0.172
10G	0.490	22.92	6	14.200	0.000	972.3	54.6	0.273	0.307
10G	0.490	22.92	7	28.400	0.000	172.2	32.6	0.466	0.575
10G	0.490	22.92	8	42.600	0.000	127.7	43.4	0.790	0.953
10G	0.490	22.92	9	56.800	0.000	89.3	16.6	0.661	1.420
11G	0.490	22.92	1	-56.800	0.000	105.0	10.2	0.460	1.452
11G	0.490	22.92	2	-42.600	0.000	0.0	0.0	0.000	0.000
11G	0.490	22.92	3	-28.400	0.000	182.7	30.5	0.406	0.578
11G	0.490	22.92	4	-14.200	0.000	861.1	80.7	0.193	0.397
11G	0.490	22.92	5	0.000	0.000	0.0	0.0	0.000	0.176
11G	0.490	22.92	6	14.200	0.000	1287.2	61.4	0.295	0.323
11G	0.490	22.92	7	28.400	0.000	292.5	35.3	0.400	0.605
11G	0.490	22.92	8	42.600	0.000	161.1	29.3	0.384	0.995
11G	0.490	22.92	9	56.800	0.000	109.6	17.8	0.457	1.433
12G	0.490	22.92	1	-56.800	0.000	100.4	19.4	0.177	1.430
12G	0.490	22.92	2	-42.600	0.000	196.2	15.3	0.316	0.995
12G	0.490	22.92	3	-28.400	0.000	215.4	19.0	0.187	0.582
12G	0.490	22.92	4	-14.200	0.000	872.3	74.4	0.377	0.314
12G	0.490	22.92	6	14.200	0.000	1274.1	46.2	0.231	0.335
12G	0.490	22.92	7	28.400	0.000	206.6	27.6	0.251	0.588
12G	0.490	22.92	8	42.600	0.000	180.4	42.0	0.497	0.984
12G	0.490	22.92	9	56.800	0.000	93.9	29.9	0.548	1.418

SUMMARY OF VERTICAL ARRAY TESTS

TEST ID	CHARGE WEIGHT (LBS)	STANDOFF DISTANCE (IN)	GAGE NO	GAGE LOCATION (IN)	CHARGE SPACING (IN)	PEAK PRESSURE (PSI)	POSITIVE IMPULSE (PSI-MS)	POSITIVE DURATION (MS)	TIME OF ARRIVAL (MS)
19M	0.490	17.40	1	-56.800	5.700	122.3	22.3	0.424	1.029
19M	0.490	17.40	2	-42.600	5.700	257.7	34.8	0.417	0.669
19M	0.490	17.40	3	-28.400	5.700	0.0	0.0	0.000	0.000
19M	0.490	17.40	4	-14.200	5.700	139.0	6.4	0.177	0.182
19M	0.490	17.40	6	14.200	5.700	784.7	52.6	0.123	0.175
19M	0.490	17.40	7	28.400	5.700	382.6	49.5	0.366	0.418
19M	0.490	17.40	8	42.600	5.700	287.3	43.7	0.406	0.699
19M	0.490	17.40	9	56.800	5.700	209.3	15.3	0.273	1.062
23M	0.490	17.40	1	-56.800	5.700	162.8	29.7	0.484	1.041
23M	0.490	17.40	2	-42.600	5.700	278.9	39.3	0.352	0.648
23M	0.490	17.40	3	-28.400	5.700	328.3	42.6	0.332	0.409
23M	0.490	17.40	4	-14.200	5.700	1508.6	48.5	0.106	0.178
23M	0.490	17.40	5	0.000	5.700	0.0	0.0	0.000	0.000
23M	0.490	17.40	6	14.200	5.700	312.3	0.0	0.000	0.167
23M	0.490	17.40	7	28.400	5.700	0.0	0.0	0.000	0.000
23M	0.490	17.40	8	42.600	5.700	299.4	51.4	0.493	0.679
23M	0.490	17.40	9	56.800	5.700	162.0	28.0	0.687	1.028
24M	0.490	17.40	1	-56.800	5.700	124.2	16.0	0.419	1.043
24M	0.490	17.40	2	-42.600	5.700	0.0	0.0	0.000	0.000
24M	0.490	17.40	3	-28.400	5.700	533.6	41.6	0.414	0.399
24M	0.490	17.40	4	-14.200	5.700	1219.5	0.0	0.000	0.172
24M	0.490	17.40	5	0.000	5.700	0.0	0.0	0.000	0.000
24M	0.490	17.40	6	14.200	5.700	887.1	83.5	0.258	0.172
24M	0.490	17.40	7	28.400	5.700	668.2	83.4	0.543	0.427
24M	0.490	17.40	8	42.600	5.700	303.3	46.3	0.402	0.684
24M	0.490	17.40	9	56.800	5.700	201.3	35.3	0.509	1.061
44M	0.490	17.40	1	-56.800	5.700	146.2	20.9	0.604	0.904
44M	.490	17.40	2	-42.600	5.700	408.2	49.3	0.435	0.600
44M	0.490	17.40	3	-28.400	5.700	531.2	41.9	0.314	0.348
44M	0.490	17.40	4	-14.200	5.700	1216.6	42.4	0.171	0.163
44M	0.490	17.40	5	0.000	5.700	7162.6	205.1	0.335	0.077
44M	0.490	17.40	6	14.200	5.700	1633.0	53.5	0.176	0.159
44M	0.490	17.40	7	28.400	5.700	343.6	28.7	0.349	0.358
44M	0.490	17.40	8	42.600	5.700	431.9	52.9	0.099	0.600
44M	0.490	17.40	9	56.800	5.700	200.2	32.7	1.136	0.909

SUMMARY OF HORIZONTAL ARRAY TESTS

TEST ID	CHARGE WEIGHT (LBS)	STANDOFF DISTANCE (IN)	GAGE NO	GAGE LOCATION (IN)	CHARGE SPACING (IN)	PEAK PRESSURE (PSI)	POSITIVE IMPULSE (PSI-MS)	POSITIVE DURATION (MS)	TIME OF ARRIVAL (MS)
28I	0.490	17.16	1	-56.800	28.50	200.8	20.8	0.708	0.499
28I	0.490	17.16	2	-42.600	28.50	662.4	47.2	1.340	0.249
28I	0.490	17.16	3	-28.400	28.50	576.2	57.2	0.203	0.154
28I	0.490	17.16	4	-14.200	28.50	4319.8	166.8	0.372	0.252
28I	0.490	17.16	5	0.000	28.50	2876.0	91.3	0.317	0.184
28I	0.490	17.16	6	14.200	28.50	3905.9	191.8	0.636	0.251
28I	0.490	17.16	7	28.400	28.50	3004.0	65.1	0.186	0.145
28I	0.490	17.16	8	42.600	28.50	890.6	75.0	0.422	0.259
28I	0.490	17.16	9	56.800	28.50	430.4	40.0	1.310	0.532
29I	0.490	17.16	1	-56.800	28.50	193.0	21.9	0.318	0.488
29I	0.490	17.16	2	-42.600	28.50	1138.3	50.3	0.348	0.245
29I	0.490	17.16	3	-28.400	28.50	4340.0	98.2	0.000	0.161
29I	0.490	17.16	4	-14.200	28.50	4132.0	149.0	0.147	0.236
29I	0.490	17.16	5	0.000	28.50	2997.0	125.0	0.154	0.159
29I	0.490	17.16	6	14.200	28.50	3950.1	216.4	0.259	0.229
29I	0.490	17.16	7	28.400	28.50	3030.3	69.4	0.117	0.154
29I	0.490	17.16	8	42.600	28.50	1397.1	54.8	0.241	0.207
29I	0.490	17.16	9	56.800	28.50	402.0	28.3	0.500	0.478
30I	0.490	17.16	1	-56.800	28.50	224.3	24.4	1.501	0.460
30I	0.490	17.16	2	-42.600	28.50	1548.4	54.3	0.328	0.219
30I	0.490	17.16	3	-28.400	28.50	1646.4	63.5	0.178	0.156
30I	0.490	17.16	4	-14.200	28.50	1076.6	140.4	0.240	0.227
30I	0.490	17.16	5	0.000	28.50	2752.9	94.1	0.117	0.134
30I	0.490	17.16	6	14.200	28.50	4215.4	217.6	0.232	0.202
30I	0.490	17.16	7	28.400	28.50	2465.4	77.8	0.267	0.141
30I	0.490	17.16	8	42.600	28.50	1221.3	55.8	0.326	0.252
30I	0.490	17.16	9	56.800	28.50	263.8	29.0	0.560	0.469
25J	0.490	22.92	1	-56.800	28.50	194.7	17.5	1.239	0.442
25J	0.490	22.92	2	-42.600	28.50	695.6	39.9	0.466	0.358
25J	0.490	22.92	3	-28.400	28.50	0.0	0.0	0.000	0.000
25J	0.490	22.92	4	-14.200	28.50	0.0	92.6	0.214	0.314
25J	0.490	22.92	6	14.200	28.50	2351.1	190.6	0.336	0.311
25J	0.490	22.92	7	28.400	28.50	0.0	0.0	0.000	0.000
25J	0.490	22.92	8	42.600	28.50	977.0	46.7	0.295	0.305
25J	0.490	22.92	9	56.800	28.50	295.5	27.1	0.594	0.653
26J	0.490	22.92	1	-56.800	28.50	214.8	23.0	0.418	0.445
26J	0.490	22.92	2	-42.600	28.50	626.6	36.9	0.458	0.376
26J	0.490	22.92	3	-28.400	28.50	0.0	6.5	0.110	0.[illegible]3
26J	0.490	22.92	4	-14.200	28.50	2231.3	96.3	0.223	0.[illegible]3
26J	0.490	22.92	5	0.000	28.50	1681.2	207.8	0.169	0.258
26J	0.490	22.92	6	14.200	28.50	2469.3	208.8	0.420	0.349
26J	0.490	22.92	7	28.400	28.50	0.0	0.0	0.000	0.000
26J	0.490	22.92	8	42.600	28.50	611.3	49.4	0.415	0.385
26J	0.490	22.92	9	56.800	28.50	239.3	25.8	0.411	0.647

SUMMARY OF HORIZONTAL ARRAY TESTS

TEST ID	CHARGE WEIGHT (LBS)	STANDOFF DISTANCE (IN)	GAGE NO	GAGE LOCATION (IN)	CHARGE SPACING (IN)	PEAK PRESSURE (PSI)	POSITIVE IMPULSE (PSI-MS)	POSITIVE DURATION (MS)	TIME OF ARRIVAL (MS)
27J	0.490	22.92	1	-56.800	28.50	226.0	28.5	0.720	0.611
27J	0.490	22.92	2	-42.600	28.50	0.0	101.9	0.365	0.365
27J	0.490	22.92	3	-28.400	28.50	1330.1	51.8	0.186	0.267
27J	0.490	22.92	4	-14.200	28.50	2664.1	127.5	0.246	0.345
27J	0.490	22.92	5	0.000	28.50	1742.4	0.0	0.126	0.279
27J	0.490	22.92	6	14.200	28.50	2719.6	103.2	0.233	0.347
27J	0.490	22.92	7	28.400	28.50	1570.3	50.1	0.086	0.267
27J	0.490	22.92	8	42.600	28.50	863.1	62.1	0.357	0.369
27J	0.490	22.92	9	56.800	28.50	318.1	36.9	0.505	0.629
31N	0.490	28.50	1	-56.800	28.50	140.9	19.7	0.441	0.732
31N	0.490	28.50	2	-42.600	28.50	336.7	63.9	0.515	0.420
31N	0.490	28.50	3	-28.400	28.50	163.3	44.1	0.171	0.378
31N	0.490	28.50	4	-14.200	28.50	2023.5	115.7	0.365	0.411
31N	0.490	28.50	5	0.000	28.50	1060.6	147.9	0.000	0.366
31N	0.490	28.50	6	14.200	28.50	1191.3	66.0	0.096	0.393
31N	0.490	28.50	7	28.400	28.50	727.3	17.9	0.056	0.383
31N	0.490	28.50	8	42.600	28.50	549.0	36.3	0.518	0.460
31N	0.490	28.50	9	56.800	28.50	198.8	21.3	0.444	0.727
32N	0.490	28.50	1	-56.800	28.50	194.2	23.5	0.345	0.771
32N	0.490	28.50	2	-42.600	28.50	677.0	53.9	0.513	0.462
32N	0.490	28.50	3	-28.400	28.50	707.8	46.0	0.147	0.388
32N	0.490	28.50	4	-14.200	28.50	0.0	0.0	0.000	0.000
32N	0.490	28.50	5	0.000	28.50	0.0	0.0	0.000	0.000
32N	0.490	28.50	6	14.200	28.50	0.0	0.0	0.000	0.000
32N	0.490	28.50	7	28.400	28.50	539.3	27.1	0.000	0.372
32N	0.490	28.50	8	42.600	28.50	565.0	51.5	0.415	0.454
32N	0.490	28.50	9	56.800	28.50	266.7	32.4	0.367	0.717
33N	0.490	28.50	1	-56.800	28.50	178.5	18.4	0.444	0.722
33N	0.490	28.50	2	-42.600	28.50	681.0	41.5	0.504	0.470
33N	0.490	28.50	3	-28.400	28.50	0.0	0.0	0.000	0.000
33N	0.490	28.50	4	-14.200	28.50	0.0	0.0	0.000	0.000
33N	0.490	28.50	5	0.000	28.50	0.0	0.0	0.000	0.000
33N	0.490	28.50	6	14.200	28.50	8051.8	802.9	0.344	0.421
33N	0.490	28.50	7	28.400	28.50	0.0	0.0	0.000	0.000
33N	0.490	28.50	8	42.600	28.50	656.6	49.6	0.401	0.457
33N	0.490	28.50	9	56.800	28.50	204.4	29.8	0.557	0.692
34N	0.490	28.50	1	-56.800	28.50	180.3	19.1	0.383	0.712
34N	0.490	28.50	2	-42.600	28.50	739.1	21.0	0.351	0.446
34N	0.490	28.50	3	-28.400	28.50	994.0	40.4	0.153	0.365
34N	0.490	28.50	4	-14.200	28.50	1814.7	113.8	0.000	0.407
34N	0.490	28.50	5	0.000	28.50	973.9	57.5	0.133	0.372
34N	0.490	28.50	6	14.200	28.50	0.0	0.0	0.000	0.000
34N	0.490	28.50	9	56.800	28.50	0.0	0.0	0.000	0.000
35P	0.490	28.50	1	-56.800	14.20	869.2	145.8	0.820	1.141

SUMMARY OF HORIZONTAL ARRAY TESTS

TEST ID	CHARGE WEIGHT (LBS)	STANDOFF DISTANCE (IN)	GAGE NO	GAGE LOCATION (IN)	CHARGE SPACING (IN)	PEAK PRESSURE (PSI)	POSITIVE IMPULSE (PSI-MS)	POSITIVE DURATION (MS)	TIME OF ARRIVAL (MS)
35P	0.490	28.50	2	-42.600	14.20	176.3	21.0	0.517	0.716
35P	0.490	28.50	3	-28.400	14.20	458.1	43.5	0.360	0.460
35P	0.490	28.50	4	-14.200	14.20	1535.8	106.3	0.458	0.362
35P	0.490	28.50	5	0.000	14.20	2523.2	91.6	0.082	0.350
35P	0.490	28.50	6	14.200	14.20	981.0	63.8	0.381	0.381
35P	0.490	28.50	7	28.400	14.20	321.8	22.7	0.407	0.474
35P	0.490	28.50	8	42.600	14.20	2149.5	318.2	0.608	0.726
35P	0.490	28.50	9	56.800	14.20	1009.3	199.6	0.608	1.156
36P	0.490	28.50	1	-56.800	14.20	81.7	16.2	0.516	1.140
36P	0.490	28.50	2	-42.600	14.20	226.9	24.9	0.537	0.691
36P	0.490	28.50	3	-28.400	14.20	475.0	41.4	0.340	0.475
36P	0.490	28.50	4	-14.200	14.20	1652.8	109.4	0.460	0.353
36P	0.490	28.50	5	0.000	14.20	2174.1	149.6	0.111	0.373
36P	0.490	28.50	6	14.200	14.20	1438.0	101.8	0.571	0.357
36P	0.490	28.50	7	28.400	14.20	253.7	19.9	0.377	0.473
36P	0.490	28.50	8	42.600	14.20	199.5	40.9	0.507	0.712
36P	0.490	28.50	9	56.800	14.20	84.3	22.7	0.697	1.153
37P	0.490	28.50	1	-56.800	14.20	84.6	13.9	0.471	1.100
37P	0.490	28.50	2	-42.600	14.20	255.5	27.4	0.752	0.675
37P	0.490	28.50	3	-28.400	14.20	291.9	40.9	0.425	0.437
37P	0.490	28.50	4	-14.200	14.20	1954.9	63.1	0.221	0.360
37P	0.490	28.50	5	0.000	14.20	2055.0	164.7	0.427	0.356
37P	0.490	28.50	6	14.200	14.20	1347.5	85.6	0.284	0.362
37P	0.490	28.50	7	28.400	14.20	351.0	22.6	0.334	0.472
37P	0.490	28.50	8	42.600	14.20	298.3	25.6	0.546	0.702
37P	0.490	28.50	9	56.800	14.20	98.4	20.5	0.611	1.136
41Q	0.490	28.50	1	-56.800	42.60	0.0	0.0	0.000	0.000
41Q	0.490	28.50	2	-42.600	42.60	0.0	0.0	0.000	0.000
41Q	0.490	28.50	3	-28.400	42.60	459.0	59.5	0.581	0.463
41Q	0.490	28.50	4	-14.200	42.60	550.6	68.5	0.633	0.478
41Q	0.490	28.50	6	14.200	42.60	546.0	67.6	0.609	0.478
41Q	0.490	28.50	7	28.400	42.60	341.4	33.3	0.498	0.461
41Q	0.490	28.50	9	56.800	42.60	600.3	43.6	0.414	0.465
42Q	0.490	28.50	1	-56.800	42.60	473.7	31.9	0.202	0.453
42Q	0.490	28.50	2	-42.600	42.60	967.3	53.0	0.347	0.393
42Q	0.490	28.50	3	-28.400	42.60	433.4	54.4	0.269	0.467
42Q	0.490	28.50	4	-14.200	42.60	445.4	67.6	0.731	0.454
42Q	0.490	28.50	5	0.000	42.60	504.7	86.4	0.358	0.417
42Q	0.490	28.50	6	14.200	42.60	707.8	71.5	0.665	0.443
42Q	0.490	28.50	7	28.400	42.60	357.7	48.4	0.580	0.438
42Q	0.490	28.50	8	42.600	42.60	820.9	44.2	0.300	0.394
42Q	0.490	28.50	9	56.800	42.60	690.6	59.0	0.404	0.457
43Q	0.490	28.50	1	-56.800	42.60	462.1	38.6	0.379	0.465
43Q	0.490	28.50	2	-42.600	42.60	1000.7	51.0	0.294	0.396

SUMMARY OF HORIZONTAL ARRAY TESTS

TEST ID	CHARGE WEIGHT (LBS)	STANDOFF DISTANCE (IN)	GAGE NO	GAGE LOCATION (IN)	CHARGE SPACING (IN)	PEAK PRESSURE (PSI)	POSITIVE IMPULSE (PSI-MS)	POSITIVE DURATION (MS)	TIME OF ARRIVAL (MS)
430	0.490	28.50	3	-28.400	42.60	0.0	0.0	0.000	0.000
430	0.490	28.50	4	-14.200	42.60	544.5	61.0	0.397	0.459
430	0.490	28.50	5	0.000	42.60	407.5	31.3	0.211	0.374
430	0.490	28.50	6	14.200	42.60	423.4	73.2	0.607	0.456
430	0.490	28.50	7	28.400	42.60	384.7	42.4	0.628	0.481
430	0.490	28.50	8	42.600	42.60	506.9	45.9	0.294	0.402
430	0.490	28.50	9	56.800	42.60	617.5	134.0	0.399	0.495

DISTRIBUTION LIST

Commander
US Army Armament Research and
Development Command
ATTN: DRDAR-CG
DRDAR-LCM-E
DRDAR-LCM-S (25)
DRDAR-SF
DRDAR-TSS (5)
Dover, NJ 07801

Chairman
Dept of Defense Explosive Safety Board (2)
Forrestal Bldg, GB-270
Washington, DC 20314

Administrator
Defense Documentation Center
ATTN: Accessions Division (12)
Cameron Station
Alexandria, VA 22314

Commander
Department of the Army
Office, Chief Research, Development
And Acquisition
ATTN: DAMA-CSM-P
Washington, DC 20310

Office, Chief of Engineers
ATTN: DAEN-MCZ
Washington, DC 20314

Commander
US Army Materiel Development
and Readiness Command
ATTN: DRCSF
DRCDE
DRCRP
DRCIS
5001 Eisenhower Avenue
Alexandria, VA 22333

Commander
DARCOM Installations and
Services Agency
ATTN: DRCIS-RI
Rock Island, IL 61299

Director
Industrial Base Engineering Activity
ATTN: DRXIB-MT & EN
Rock Island, IL 61299

Commander
US Army Materiel Development
and Readiness Command
ATTN: DRCPM-PBM
DRCPM-PBM-S
DRCPM-PBM-L (2)
DRCPM-PBM-E (2)
Dover, NJ 07801

Commander
US Army Armament Materiel
Readiness Command
ATTN: DRSAR-SF (3)
DRSAR-SC
DRSAR-EN
DRSAR-PPI
DRSAR-FPI-C
DRSAR-RD
DRSAR-IS
DRSAR-ASF
Rock Island, IL 61299

Director
DARCOM Field Safety Activity
ATTN: DRXOS-ES (2)
Charlestown, IN 47111

Commander
US Army Engineer Division
ATTN: HNDED
PO Box 1600, West Station
Huntsville, AL 35809

Commander
Badger Army Ammunition Plant
Baraboo, WI 53913

Commander
Indiana Army Ammunition Plant
Charlestown, IN 47111

Commander
Holston Army Ammunition Plant
Kingsport, TN 37660

Commander
Lone Star Army Ammunition Plant
Texarkana , TX 75501

Commander
Milan Army Ammunition Plant
Milan, TN 38358

Commander
Iowa Army Ammunition Plant
Middletown, IA 52638

Commander
Joliet Army Ammunition Plant
Joliet, IL 60436

Commander
Longhorn Army Ammunition Plant
Marshall, TX 75760

Commander
Louisiana Army Ammunition Plant
Schreveport, LA 71130

Commander
Ravenna Army Ammunition Plant
Ravenna, OH 44266

Commander
Newport Army Ammunition Plant
Newport, IN 47966

Commander
Volunteer Army Ammunition Plant
Chattanooga, TN 37401

Commander
Kansas Army Ammunition Plant
Parsons, KS 67357

District Engineer
US Army Engineering District, Mobile
Corps of Engineers
PO Box 2288
Mobile, AL 36628

District Engineer
US Army Engineering District, Ft. Worth
Corps of Engineers
PO Box 17300
Ft. Worth, TX 76102

District Engineer
US Army Engineering District, Omaha
Corps of Engineers
6014 US PO & Courthouse
215 N 17th Street
Omaha, NB 78102

District Engineer
US Army Engineering District, Baltimore
Corps of Engineers
PO Box 1715
Baltimore, MD 21203

District Engineer
US Army Engineering District, Norfolk
Corps of Engineers
803 Front Street
Norfolk, VA 23510

Division Engineer
US Army Engr District, Huntsville
PO Box 1600, West Station
Huntsville, AL 35807

Commander
Naval Ordnance Station
Indianhead, MD 20640

Commander
US Army Construction Engr Research
Laboratory
Champaign, IL 61820

Commander
Dugway Proving Ground
Dugway, UT 84022

Commander
Savanna Army Depot
Savanna, IL 61704

Civil Engineering Laboratory
Naval Construction Battalion Center
ATTN: L51
Port Hueneme, CA 93043

Commander
Naval Facilities Engineering Command
(Code 04, J. Tyrell)
200 Stovall Street
Alexandria, VA 22322

Commander
Southern Division
Naval Facilities Engineering Command
ATTN: J. Watts
PO Box 10068
Charleston, SC 29411

Commander
Western Division
Naval Facilities Engineering Command
ATTN: W. Moore
San Bruno, CA 94066

Officer in Charge
Trident
Washington, DC 20362

Commander
Atlantic Division
Naval Facilities Engineering Command
Norfolk, VA 23511

Commander
Naval Ammunition Depot
Naval Ammunition Production
Engineering Center
Crane, IN 47522

US Army TRADOC Systems
Analysis Activity
ATTN: ATAA-SL (Tech Lib)
White Sands Missile Range, NM 88002

Commander
US Army Armament Materiel and
Readiness Command
ATTN: DRSAR-LEP-L
Rock Island, IL 61299

US Army Materiel Systems
Analysis Activity
ATTN: DRXSY-MP
Aberdeen Proving Ground, MD 21005

Weapon System Concept Team/CSL
ATTN: DRDAR-ACW
Aberdeen Proving Ground, MD 21010

Technical Library
ATTN: DRDAR-CLJ-L
Aberdeen Proving Ground, MD 21005

Technical Library
ATTN: DRDAR-TSB-S
Aberdeen Proving Ground, MD 21010

Technical Library
ATTN: DRDAR-LCB-TL
Benet Weapons Laboratory
Watervliet, NY 12189

Commander
Radford Army Ammunition Plant
Radford, VA 24141

Commander
Newport Army Ammunition Plant
Newport, IN 47966

Officer in Charge of Construction
Trident
Bangor, WA 98436